Development of the visual pathway in Xenopus laevis (Daudin)

Bertram P. Payne,

CHAPTER IV

Development of the receptive field properties of retinal ganglion cells

INTRODUCTION

Few physiological studies have been carried out on the developing vertebrate retina. Hamasaki and Flynn (1977) studied the kitten retina and found that the excitatory regions of receptive fields were similar to those of adults, however, the inhibitory regions were underdeveloped and the ganglion cell discharges were "sluggish".

Studies on developing retinas have mainly concentrated on amphibians. Studies of the developing retina of Xenopus have been mainly concerned with the time of origin and location of developing ganglion cells (Hollyfield, 1971; Straznicky and Gaze, 1971; Jacobson, 1976; Straznicky and Tay, 1977). Other studies have examined the ultrastructural pattern of synaptic connexions (Fisher, 1976). Witkovsky et al (1976) have correlated their ultrastructural findings with the development of the electroretinogram (ERG) and have shown that the photoreceptors function at Stage 38 prior to synapse development and that photoreceptor synaptic ribbons were present and functional at Stage 39.

Fisher (1976) studied the inner plexiform layer of Xenopus retina and found that synapse formation increased explosively at Stage 40, and that the rate of increase in the numbers of synapses fell after Stage 47 in the region of the central retina. However, the retina is by no means structurally mature at this stage.

In view of the evidence of previous work establishing the physiological and morphological integrity of the developing retina and tectal input it should be possible to examine the responses and assess the extent to which visual information is processed and transmitted to the tectum at various stages during development. The responses of retinal ganglion cells were studied throughout development since it was clear that the receptive field properties of tadpole ganglion cells were very different to those recorded in the adult.

METHOD

A. PREPARATION OF THE ANIMAL

(i) Adults

Animals were prepared in order to expose the optic tectum to enable the recording of action potentials from ganglion cell terminals. Adults of at least two months of age were anaesthetized with ether. The eyes were shielded from the dissecting light and the skin overlying the skull and the surrounding muscle was removed. The two large dorsal blood vessels were sutured and cut. The dorsal surface of the skull was removed with the aid of a dental burr and the forebrain was removed by suction. 2-12 mg of succinyl choline were administered to the dorsal lymph sac to immobilize the preparation. Cotton threads soaked in Xylocaine (Astra) were placed along all cut edges. All exposed surfaces, especially the eyes, were covered with paraffin oil. The animal was then draped with a fresh medical wipe tissue and placed in a shallow bath containing Niu-Twitty solution.

(ii) Tadpoles and toads up to two months of age

The toads were anaesthetized by ether and the tadpoles by immersion in a 1:1000 (w/v) solution of MS 222. All individuals were half-submerged in a Niu-Twitty solution. The skin overlying the brain was cut away and the roof of the skull which required gentle burring in older juveniles was cut and removed. The forebrain was removed by suction and the animals were immobilized with 0.02 - 0.05 mg d-tubocurarine. This was injected into the thigh in young toads and behind the non-experimental eye in tadpoles. Many of these animals were then placed in a glass hemisphere (Beazley et al, 1972; Gaze et al, 1974). With a Sylgard (Dow Corning) base and filled with Niu-Twitty solution.

The pia of Xenopus tadpoles is tough and elastic and when platinum-tipped indium electrodes were used penetration of the tectal membrane was often accompanied by loss of the Platinum tip. It was therefore decided to attempt to soften the membrane by digestion (Chung et al, 1975; George, 1970) with Protease Type 1 (Sigma). Over a five minute period a solution of protease (10 mg/ml) in Niu-Twitty solution was dropped gently onto the tectal surface using a Pasteur pipette. The preparation was then transferred to Niu-Twitty solution to wash.

A number of Rana pipiens and R. temporaria were also used in this study for comparison. These were prepared in a similar manner, but were immobilized with 0.05 - 0.5 mg of d-tubocurarine, the quantity depending on the time of year.

Electrophysiological recording was delayed for half an hour after operative surgery in adults and for five to ten minutes in tadpoles to allow the animals to recover from the anaesthetic.

B. ELECTRODES

Metal-in-glass pipettes and stainless steel recording electrodes were used to investigate the location of ganglion cell terminals in the optic tectum.

(i) Metal-in-glass pipettes

The electrodes comprised a mixture of indium (BDH) and Woods metal (BDH) in glass micropipettes and were manufactured according to a method similar to that of Gesteland et al (1959).

The micropipettes were produced from borosilicate glass tubing with an internal diameter of 1 mm, using an automatic glass puller. The tips of the micropipettes were broken to give a diameter of approximately 3 μm.

The Woods metal and indium were heated to a temperature slightly above their melting point and the liquid was drawn up into a PVC tubing which had an internal bore slightly smaller than that of the micropipettes. After cooling, the PVC tubing was gently cut away and the Woods metal/indium alloy wire was inserted into the micropipette. Tinned

copper wire was used to force the alloy to the tip of the micropipette which was then warmed on the bit of a soldering iron. Firm pressure was applied to the tinned copper wire until a small bubble of alloy appeared at the tip and the copper wire became embedded in the alloy. The micropipette was removed from the heat and pressure was maintained until the alloy had solidified.

These electrodes were plated individually prior to use. Each electrode was placed in a microdrive and the tip was lowered to the surface of an aqueous solution of 1% auric potassium cyanide (BDH). A negative 3V square wave pulse train at a frequency of 1 KHz was applied to the tip for 15-30 seconds from a Servomex waveform generator type LF 141. A carbon rod was used as the indifferent electrode. This process was repeated using a solution of 1% chloroplatinic acid (BDH) containing 0.01% (w/v) lead acetate and a few granules of gelatin. The gelatin was dispersed throughout the solution by the heat of the bench light. A negative square wave of 1.5V produced from the same waveform generator was used to plate the electrode tip with platinum. The alternating current which passed through the tip was monitored on an oscilloscope and was used to determine the electrode impedance. Plating was continued until the impedance was reduced to about 100 KΩ. The electrodes were viewed under a microscope and any tips which were too large or uneven were removed and replated. Electrodes produced in this manner were used immediately.

(ii) Stainless steel electrodes

Stainless steel electrodes were prepared according to the method of E. Schürg-Pfeiffer (personal communication). Size 'O' insect pins were cleaned in acetone and the heads were dipped repeatedly 2-3 mm into a 25% solution of hydrochloric acid (v/v). An alternating current of 3A driven by 12V from a Radford Lab 59 R Labpack was passed between the insect pin and a copper coil in the acid. After a small spark had passed between the pin and the etching fluid, the pin was dipped in the acid twice more, washed in distilled water and observed under a microscope. Etching was continued until a tip diameter of 1-2 μm was produced.

Some electrodes were polished in a mixture of H_3PO_4, H_2SO_4 and water in the ratio 21:17:12 (Cross and Silver, 1963). These electrodes seemed to have no improved qualities over unpolished electrodes, and therefore the method was discontinued.

The electrodes were insulated by immersion in a 50% solution of Insl-X and acetone. They were removed and rapidly inverted and allowed to dry in air. Prior to use the electrode tip was gently wiped on a soft piece of paper. This enhanced the signal to noise ratio, presumably by removing a little of the insulation.

C. VISUAL STIMULI

Visual stimuli were black paper discs mounted on glass wands, varying in size from 2^{o}-30^{o} of visual arc. These stimuli were moved manually in front of a tangent screen which was positioned 28 cm from the eye of the animal. This screen was matt white and was flooded by light with a luminance of 4.8 $cd.m^{-2}$ and could be dimmed over a range of 3 log units.

The criterion for the edge of the receptive field of a neuron under study was set as the position of the leading edge of the disc when the first spike was recorded. When delineating a receptive field, each scan of the wand in a particular direction was not repeated until one minute had elapsed.

Neuronal responses in adults, and where possible in young toads and tadpoles, were classified according to the scheme of Grüsser and Grüsser-Cornehls (1976), which is outlined in figure 4:1.

These two tests consisted of the responses to the switching off and on of the background illumination and the response to the movement of a small black object (2^{o}) into the receptive field. However, class I and II cells are extremely sensitive to slight movements of the wand. This problem was overcome by attaching a black stimulus

Fig. 4.1: Schematic diagram of the responses of adult amphibian retinal ganglion cells.

Two tests were used routinely to classify the responses of adult Xenopus retinal ganglion cells. The two tests were either the switching on and off of background illumination (a) or moving a 2° black target into the receptive field and holding it stationary (b).

(a) Class I and II ganglion cells do not respond to the switching on and off of the background illumination. Class III ganglion cells have a phasic response to both the 'on' and 'off' of the light. Class IV units have a maintained low level discharge in the dark (start of trace) which is inhibited by the light 'on'. When the light is switched off an intense discharge is produced, the rate of which decreases to the level prior to the light 'on'.

(b) Class I and II ganglion cells respond with a discharge of action potentials when a small (2°) black object is moved into the receptive field and this discharge is maintained if the object is held stationary. Class I and II response may be distinguished from each other by combining the test illustrated in (a) with that in (b) since class II show the phenomenon of 'erasability' (Maturana et al, 1960). Class I ganglion cells produce the maintained discharge when a small object is moved into the receptive field, when the background illumination is switched off the response stops, however at 'on' the response continues. In contrast, after the discharge has stopped at light 'off' in Class II ganglion cells, at light 'on' no further discharge is produced. Class III ganglion cells give only a transient response to the movement of the target. Class IV ganglion cells do not respond to this stimulus.

4-1

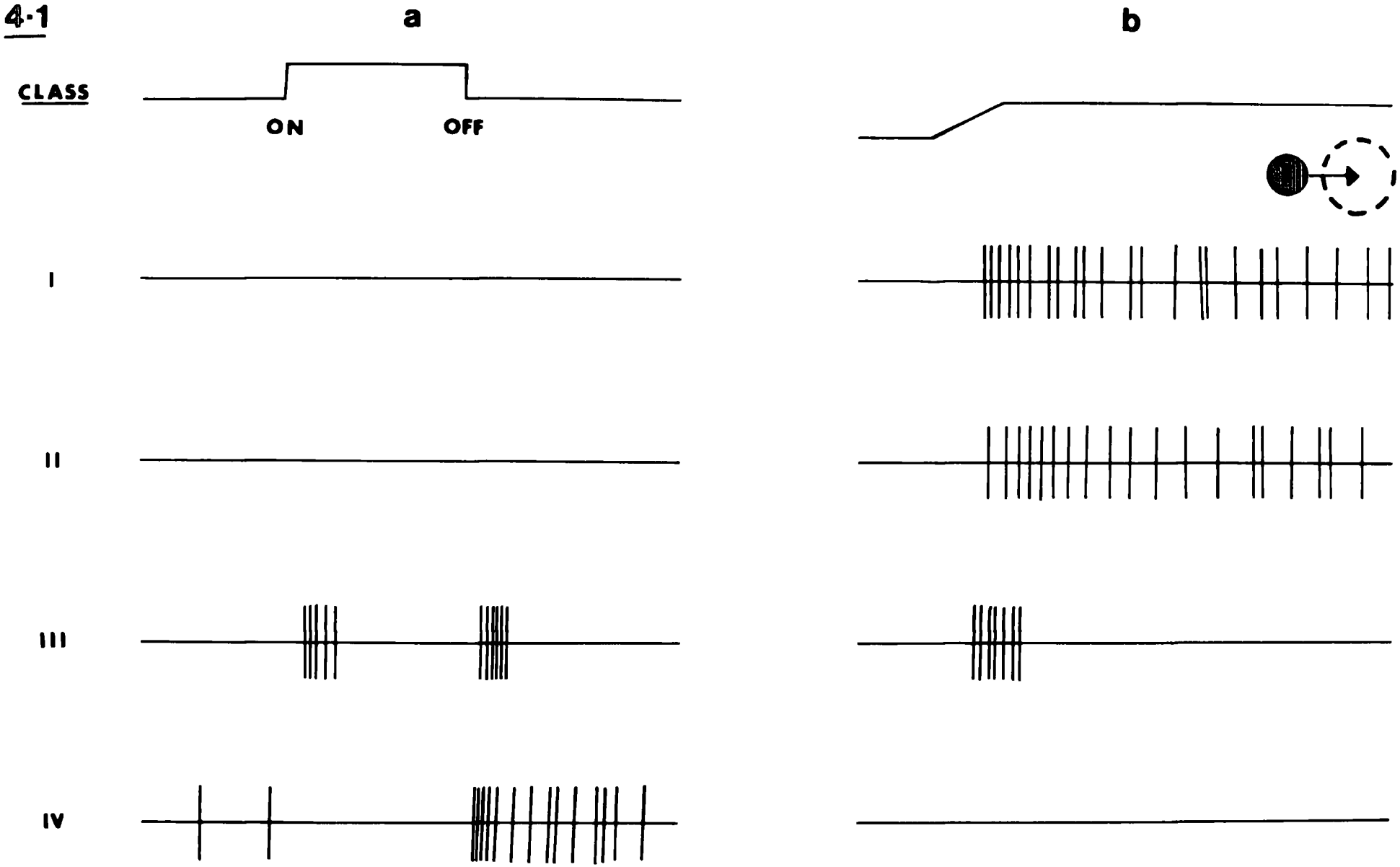

object to the screen, so the stimulus could be introduced into the receptive field by movement of the screen. In all cases controls were performed to determine if any responses were produced to movement of the screen alone and neurons which did respond in this way were ignored.

D. RECORDING PROCEDURE

Electrodes were lowered into the optic tectum using Prior micromanipulators. Action potentials (spikes) in response to visual stimuli were recorded by means of metal-filled micropipettes or stainless steel electrodes. The silver indifferent electrode was located in the Niu-Twitty solution surrounding the animal. The responses were amplified 1000 times by an AC-coupled high input impedance amplifier. A band pass filter was used to eliminate signals below 700 Hz and above 2KHz. The signal from the amplifier was passed through two Tektronix 502 A oscilloscopes, one for observation and one for photography, to a Pioneer CT-F2121 FM tape recorder to produce a permanent record for later analysis. The signal was also passed to a window discriminator, the output of which was used to brighten spikes of selected amplitude on a third oscilloscope by Z-axis modulation. This signal was also led to the tape recorder for permanent storage. Action potentials were monitored on the oscilloscope screens and by means of a loudspeaker. Photographs were taken using a 35 mm Nihon-Kohden oscilloscope camera both on- and off-line.

E. HISTOLOGICAL CONTROL OF RECORDING SITE

The location of units was confirmed by producing a small lesion at the recording site by passing 7.5 μA for 10 seconds through the metal filled micropipettes with the electrode negative. The animals were then fixed and processed as described in the general methods. Alternatively, recording sites were marked by using the Prussian Blue technique of Adrian and Moruzzi (1939). This involved passing a direct current of 7.5 μA for one to two seconds with the electrode positive. The tissue was fixed with 0.9% Saline containing 10% formaldehyde and 1% ferrocyanide.

RESULTS

Retinal ganglion cell axon terminals were classified according to the schema of Grüsser and Grüsser-Cornehls (1976) which is based on the responses to either the "on" and "off" of a background light or the movement of a small black object into the receptive field. Class I and II ganglion cells were differentiated by the presence or absence of erasability (Maturana et al 1960). Using these two criteria, responses in both adults and tadpoles could be well characterized. Most recordings from retinal ganglion cell terminals were made from the part of the tectum which receives terminals from central retinal ganglion cells.

Adults

The responses of ganglion cell axon terminals were characterized in twenty-three Xenopus laevis which were either two years old and bred in the laboratory or older and purchased from suppliers. Twelve frogs (Rana species) were also studied for comparative purposes.

Four response types were recorded which correspond to the classes I to IV of Maturana et al (1960) and Grüsser and Grüsser-Cornehls (1976). Responses from classes I and II could be recorded in the more superficial

part of layer 9 of the tectum. Typical depths for class I and II terminals were 50 μm and 100 μm respectively. However, some class I responses could be recorded in the region of class II terminals and vice versa. Accurate depth measurements were difficult to make because of tissue dimpling and the collapse of the ventricle on electrode penetration. However, using the Prussian blue method (Adrian and Moruzzi, 1939) of electrode tip localization, class I terminals were usually found more superficial to class II (fig. 4:11 a, b).

Figure 4:2 shows the activity of a Class I terminal recorded in response to the movement of a small 4^{o} black object into the receptive field. The activity was maintained if the stimulus remained stationary within the receptive field. Similar responses were obtained from class II terminals (fig. 4:3) although the discharge in this case was at a lower rate. The ability to erase the neuronal response was used routinely to differentiate class I and II responses. If, after the stimulus had been moved into the receptive field, the background light was switched off, both classes of fibres stopped firing. But when the lights were switched on again after a short delay, class I fibres continued their maintained discharge, whereas class II fibres did not (figs. 4:2 and 4:3).

Responses of adult Class I and II ganglion cells

Fig. 4.2: The response illustrated is from a class I ganglion cell terminal. A small 4^{o} black target was moved into the receptive field (sloping line) and held stationary. The response was intense during the movement of the target. The maintained discharge stopped at light 'off' (downward deflection of the lower line) and restarted at 'on' (upward deflection of the lower line.)

Fig. 4.3: Similar maintained responses were recorded from Class II terminals. A target moved into the receptive field elicited a response which was maintained when the target was held stationary. When the light was switched off the response stopped and was not re-established at light 'on'. Thus the response was erasable.

Fig. 4.4: The presence of an inhibitory surround to the class I and II ganglion cells was investigated by moving a black 30^{o} target into the receptive field periphery. A maintained discharge was evoked from a class II ganglion cell when a 4^{o} target was moved into the receptive field and held stationary (a). This maintained activity was inhibited by the movement of a 30^{o} target into the peripheral region of the receptive field (bar in b). Note that the discharge almost ceased. When the second stimulus was removed the maintained response continued (b). The larger spikes at the time of entry and exist of the second stimulus were from a second ganglion cell.

Time calibration for all figures are as indicated.

4·2

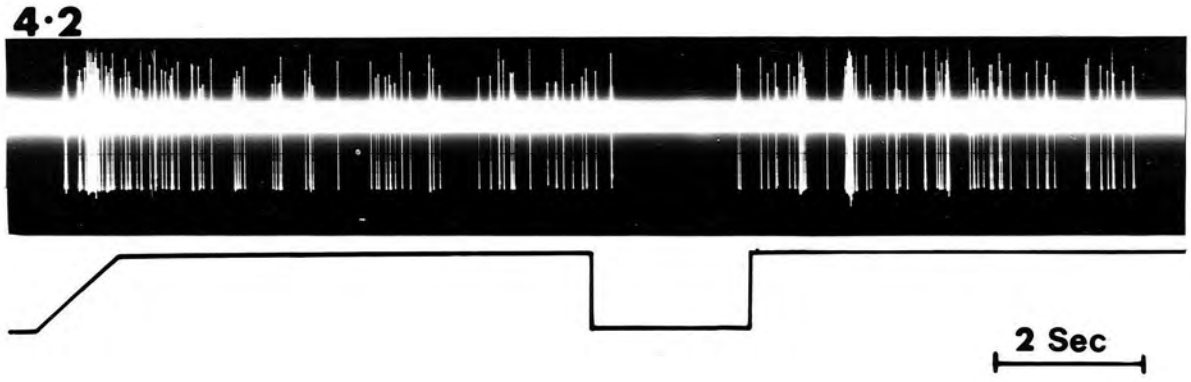

4·3

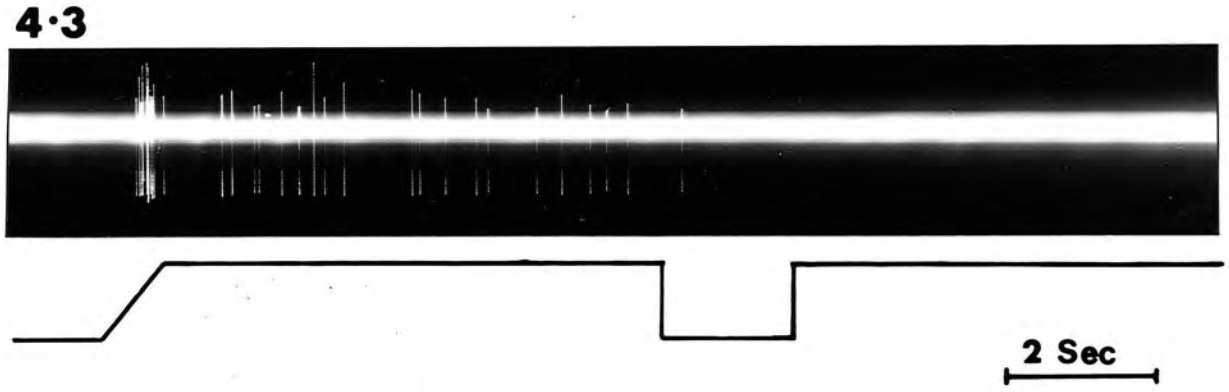

4·4a

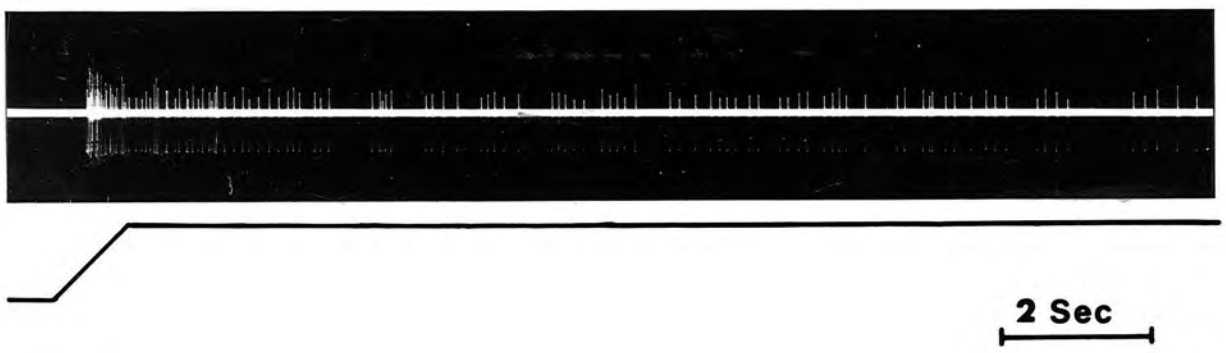

4·4b

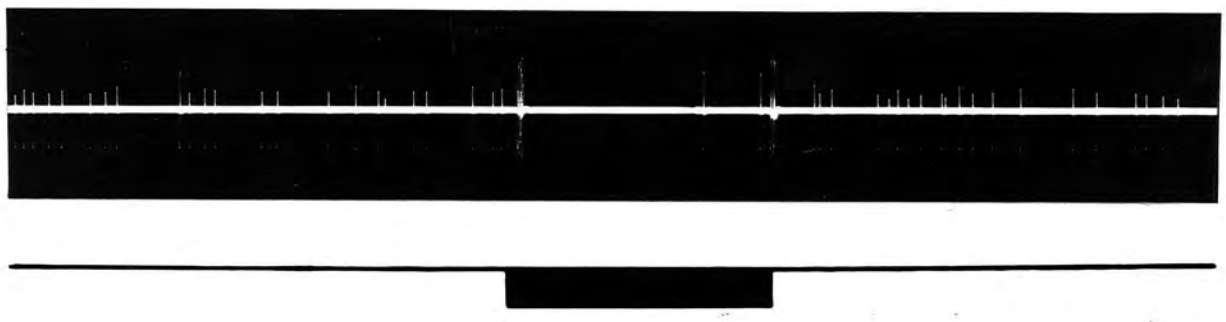

The presence of an inhibitory surround to the excitatory centre of the class I and II receptive fields was also investigated. A 4^{o} object was moved into a class II excitatory receptive field and held stationary. This produced a maintained response from the neuron (fig. 4:4 a). After several seconds, a black 30^{o} stimulus was moved to a position 60^{o} away from the excitatory receptive field. This movement led to the inhibition of the maintained response of the class II ganglion cell and also to the excitation of another ganglion cell, as evidenced by the larger spikes at the point of entry and removal of the larger stimulus (fig. 4:4 b). Once the second stimulus had been removed, the maintained activity was re-established. The inhibition was produced by the movement of the second stimulus to within 60^{o} to 100^{o} of the excitatory receptive field in class II fibres and to within 30^{o} to 80^{o} in class I fibres. The excitatory receptive field sizes for both class I and class II ganglion cells in the adult were usually between 3^{o} and 6^{o}.

Class III ganglion cells responded with a brief burst of action potentials to both the switching on and off of the background illumination (fig. 4:5). They also responded to small and medium size objects (2^{o} to 12^{o}) traversing the receptive fields, which were 8^{o} to 12^{o} in diameter. The class III discharges could be recorded between depths of 120 μm and 240 μm in the

Responses of adult Class III and IV ganglion cells.

Fig. 4.5: Class III ganglion cells respond to the 'on' and 'off' of the background light with a brief transient discharge. The downward deflection of the lower line in the figure indicates light 'off' and notice that the 'off' discharge was more prolonged than the 'on' (upward deflection of the lower line.)

Fig. 4.6: Class IV ganglion cells are easily characterized by their response to the 'on' and 'off' of the background illumination. This figure shows a 'bursty' endogenous discharge in the dark (start of trace) which was totally inhibited by the light 'on' downward deflection of the lower line. When the light was switched on an intense discharge was produced, the rate of which decreased to the endogenous level prior to the test. Note the 'bursty' appearance of the endogenous discharge at the right of the trace.

Time calibrations for both traces are as indicated.

4·5

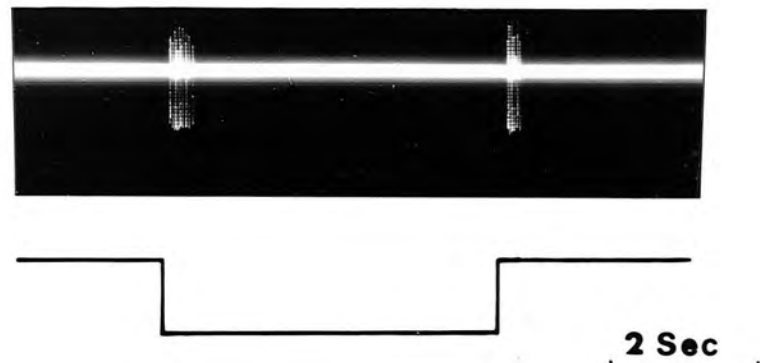

4·6

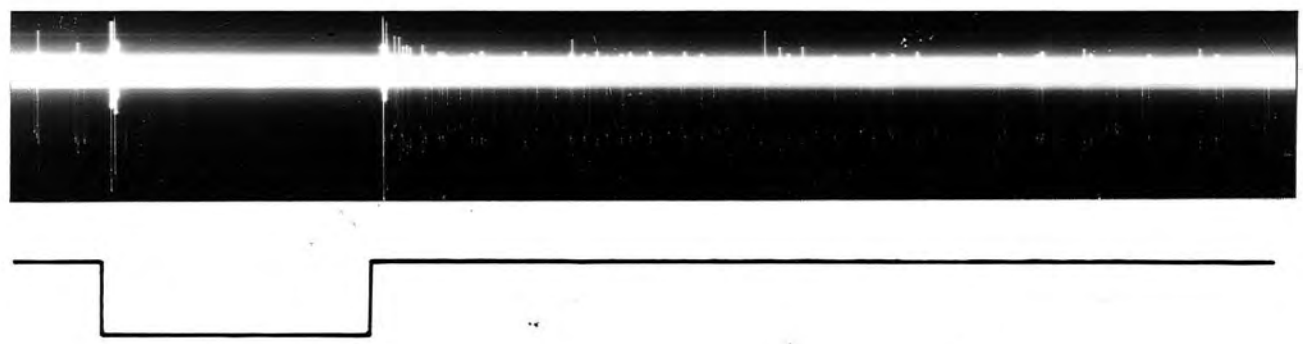

tectum, with a depth of 170 μm being typical. Class III responses were always deeper than class II responses (fig. 4:11 c).

Class IV ganglion cell terminals were not commonly encountered and responded only to moving black stimuli at least 4^{o} in diameter. The receptive field sizes were usually 16^{o} to 21^{o} with some as large as 28^{o}. Class IV neurons could easily be characterized by their massive discharge when the background illumination was switched off, and the total inhibition of the endogenous activity in the light. A typical response is exhibited in figure 4:6, where the bursts of endogenous activity were inhibited by switching on the background illumination. When the light was switched off, an intense response was produced which returned to the endogenous rate of activity seen prior to the light "on". Class IV responses were always found to be the deepest of all four ganglion cell terminals from which recordings were taken, and Prussian blue electrode markings were always in layer 7 or layer 8 (fig. 4:11 d).

Tadpoles

Responses were recorded from the tecta of 123 tadpoles and where possible were classified using the same criteria that were used to define the responses of adult retinal ganglion cells.

Stages 46 to 49

The earliest visually evoked responses which could be recorded were from Stage 46 tadpoles and responses were recorded from 37 tadpoles between Stages 46 and 49. Action potentials could be evoked and recorded in the tectum in response to switching the background illumination on and off. The responses consisted of two to six spikes at either "on" or "off", usually with a greater response at "on" (fig. 4:7 a). These responses could be evoked only once or twice, with the second response much diminished relative to the first. These ganglion cells also responded to large (at least 30^{o}) black visual stimuli traversing the receptive field (fig. 4:7 b). Responses were weak and readily habituated to subsequent stimuli presented within an interval of one minute, although if a different direction of movement for the stimulus was used, the responses improved markedly. By Stage 49, units typical of this kind were recorded regularly in the most superficial part of the tectum. Units could also be recorded whose discharges were more stable to repetitive stimuli and produced spike bursts with a greater number of action potentials.

Stages 50 to 54

Responses were recorded from 23 tadpoles in Stages 50 to 54 inclusive and these could be classified into two major types.

Responses of tadpole stage 46 ganglion cells

Fig. 4.7: The discharge illustrated in (a) was produced in response to the background light 'off' (upward deflection of the lower line) which elicits five spikes with long (approx. 400 msec) interspike intervals. Light 'on' (donward deflection of the lower line) evoked three spikes.

The discharge illustrated in (b) was evoked in response to a 40^{o} target traversing the receptive field and the traverse is shown diagrammatically by the sloping lower line.

Fig. 4.8: Responses of tadpole stage 50 and 53 ganglion cells

(a) A stepwise brightening of the background light (stepped lower line) in (ai) evoked single spikes or pairs of spikes shortly after the illumination change in a stage 50 tadpole. Decremental light changes, (stepped lower line) evoked discharges of two or three spikes after each step and in total darkness a maintained discharge was produced (right end of trace).

(b) A low level endogenous activity was present in the class IV type response from a stage 53 tadpole. At light 'off' (downward deflection of the lower line) an intense discharge was produced which was reminiscent of an adult class IV response to the 'off' of the background illumination. Responses such as illustrated here could only be evoked by large illumination changes, in contrast to those illustrated above in (a).

Time calibrations are as indicated.

4·7a

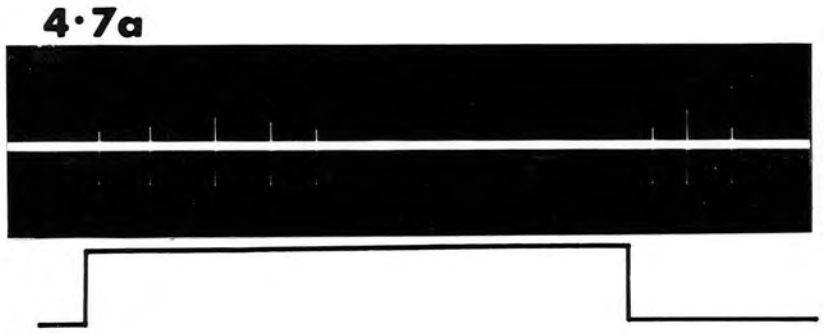

4·7b

1 Sec

4·8ai

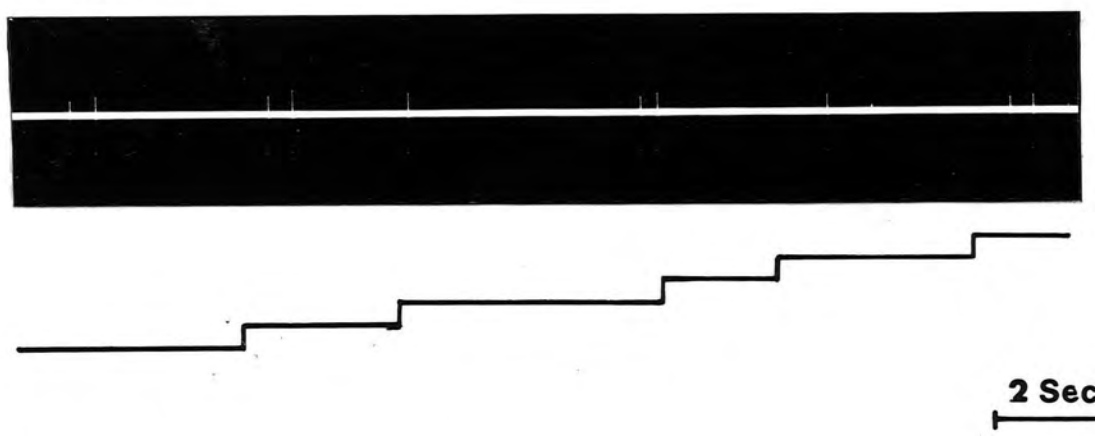

2 Sec

4·8aii

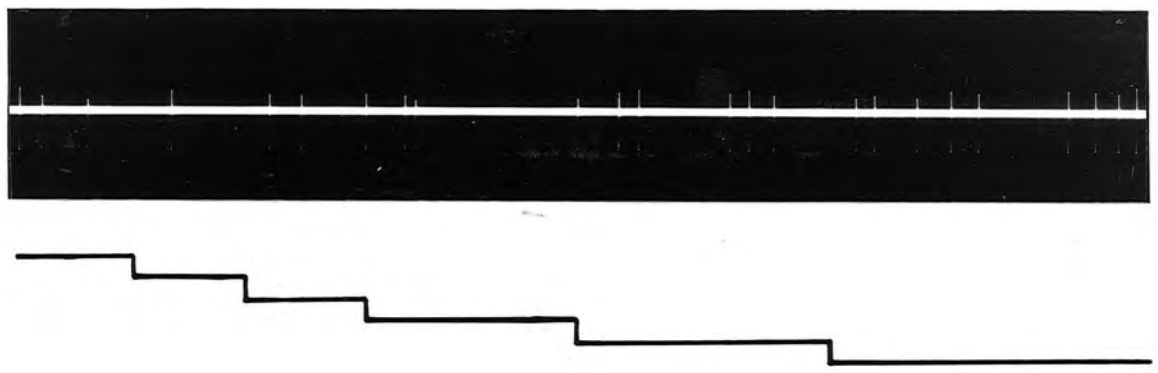

2 Sec

4·8b

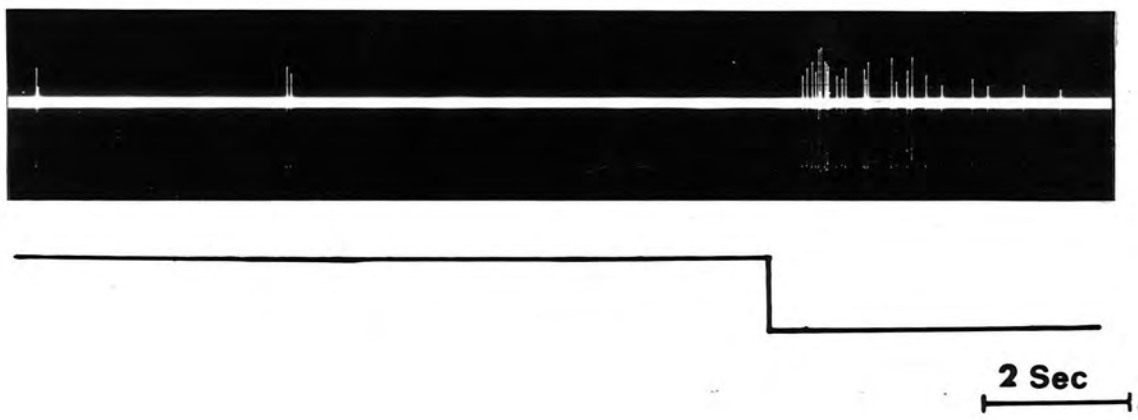

2 Sec

The two prominent types responded phasically to large objects traversing the receptive field. The most effective stimuli for evoking responses were brightening or darkening the visual field. The first of these prominent types responded not only to a small stepwise brightening of the visual field (fig. 4:8 ai) with one or two spikes, but also to a stepwise dimming with bursts of three or four spikes at the time of the actual change in the illumination (fig. 4:8 aii). During the interval between changes in illumination, some endogenous activity was apparent. These neurons habituated readily after two or three repetitions of the stimuli.

Another type of response could also be evoked which responded only to stepwise reductions of the illumination, and therefore showed similar characteristics to class IV units of an adult. However, these units had a low endogenous activity in the light (fig. 4:8 b), whereas light inhibits activity of class IV neurons in the adult.

The dimming responses of the tadpole class IV units were somewhat different from those of the adult in that they could only be evoked by large decremental shifts of background illumination. A third minor type was also present more medially and caudally in the tectum and these responses were similar to those described for Stages 46 to 49.

Stages 55 to 60

Responses were recorded from 21 animals between Stages 55 and 60. Units could be recorded in the antero-lateral pole of the tectum which produced responses which were similar to class III and IV units recorded in the adult tectum. Tadpole class III units responded phasically to the movement of a stimulus object within the receptive field or to large increasing and decreasing illumination (fig. 4:5) whereas class IV tadpole units produced a tonic discharge that only increased on the reduction of illumination (fig. 4:6). These responses were recorded at deeper levels than those recorded in tadpoles staged between 46 and 54, although depth measurements must be regarded as being inaccurate in these stages. However, in animals from Stages 55 to 60, class IV responses tended to be evoked deeper in the tectum than class III responses. Responses similar to those recorded prior to Stage 55 were recorded more caudally and medially in the tectum than the class III and IV type responses.

Stages 61 to 66

Forty-two metamorphic animals between Stages 61 and 66 were used for recording responses to visual stimuli. At these stages responses could be recorded

from the whole surface of the tectum. At the antero-lateral pole responses to illumination change were recorded at typical depths of 60 μm to 100 μm from the surface. These were class III and IV responses which were very similar to the responses recorded from adult ganglion cell terminals, however they did tend to habituate more readily. More superficial to those units, maintained responses could be evoked in response to a black disc of 16^{o} to 24^{o} moving into and being held stationary within the receptive field (fig. 4:9). The neuronal discharge was very similar to the maintained activity of an adult class II ganglion cell, although with the initial movement of the stimulus into the receptive field no high frequency activity could be recorded (compare fig. 4:4). Switching the background light off and on again caused the response to be lost. The response habituated to repeated movements of the disc along the same path, and movements along different paths eventually induced habituation. Responses of this type were rarely recorded at Stage 61, but by the end of metamorphic climax they could be recorded from a far larger area of the tectum and more regularly during a single electrode penetration. These units produced a weak sustained discharge reminiscent of class I and II terminals in the adult. The responses were difficult to study because they habituated readily. When they were first detected in stages prior to metamorphosis

Traces of Class I and II type responses evoked prior or after metamorphosis.

Fig. 4.9: A class II type response in a stage 62 tadpole was evoked by movement of a 20° black target into the receptive field (sloping bottom line). Note that the initial high frequency discharge is absent (compare with figures 4.3 and 4.4). The ganglion cell produced a maintained discharge when the target was held stationary. This maintained discharge stopped when the background light was switched off and could not be re-established at light 'on'.

Fig. 4.10: A burst of spikes was evoked by the movement of an 8° target into the receptive field of a class I type ganglion cell. When the target was held stationary a maintained response was evoked. When the background light was switched off the response stopped, and reappeared at light on. This record was taken from an animal one week after metamorphosis.

4·9

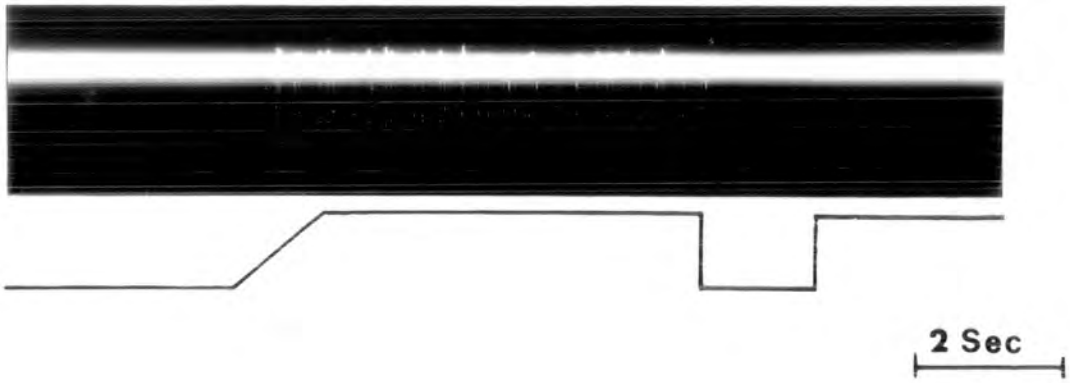

4·10

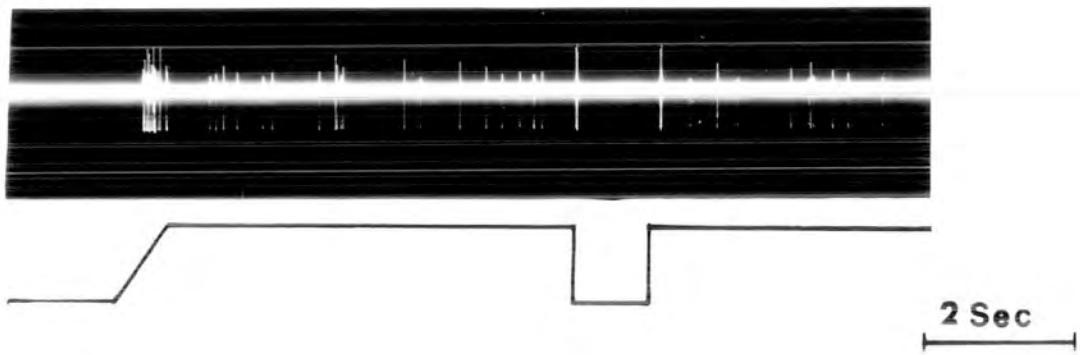

it was not possible to inhibit them by movement of a large stimulus in the periphery of the receptive field, as in adults.

Juvenile Toads

Responses were recorded from 51 animals between the completion of metamorphosis and one year of age, by which time the responses were indistinguishable from those recorded in the adult tectum in response to the same stimuli. These responses could be recorded from the most superficial part of layer 9 over the whole surface of the tectum. In the period immediately after metamorphosis, the responses appeared to be similar to those recorded in adult tecta, but class I responses were absent. Classes II, III and IV could be recorded at typical depths of 0 to 25 μm, 60 to 100 μm and 120 to 145 μm respectively. Because of the thinness of the immature tectum, present metal electrode marking techniques were too crude to give a more accurate estimation of position. With advancing age, the responses of these ganglion cell terminals became indistinguishable from those of the mature adult, and became especially resistant to habituation. Between six and twenty days after metamorphosis, class I type responses could be recorded. The movement of a black 8^{o} disc into the receptive field led to a burst of activity and if the stimulus was halted within the

Fig. 4.11: Prussian Blue Marked Electrode sites

A. Superficial recording site of a Class I terminal (arrow), marked by the Prussian Blue method.

B. Site of recording of a class II terminal (arrow), which is deeper (100 µm) than the class I terminal in A.

C. Site of recording of a class III terminal (arrow) and the dye mark is located superficial to the cell bodies of layer 8 cells at a depth of 100 µm.

D. Prussian blue marked site of recording a class IV terminal (arrow). The location of the recorded fibre is situated below the cell bodies of layer 8 at a depth of 200 µm.

Figure '8' in all figures shows the location of layer 8 in the tectum.

Calibration scale applies to figures A, C and D. Note the different calibration bar in figure B.

4·11

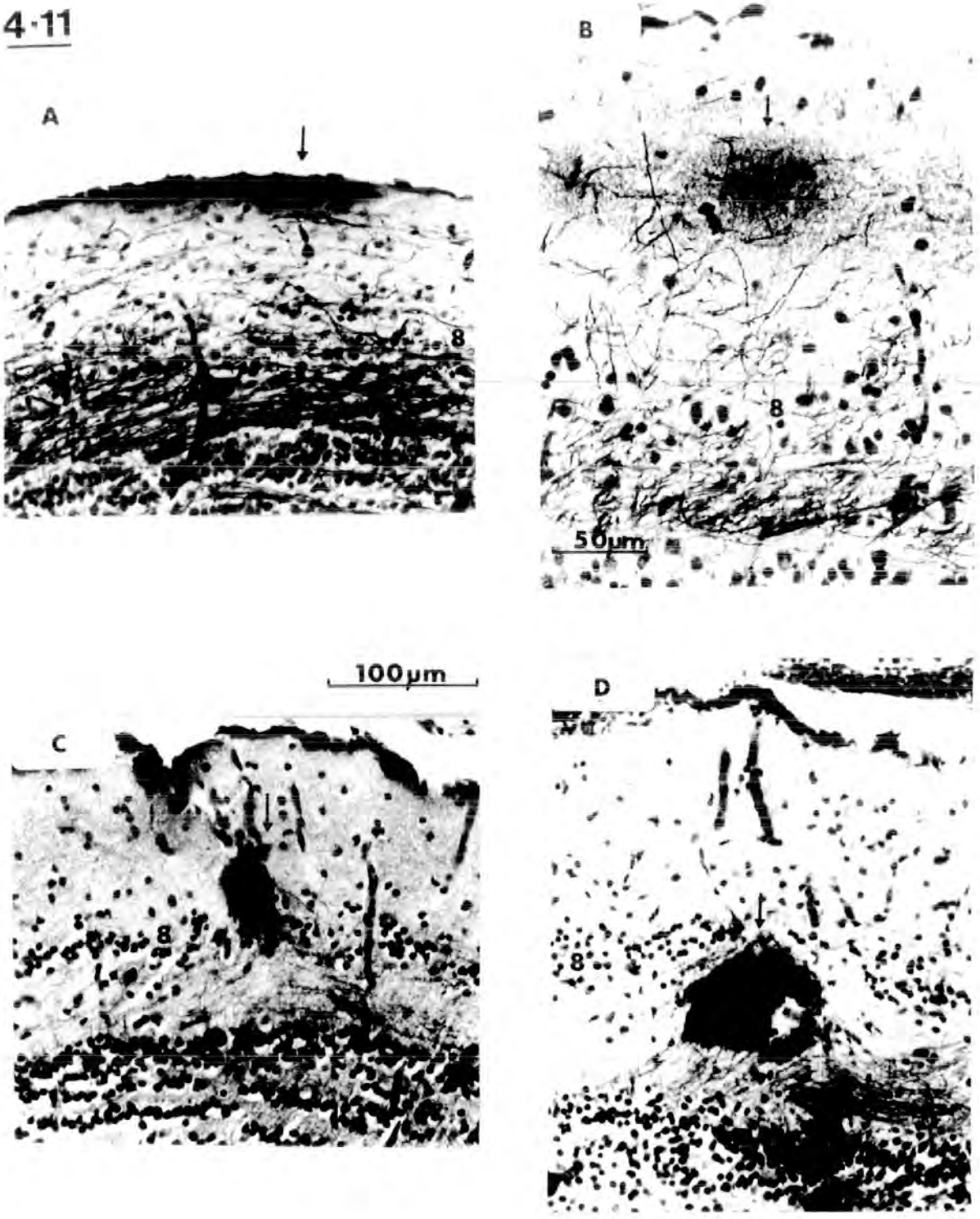

receptive field a maintained discharge was produced which was not erasible when the illumination was switched off and on (fig. 4:10). If this procedure was carried out three or four times, the response did become erasible and therefore indistinguishable from a class II response. Within the tectum, these class I responses, occurred with the same depth distribution as class II terminals. Neither type was inhibited by the movement of a large dark object into the peripheral receptive field, as in the adult (fig. 4:3). However, surround inhibition of the maintained discharge was induced in one animal two weeks after metamorphosis and occurred quite regularly in animals three weeks after metamorphosis.

Between metamorphosis and one month of age the receptive fields of class I and class II ganglion cells decreased in size from 40^{o} to 5 - 15^{o} for most of the responses recorded. Coupled with this was an increased tendency to respond to smaller stimuli, larger stimuli producing a less vigorous response. Similarly, class III and IV ganglion cell receptive fields generally reduced in size from about 40^{o} to 10 - 15^{o} for class III and from about 60^{o} to about 20^{o} for class IV. Throughout the remainder of the first six months, the responses to repetitive stimuli became more robust and the discharge rates increased. The responses were indistinguishable from those recorded in mature adults and the depth at which the units were recorded developed into the adult pattern with time.

Depth of Ganglion Cell Terminals

The first responses which can be recorded in Stage 46 tadpoles are derived from the most superficial part of the tectum to a depth of 50 μm by micrometer readings. This area cannot be differentiated into cell and plexiform layers. These responses are derived most probably from the marginal zone (Boulder committee, 1970). During the next few stages of development, neurons migrate superficially and responses can also be recorded from slightly deeper positions to approximately 80 μm. No correlation between ganglion cell type and depth can be made prior to about Stage 55. At this time responses indicate a tendency for class IV type responses to be located slightly deeper than the class III type, and this is quite marked by Stage 60 when units were recorded to a depth of 100 μm. Although class III type units could still be recorded close to the surface at this time, class IV could not. During metamorphic climax, the class II type responses were always recorded immediately below the pial surface.

After metamorphosis had been completed, typical depths for the recording of responses were 0 to 25 μm for Class II, 60 to 100 μm for class III and 120 to 145 μm for Class IV. With time the layering of the terminals from which responses could be recorded diverged even more, class III and IV being situated deeper within the tectum. At the same time, the class I and II responses diverged, but remained close to

the pia. Although this is not to imply that there were strata within layer 9 from which afferent activity could not be recorded, since there was often still some degree of overlap of terminals in the adult.

All of the depths given refer to the anterolateral pole of the tectum. In other regions, the tectum is much thinner and consequently depth values for the different classes are less.

DISCUSSION

In adult Xenopus laevis, four ganglion cell response types could be recorded from terminals at different depths within the optic tectum. The four functional response types are in agreement with the results obtained from other anuran species (see review by Grüsser and Grüsser-Cornehls, 1976). The responses conformed to the basic plan and classification devised by Lettvin et al (1959, 1961) and Maturana et al (1960). However, this classification scheme with respect to class I and II retinal ganglion cell responses has since been questioned (Keating and Gaze, 1970 a). Both types have excitatory receptive fields which are sensitive to sharp borders, and an inhibitory region which can suppress the responses generated by the excitatory field. Keating and Gaze argue that the response types are quantitatively rather than qualitatively different. However, Maturana et al (1960) reported that the sustained edge detectors (class I) respond with a longer lasting response than the convex edge detectors (class II). Keating and Gaze (1970 a), while in agreement with this observation, found the effect to be less distinct. Maturana et al (1960) reported the phenomenon of erasability, although in a

small proportion of cells a mixed response was obtained and Keating and Gaze report this feature to be even more variable.

Although variations similar to those reported by Keating and Gaze were noted in preparations of Xenopus laevis, class I and II responses could easily be distinguished using the criterion of erasability, provided that at least one minute elapsed between presentations of stimuli to the receptive field. A response was classified as class I if it was not erasible and as class II if the response was lost, regardless of the discharge rate.

Using a technique similar to Keating and Gaze (1970 a) the presence of an inhibitory surround was detected for class I and II ganglion cell responses, indicating that these response types are similar to those recorded from Ranid anurans. The layering of responses of ganglion cell axon terminals in the optic tectum of Xenopus is in agreement with previous findings of Maturana et al (1960). Gaze and Keating (1969) and Keating and Gaze (1970 b), with the class I responses found nearest to the tectal surface, whereas the deepest terminals are class IV units, occurring in layer 8 or at the junction of layers 7 and 8. Recently, however, Witpaard and ter Keurs (1975) have questioned both the classification and depth distribution of the terminals. They suggest that, the class I and II

responses should be considered as a functional group and termed contrast units; that class III response types should be differentiated into slow and fast "on-off" units; and that class IV are the "off" units. Their classification scheme is derived from response characteristics and micrometer depth readings which they have compared with the physiological data of Maturana et al (1960) and Gaze and Keating (1969), the morphological data of Potter (1969) and the data on the distribution of degenerative debris after eye enucleation (Scalia et al, 1968; Lázár and Székely, 1969). However, their micrometer depth measurements were not substantiated by lesion marking.

These studies were carried out on the Rana species, R. temporaria, R. esculenta or R. pipiens. Ewert and von Wietersheim (1974 a), using the toad Bufo bufo, found a good correspondence between the electrolytically marked electrode sites of recording and the location of degenerative debris after eye enucleation for the three layers of ganglion cell terminals in the optic tectum of this animal.

The location of the four groups of activity reported here are in agreement with the locations of synaptic activity determined by current source density analysis (Chapter 5).

Tadpoles

Numerous studies have been carried out on the developing visual system of Xenopus laevis, although most of these studies have been concerned with determining how an orderly retinotopic map of the ganglion cell terminals in the optic tectum is formed and when axial specification of this map occurs. All this work stemmed from the experiments of Jacobson (1967, 1968 a, b) which localized Stage 30 as the period for the specification of the antero-posterior axis, and prior to stage 31 for the dorsoventral axis. Investigations into the structure of the eye at this period in development have correlated the cessation of DNA synthesis in the central portion of the retina with the time of this specification (Jacobson, 1968 b) although DNA synthesis and cell proliferation continues at the periphery of the retina (Hollyfield, 1971; Straznicky and Gaze, 1971; Jacobson, 1976; Straznicky and Tay, 1977) until after metamorphosis has been completed. Electron microscopical studies indicate that, as specification of the retina occurs, gap junctions are lost (Fisher and Jacobson, 1970; Dixon and Cronly-Dillon, 1972; Hayes, 1976). They are however maintained at the periphery in the region of cell proliferation.

Only two electron microscopical studies have been carried out on the normal tadpole retina (Fisher, 1976; Tucker and Hollyfield, 1977) and the results of the two are partially at variance with each other. This is probably due to the quantitative nature of the work and may be associated with the aim of the latter work to compare light and dark reared animals.

Fisher (1976) found that, from an undifferentiated mass, the retina was produced in a very short time (28 hours from Stage 31 to Stage 40). Witkovsky et al (1976) showed that the photoreceptor outer segments start to differentiate at Stage 37 to 38 and are functional immediately as evidenced by the presence of the 'a'-wave in the electroretinogram (ERG). They found that by Stage 39, 40% of the tadpoles examined exhibited a 'b'-wave in the ERG, which indicates the presence of 'mature' synapses, involving a synaptic ribbon, synaptic vesicles and an invaginated second-order neuron (Witkovsky et al, 1976). The time-interval between the onset of the 'a' and 'b' waves of the ERG is equivalent to nine and a half hours. After Stage 40, retinal synapses differentiate rapidly, especially in the inner plexiform layer where, between Stages 40 and 46, there is an explosive increase in the number of conventional ribbon synapses and serial synapses (Fisher, 1976). Bipolar cells carry information from the outer to the inner plexiform layer, where they form ribbon synapses with amacrine and ganglion cells. In this context, it is interesting to note that the

intracellular recordings by Werblin and Dowling (1969) indicate that the outer plexiform layer is responsible for the static properties of the centre-surround receptive field, whereas transient features are attributable to the inner plexiform layer. Dubin (1970) determined that in a variety of vertebrates the numbers of ribbon synapses were relatively constant regardless of species. Fisher (1976) found in Xenopus tadpoles that, once a bipolar cell had formed ribbon synapses the number of synapses in a particular region was constant, although Tucker and Hollyfield (1977) indicate that the number of bipolar ribbon synapses decrease after the initial differentiation. Contrary to this, Fisher (1976) found that after the initial explosive formation of conventional synapses between Stages 40 and 46, conventional synapse density hardly increased between Stage 46 and a juvenile postmetamorphic age. However, if the numbers of conventional synapses are expressed in terms of inner nuclear layer nuclei, then the numbers may be seen to have increased four-fold between Stage 46 and a postmetamorphic juvenile. Concomitant with this increase in conventional synapses is an increase in serial conventional synapses which, after their initial increase, double in number. This represents a six-fold increase per inner nuclear layer nucleus. The rate of this increase in conventional synapses and serial synapses is constant. This contrasts to the results of Fisher (1972) in a study of Rana pipiens, which reports that the rate of formation

of serial and conventional synapses increases dramatically at the time of forelimb emergence. In this context the conclusion of Dubin (1970) is important since he correlates the numbers of serial and conventional synapses with the receptive field complexity of the retinal ganglion cells (e.g. in the frog and the pigeon). The increasing complexity of receptive fields presumably arises as a consequence of increased interaction between amacrine cells. The results of Fisher (1976) suggest that complex receptive fields of Xenopus are gradually produced by addition of conventional and serial synapses. The results of the present study support this since no sudden changes in receptive field organization were observed during development. On the other hand in a study of Rana pipiens (Fisher, 1972) observed that not only is there a steady increase in the numbers of synapses during larval life but there is also a sharp increase in the number of amacrine to amacrine synapses at the onset of metamorphosis. This would indicate a sharp change in receptive field complexity during development, but this possibility has yet to be investigated fully. Two studies of the responses of retinal ganglion cells (Chung, Stirling and Gaze, 1975) and of the development of the retinotectal map (Gaze, Keating and Chung, 1974) in Xenopus indicate that it is possible to record from ganglion cell terminals in the tectum as early as Stage 43, although this is not routinely possible prior to Stage 46 when the tectum is still

undifferentiated (Gaze, Keating and Chung, 1974). No investigations were carried out in animals younger than this stage in the present study.

At Stage 46, which is forty hours after the onset of the full ERG (Witkovsky et al, 1976), tectal responses of ganglion cell terminals could be evoked to "on" and "off" of light or to a large moving target, but these responses habituated readily. The large excitatory receptive fields at this stage indicate a considerable degree of convergence within the retina without the differentiation of the characteristics of class types.

By Stage 50 the responses had become less susceptible to repetitive stimulation and produced responses which were akin to those obtained from class III and IV ganglion cells in the adult. A subgroup of the units with "on-off" characteristics could be interpreted as possessing responses intermediate between those of the "on-off" and "off" response units since their responses included sensititivity to the dimming and brightening of the light stimulus.

By Stage 55, class III and IV units were present with similar properties to those of the adult although their receptive fields were larger. All the responses which could be recorded in animals up to Stage 60 showed small variation from class III and IV type response characteristics. The increase in complexity of receptive fields from Stage 46

to Stage 60 could be explained in terms of either a loss of excitatory inputs or an increase in inhibitory connexions. The number of bipolar ribbon synapses remains constant (Fisher, 1976) but since the numbers of conventional and serial synapses are increasing continually this could favour the latter explanation. Since, in the adult, class III and IV ganglion cells have simple receptive fields in comparison to class I and II, the lateral contacts between amacrine and amacrine or amacrine and ganglion cells would be expected to be smaller in number.

However, at Stage 61 not only are the responses of the Class III and IV ganglion cells becoming more refined and more resistant to habituation, but a new type of unit (Class II) appears. Habituation, lack of peripheral inhibition, size of the receptive field and size of the stimulus required to evoke a response all indicate that the number of synapses between the receptors and the ganglion cells and the lateral connexions between amacrine cells are few in number. However, as the animal ages not only does the excitatory receptive field decrease in size but a marked inhibitory area develops. Within this area, it is possible to inhibit the sustained discharge of a class I or II ganglion cell. Class I units do not appear until at least six days after metamorphosis. These two observations are in good agreement with Fisher (1976). However, in the tadpole and young toad the responses are still very immature compared to those of the adult. Fisher did not report results from the inner plexiform layer from a mature adult for comparison.

The sustained responses which could be recorded just prior to the end of metamorphic climax could be completely erased by a transient step to darkness (Lettvin et al, 1959, 1961; Maturana et al, 1960). However, within a week of the completion of metamorphosis responses were evoked which were not erasable in this way, although after a few repetitions of the stimulus, the secondary response was lost, indicating that the basis for the erasability is labile. The second point to arise from this observation is that the class I type responses possibly differentiate from those of class II. It would be interesting to determine whether any structural basis could be found for the non-erasability of class I units.

After metamorphosis, the properties of the ganglion cell receptive fields do not cease to change. The transient response characteristics of class III and IV units in juvenile Xenopus are similar to those in adults, but the peripheral inhibition is underdeveloped and only appears with time. Chung et al (1975) suggest that the inhibitory surround of class I and II units expands to include the entire retina in mature Xenopus. Daw (1968) found that the inhibitory receptive fields of goldfish retinal ganglion cells may extend to cover the remainder of the visual field. It is interesting to note that the appearance of class II inhibitory fields after metamorphosis coincides with the lack of erasability in class I units.

Both these points indicate the formation of extensive lateral connexions at this time.

Chung et al (1975) have suggested that the sustained responses which appear at metamorphosis may be related to the appearance of a new type of ganglion cell in the retina. The origin of this new type of ganglion cell is unknown, but there are three possibilities: (i) the cell has differentiated from an undifferentiated cell, (ii) the cell has migrated laterally within the retina and differentiated, or (iii) the cell has differentiated further from ganglion cells which are already present prior to metamorphosis. The first possibility cannot be discounted. Hollyfield (1971) found possible evidence for cell migration within the tadpole retina and has shown that extensive mitosis occurs within the inner nuclear layer. He suggests that while some cells may differentiate and become neuronal, the majority are either neuroepithelial germinal cells, glioblasts or both. The results from Xenopus are unlike those obtained from his study of Rana pipiens (Hollyfield, 1968) in which he found extensive migration of retinal cells. The third possibility has been suggested by Chung et al (1975) on the basis of the evidence that at the time of the appearance of these new functional types, their evoked responses had features in common with those of the class III type.

Similar studies to those reported here have been carried out on four species of Rana, R. temporaria, R. catesbeiana, R. pipiens and R. clamitans (Reuter, 1969; Pomeranz and Chung, 1970; Pomeranz, 1972). However, there is some confusion between these workers, since Reuter (1969), in a limited study on tadpoles, recorded from a number of units which were similar to class I fibres, but from only one unit similar to a class II fibre. However, Pomeranz and Chung (1970 a) and Pomeranz (1972), in a far more comprehensive study, found that class II responses could be recorded from the tadpole tectum, although from a restricted area, and that class I responses were absent. Chung et al (1975) in their study of Xenopus tadpoles avoid this problem by referring to both class I and II responses as 'sustained' units on the basis of the comments of Keating and Gaze (1970) who question the distinctness of the two populations. Chung et al (1975) found that sustained units appeared only at metamorphic climax, in agreement with the present results. One difficulty arising from previous work on Rana (Reuter, 1969; Pomeranz and Chung, 1970; Pomeranz, 1972) is that no mention is given of either the stage or age of the tadpoles from which responses were evoked. If recordings were made at the time of forelimb emergence, when the numbers of serial and conventional synapses increase

rapidly (Fisher, 1972), then the presence of sustained units (either class I or II) would be expected. However, on the basis of the results reported here, it is likely that had the studies involved the use of younger tadpoles, no sustained units would have been detected.

Pomeranz (1972) concludes that because class II responses can be recorded in tadpoles and that the fibres transmitting class I and II information are of a similar size, then the absence of class I responses in tadpoles is not a technical artifact. Using similar reasoning, Maturana et al (1960) and Chung, Bliss and Keating (1974) have stated that class I and II responses are both mediated by unmyelinated fibres (see also Chapter 5). Since responses from retinal ganglion cell axons can be recorded in the tectum of Stage 46 tadpoles, and it is known (see Chapter 1) that all the axons within the optic nerve at this time are unmyelinated, it is unlikely, therefore, that class I and II responses in tadpoles would not have been selected by the electrodes used in this study.

Additional evidence regarding further maturation of the visual system after metamorphosis has been provided from studies of the prey-catching behaviour of the midwife toad Alytes obstetricans (Ewert, 1977; Ewert and Burghagen, 1977) and Salamandra salamandra (Himstedt et al, 1976). Ewert (1977) and Ewert and Burghagen (1977) found that

directly after metamorphosis Alytes showed visual angular size constancy in its prey selection, whereas six months after metamorphosis the individuals showed true size constancy selection. Ewert (1977) also reports that the prey catching behaviour of six months old Alytes involves the preferential selection of worm-like prey dummies, in contrast to the immediately postmetamorphic toad whose prey catching activity is determined purely by the visual angular size of the stimulus, not by its real size or form. It is known that extensive interactions occur between the caudal thalamus and the optic tectum in determining prey catching or predator avoidance behaviour (Ewert, 1970; Ewert and von Wietersheim, 1974 b, c; Ewert et al, 1974). Himstedt et al (1976) obtained similar results from the urodele Salamandra salamandra and found that the prey catching response of the larvae depended on the size of the prey dummy in either the horizontal, vertical or both axes. However, after metamorphosis, their behaviour changed in respect to prey dummies which had a vertical component and by eight to ten months, all the salamanders responded purely to worm-like objects, with an elongation in the horizontal plane and the direction of movement. Presumably the responses of central neurons change during this period and it would be interesting to compare the responses of retinal ganglion cells prior and subsequent to metamorphosis in this animal.

Depth of ganglion cell terminals
in the optic tectum

The distribution of ganglion cell terminals in the optic tectum of the adult Xenopus determined by electrophysiological methods are in good agreement with those derived from other anurans (Maturana et al, 1960; Gaze and Keating,1969; Keating and Gaze 1970 b; Ewert and von Wietersheim, 1974 a; Grüsser and Grüsser-Cornehls, 1976; but also see Witpaard and ter Keurs, 1975). Interpretation of the anatomical distribution of terminals in the tectum is somewhat dependent on the histological method used. Three or four layers may be distinguished according to whether the distribution has been mapped by Fink-Heimer degeneration, autoradiographic labelling or horseradish peroxidase incubation (for review see Scalia, 1976). The location of ganglion cell terminals determined by unit recordings and subsequent histological localization is an good agreement with the results obtained by current source density analysis (see Chapter 5).

The electrophysiological localization of terminal distributions in tadpoles was not precise because the tectum is thin and soft and accurate depth measurements were difficult to make because of dimpling. The use of the Prussian blue marking technique was precluded by the inaccuracy of the method due to the size of the spot relative to the thickness of the tectum.

The development of the laminar arrangement of optic afferents in the tectum is a complex process. In tadpoles prior to Stage 55 the optic afferent layer is thin and lamination cannot be resolved. After Stage 55, responses of class III and IV terminals can be recorded at different depths. At metamorphic climax and shortly afterwards, class I and II terminals can be recorded most dorsally in the tectum and, with further growth, the separation of terminal layers becomes more distinct.

CHAPTER V

Innervation of the adult *Xenopus* tectum by optic afferents

INTRODUCTION

Intracellular electrical recording can yield precise data concerning information processing within neuronal elements. It is often impossible, however, to make stable intracellular recordings from cells in the central nervous system and in such cases it is necessary to use extracellular potentials as indicators of neuronal activity (Nicholson and Freeman, 1975). This applies to the amphibian tectum where the vast majority of the cells have a diameter of approximately 8 μm.

Deductions about the site of synaptic action and the site of the postsynaptic cell bodies may be made from an analysis of the amplitude and polarity of extracellular potential waves at various depths in a penetration through a neuronal ensemble. This is only possible if the neurons form a population whose constituent somata and dendrites are organized in a similar manner. In the case of the tectum, most somata are located in cellular sheets, and the dendrites of the somata are radially orientated. Field potential analytical methods enable determination of some of the interconnections and interactions within a neuronal population. The method of current source density analysis provides a significant improvement in

the ability to resolve the location and time course of neuronal activity, compared with the traditional methods of analysing extracellular potentials (Hubbard et al, 1969; Freeman and Nicholson, 1975).

Extensive work has been carried out on the optic tectum and its optic afferent innervation in amphibians, including both structural (reviews by Székely and Lázár, 1976; Scalia, 1976) and physiological (review by Grüsser and Grüsser-Cornehls, 1976) studies. Most of the work to date has produced data only on the properties of ganglion cells (conveniently recorded in the tectum) and on the morphology of the neuronal components. Very little work has been carried out on the interaction of elements, their circuitry and their properties, the notable exceptions being reports by Chung, Bliss and Keating (1974) and by Ewert and his coworkers (Ewert and von Wietersheim, 1974 b, c; Ewert, Hock and von Wietersheim, 1974). Chung and colleagues carried out a study similar to this report, in Rana, and Ewert's group have been stydying the responses of neurons within the tectum and their interaction with thalamic neurons.

Relatively little attention has been paid to the location and properties of the synapses of optic afferent fibres and the location of their postsynaptic neurons. Chung, Bliss and Keating (1974), using laminar profile analysis in Rana pipiens, located three synaptic layers superficial to layer 8 cells and one synaptic layer immediately beneath this stratum.

In this report the technique of current source density analysis was employed on the optic tectum of Xenopus in an attempt to gain information concerning the location and properties of afferent synapses and their postsynaptic neurons using responses to an electrical stimulus applied to the contralateral nerve.

METHOD

A. PREPARATION OF THE ANIMAL

Twenty-two adult Xenopus laevis were used in this study. The brains were exposed as described in Section B of the General Methods. The forebrain was removed by suction and a small hole was made in the sclera of the eye or in the thick connective tissue sheath of the intracranial portion of the optic nerve to facilitate entry of a stimulating electrode. The preparation was immobilized with an injection of 2 to 12 mg of succinyl choline into the dorsal lymph sac. The animal was covered by a fresh medical wipe tissue and was placed in a shallow bath containing Niu-Twitty solution. Cotton threads soaked in Xylocaine (Astra) were placed along all cut edges, although great care was taken to avoid contact with either the optic nerve of the brain. Contact of electrolytes with the optic tectum was also avoided since this reduced the size of evoked potentials (Nicholson and Llinás, 1971; Klee and Rall, 1977). All surfaces exposed to the air were covered with paraffin oil. All animals were allowed to recover from the anaesthetic for half an hour prior to the start of the recording procedure.

Sixteen Rana pipiens and R. temporaria were also used in this study for comparison. These animals were prepared in a similar manner, but were immobilized with varying amounts of d-tubocurarine (0.05 - 0.4 mg) depending on the time of year.

At the termination of each experiment, the animal was decapitated and the head was fixed for at least one day in 0.9% saline containing 10% formaldehyde. The brain was removed, dehydrated, embedded and sectioned, and all sections were stained either with Cresylecht Violet or by the Klüver-Barrera method for cell bodies and fibres, as described in section C of the General Methods.

B. ELECTRODES

Four types of electrodes were used in this study; two for stimulation and two for recording purposes.

Stimulating Electrodes

Woods Metal-in-glass or stainless steel electrodes were used to deliver stimulating pulses and were manufactured as described in the Methods section of Chapter 4.

Recording Electrodes

One hundred micron diameter silver/silver chloride wire electrodes were used to record surface evoked potentials and were used mainly to optimize the position of the stimulating electrode. Glass micropipettes were used to record not only the surface potentials but also potentials at depth and any associated spike responses. The electrodes were manufactured from two millimeter external diameter borosilicate glass tubing (Dial Glassworks, Stourbridge, Worcs.). In the later experiments glass tubing containing an integral glass rod was used. The glass was cut into convenient lengths and was washed in warm water containing 'Quadralene' detergent. After the glass was rinsed several times in tap and then distilled water it was placed upright and allowed to dry in an oven at 60^{o}C.

The microelectrodes were made using a C.F. Palmer horizontal puller. The electrodes were filled by methanol under reduced pressure. The methanol was later displaced by transferring the electrodes to distilled water for at least half an hour. The electrodes were then transferred to a solution of either 2 M or 4 M sodium chloride overnight to allow adequate diffusion of the electrolyte into the electrode tip. The electrolyte solutions were filtered through a Millipore filter (0.45 μm) prior to use. The electrode tips were broken

carefully to give a diameter not greater than 2 μm. The electrodes which contained an integral glass rod were filled by direct injection of the electrolyte solution using a syringe and a fine needle inserted as far as the shoulder of the micropipette. The solution was carried to the electrode tip by capillarity. More commonly, the electrolyte solution used contained basic dyes for the purpose of marking the recording sites in the tectum. Fast Green FCF or Pontamine Sky Blue 6 BX were used and both were obtained from George T. Gurr, London. The solution of Fast Green FCF was made by adding excess dye to a warm (40°C) 2 M sodium chloride solution and then filtering. The Pontamine Sky Blue was made as a 4% (w/v) solution in 0.5 M sodium acetate (Potter et al, 1966; Hellon, 1971) and hydrochloric acid was added until a pH of 7.7 was obtained. These electrodes had resistances of either 3 - 8 MΩ or 2 - 5 MΩ (Thomas and Wilson, 1965; Hellon, 1971).

C. RECORDING PROCEDURE

Constant voltage negative pulses, usually of 50 μsec duration, were delivered by metal-in-glass or stainless steel electrodes either to the optic nerve head or to the optic nerve. The position for the stimulating electrode was chosen so that the maximum amplitude of

the tectal evoked potential in response to a 20 V 0.1 msec pulse was obtained. The indifferent stimulating electrode was placed on the cornea. The distance between the stimulating and recording electrodes was measured using a microscope with a calibrated eye-piece graticule. Shielded electrode holders were used throughout to minimize the stimulus artifact. Pulses of up to 90 V were produced as described in the Methods section of Chapter 3 and were delivered from a stimulus isolation unit. The evoked potentials were led to a high input impedance amplifier of 1,000 times gain, either DC or occasionally AC coupled with a time constant of two seconds. The output was displayed on a triggered Tektronix 502 A oscilloscope and single frame photographs were taken with a Nihon-Kohden PC-2A oscilloscope camera. Responses from sequential depths of the tectum and other events of interest were photographed.

Recordings in a depth sequence were usually made as the electrode was withdrawn, as the tectum often dimpled during penetration. Recordings were regarded as valid only if the micrometer measurement at the tectal surface was the same before and after a penetration. Dye spots were deposited by passing a direct cathodal current of 7.5 μA for eight minutes for the Fast Green FCF dye and for two minutes for the Pontamine Sky Blue dye. Successful marking could be observed during current flow since the tectum is semi-transparent.

D. DATA COLLECTION AND COMPUTATIONAL METHODS

Responses were recorded at sample intervals of 10 μm since it has been suggested that sample points must be spaced at intervals of less than 50 μm for accuracy in calculating the second spatial derivative (Freeman and Nicholson, 1975). The evoked potential was measured at a fixed latency. This was not necessarily at the peak of the evoked wave since the sites of current sources and sinks are dependent on the rate of change in the voltage field.

Calculation of the current density in one dimension under ideal conditions can be carried out using the following rationale:

I_x (t) is the current density at time t under ideal conditions in a direction normal to the surface of the tectum and may be expressed in terms of the first and second derivatives of the potential at a given depth, as follows:

$$I_x(t) = \frac{\delta^2 V(t)}{\delta x^2} \cdot \sigma x + \frac{\delta V(t)}{\delta x} \cdot \frac{\delta \sigma x}{\delta x} \qquad (1)^*$$

* Freeman and Stone (1969)

where V(t) = the potential of time (t) with respect to a distant electrode

and σx = the conductivity of the tissue in the x direction

Let V_1, V_0 and V_2 be three consecutive potential values at time t in a depth profile such that:

$$V_1 = V(x - \Delta x, t)$$

$$V_0 = V(x, t)$$

$$V_2 = V(x + \Delta x, t)$$

and let σ_1 = the conductivity for the interval $(x - \Delta x)$ to x

and σ_2 = the conductivity for the interval x to $(x + \Delta x)$

From the definitions of the first and second derivatives:

$$\frac{\delta V(t)}{\delta x} \simeq \frac{V_2 - V_1}{2\Delta x}$$

$$\frac{\delta^2 V(t)}{\delta x^2} \simeq \frac{(V_2 - V_0) - (V_0 - V_1)}{\Delta x^2}$$

$$\frac{\delta \sigma_x}{\delta x} \simeq \frac{\sigma_2 - \sigma_1}{\Delta x}$$

substituting into equation (1):

$$Ix(t) \simeq \left[\frac{(V_2 - V_0) - (V_0 - V_1)}{\Delta x^2}\right]\left[\frac{\sigma_1 + \sigma_2}{2}\right] + \left[\frac{V_2 - V_1}{2\Delta x}\right]\left[\frac{\sigma_1 - \sigma_2}{2}\right]$$

$$\simeq \frac{\sigma_2 (V_2 - V_0) - \sigma_1 (V_0 - V_1)}{\Delta x^2} \qquad (2)$$

A simple graphical interpretation is permitted by equation (2) to convert potential depth profiles into net current density profiles when the conductivity values are known. The degree of accuracy of the values of $I_x(t)$ will be inversely proportional to the length of Δx. With constant resistivity, equation (2) reduces to the following:

$$\frac{I_x(t)}{\sigma} \simeq \frac{V_1 + V_2 - 2V_0}{\Delta x^2} \qquad (3)$$

Equation (3) permits the conversion of potential depth profiles into 'second-derivative' curves that are directly proportional to $I_x(t)$ at every point under ideal conditions and constant conductivity. In a single penetration the potential values measured at a fixed latency were plotted for depth intervals af 10 μm and a depth profile was obtained by drawing a smooth curve by eye through the plotted points. The smooth curve reduced the scatter of the 20 μm increment values used to calculate the second spatial derivative from equation (3) .

Figure 5:1 illustrates schematically the experimental basis of laminar field potential analysis. In figure 5:1 a, a negative square wave constant voltage electric shock is delivered to the optic nerve at time t_o and this evokes extracellular field potentials in the tectum which vary in both form and polarity according to depth. The ampli-

Fig. 5:1 Schematic diagram illustrating the theoretical basis of laminar field potential analysis

(a) The extracellular voltage waveforms produced by current flow generated in a postsynaptic population of neurons are recorded at various depths in the neurone field. The postsynaptic activity is produced in response to a stimulus applied (at time t = 0) to the presynaptic fibre population. The amplitude and polarity of the evoked wave is measured at a fixed time (t_1) after the stimulus.

(b) The amplitude and polarity of the evoked waveform at time t = t_1 is plotted in a depth profile and a smooth curve fitted by eye to the points.

(c) The second spatial derivative of the smooth curve of voltage/depth profile is calculated by the procedure described in the text and reveals the relative magnitude and direction of transmembrane current.

(c) Current enters the postsynaptic membrane and is distributed to the remainder of the idealized neuron. A small current leaks out of the dendrites but the major portion leaves from the cell body. The outward current is divided and flows either radially to the synapse or via an external current path. An equivalent circuit diagram consists of two potentiometers. The position of the wipers correspond to the locations of the recording and indifferent electrode. (Redrawn from Chung, Bliss and Keating, 1974.)

5·1

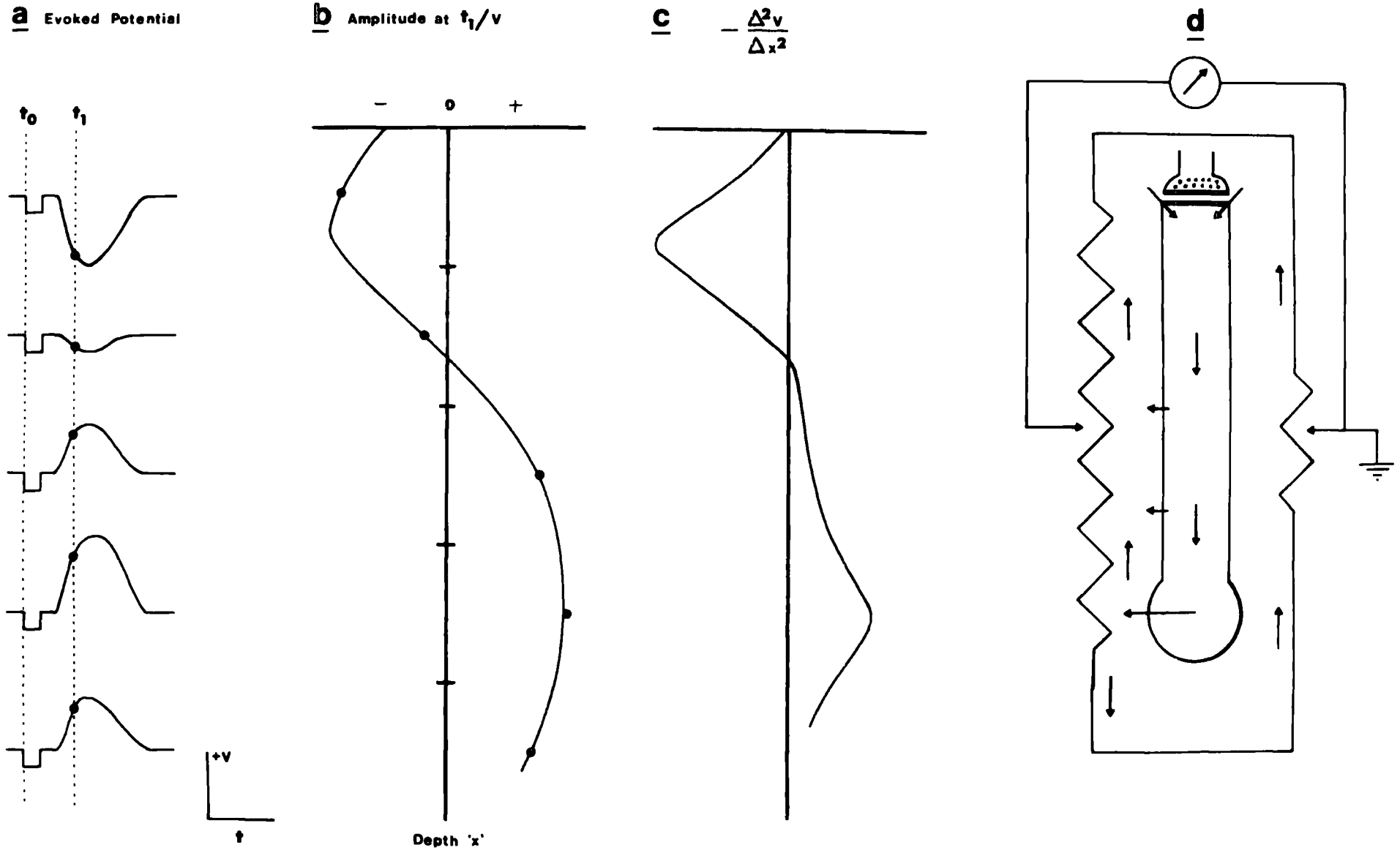
a Evoked Potential
t_0
t_1
+V
t
b Amplitude at t_1/V
−
0
+
Depth 'x'
c $-\frac{\Delta^2 V}{\Delta x^2}$
d

tude of these evoked potentials are measured at a constant time interval of t_1 and a depth profile is constructed by plotting these values as a function of successive depths (fig. 5:1 b). The relative direction and magnitude of the transmembrane current can be calculated from these values using the second spatial derivative which is shown in figure 5:1 c. Figure 5:1 d shows an idealized neuron of the optic tectum. At the synaptic region, current is absorbed from the surrounding medium when the dendrite is depolarized. The intracellular current flows along the dendrite, and a small amount leaks to the outside through the dendritic membrane. The majority of this current passes to the cell soma and then outwards, since in this region the space constant decreases abruptly. The principal outward current passes from the cell soma directly to the synapse, although a second minor outward current takes an external path via the indifferent electrode.

RESULTS

A. PHYSIOLOGY

The results illustrated and discussed here are taken from adult Xenopus, although depth profiles obtained from Rana pipiens are also presented for comparative purposes.

Stimulation of the optic nerve of adult Xenopus with brief electrical stimuli produced three distinct negative waves at the surface of the contralateral tectum (fig. 5:2 a, b). These waves have been labelled m_2, u_1 and u_2 in accordance with the terminology of Chung, Bliss and Keating (1974). Occasionally a small negative wave with a very short latency, termed m_1, could be recorded at the tectal surface. This wave was often obscured by the stimulus artifact in many recordings. As the recording electrode penetrated the tectum, the m_2 wave became more distinct with the m_1 wave superimposed on the initial negative going phase of the m_2 wave (fig. 5:2 c). The relationship between the m_1 and m_2 waves is shown more clearly in figure 5:2 d which is a recording made from a depth of 190 μm in the tectum, at which depth

Fig. 5:2 Extracellular potential waves recorded in the optic tectum in response to stimulus applied to the contralateral optic nerve

(a) Recordings made at the surface of the tectum reveal the presence of three distinct waves of negative polarity. These waves are labelled m_2, u_1 and u_2 according to their respective latencies (see text).

(b) Same recording conditions as in (a) except that the time scale has been expanded and the stimulus voltage has been reduced (to minimise stimulus artefact) in order to reveal the relative latencies and waveforms of the m_2 and u_1 waves.

(c) Records of m_1 and m_2 waves made at a tectal depth of 190 μm. The amplitudes of these two negative waves is maximum at this depth whereas the amplitudes of the 'u' waves are small (compare this record with record (a)). The latencies and waveforms of the 'm' waves is more clearly revealed on the faster time display of record (d).

(e) and (f) Record (e) shows the tectal responses (labelled 1 and 2) to a stimulus of the ipsilateral optic nerve (e) compared with those evoked by stimulation of the contralateral nerve (f).

Time and voltage scales are indicated in each record. In all records, positive polarity is displayed upwards.

5·2

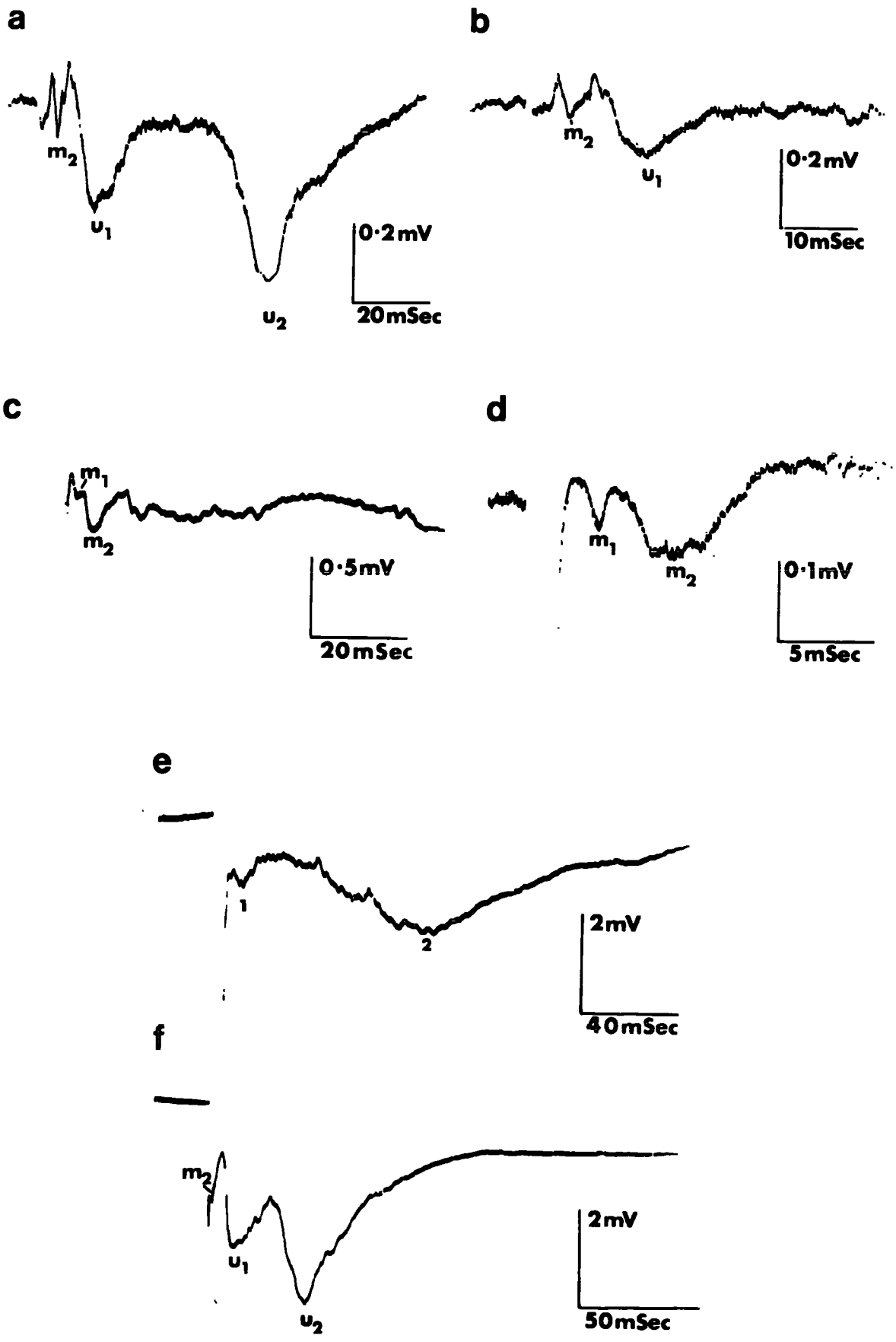
a
m2
u1
u2
0·2mV
20mSec
b
m2
u1
0·2mV
10mSec
c
m1
m2
0·5mV
20mSec
d
m1
m2
0·1mV
5mSec
e
1
2
2mV
40mSec
f
m2
u1
u2
2mV
50mSec

the amplitudes of the 'm' waves are near maximal (see depth profiles). The latencies of the peaks of the waves in figures 5:2 a and 5:2 b are 6, 16 and 61 msecs for the m_2, u_1 and u_2 waves respectively. The responses from a different preparation, shown in figure 5:2 d, have latencies of 4 and 8 msec for the m_1 and m_2 waves. Typical values for the latencies of the peaks are 3 - 4 msec, 6 - 8 msec, 12 - 16 msec and 50 - 60 msec for the m_1, m_2, u_1 and u_2 evoked potentials respectively. Similar responses were obtained in the Rana sp. used.

Figures 5:2 e and 5:2 f show the responses to the same stimulus recorded from the surface of the ipsilateral and contralateral tectum respectively. The ipsilateral response consisted of a complex wave in which a short latency peak (7 msec) and a longer latency wave (80 msec) were prominent (fig. 5:2 e). The wave, comparable in latency to the m_2 wave of the contralateral tectum is superimposed on the stimulus artifact, whereas the longer latency ipsilateral response is clearly evident. Since the ipsilateral response could not be distinctly characterized into a number of components in the same way as the contralateral response this pathway was not studied further.

The contralateral response shows the m_2 wave superimposed on the stimulus artificat and two clearly evident 'u' waves with latencies of 5, 12 and 40 msec respectively.

Stimulus Strength - Tectal Response Characteristics

Figure 5:3 shows the characteristics of the m_1 and m_2 waves recorded at a depth of 240 μm in response to stimuli of increasing intensity applied to the optic nerve. These results are represented graphically in figure 5:4. A stimulus of 4 V elicited no response from the tectum (fig. 5:3). A 5 V stimulus produced a small negative deflection which increased in size in response to a 6 V stimulus. The latency of this wave indicated that it was an m_1 wave. At 6 V, a second wave appeared the latency of which was indicative of the m_2 wave. The m_1 wave amplitude saturated with stimuli of 12 to 14 V, whereas the m_2 wave amplitude continued to increase up to a maximum for a 20 V stimulus (figs. 5:3 and 5:4).

Figure 5:5 shows the stimulus strength-tectal response characteristics for 'u' waves recorded from the surface of the tectum. These are represented graphically in figure 5:4. A stimulus of 6 V evoked no response from the tectum, but a wave with a latency of 20 msecs was produced by a stimulus of 10 V which can be identified on the basis of its latency as the u_1 wave. At 15 V, the tail of this wave was distorted by the overlapping u_2 wave. An 18 V stimulus evoked waves of larger amplitude. With stimuli of 20 V the u_1 wave amplitude was maximum but the u_2 wave

Fig. 5:3 Stimulus voltage - contralateral tectal response characteristics 'm' waves

Responses recorded in the tectum at a depth of 240 μm. A 5 V stimulus produces a small negative deflection at a latency which indicates an m_1 wave. A 6 V stimulus evokes a second wave with a longer latency which is indicative of an m_2 wave. The m_1 wave increases in amplitude with increasing stimulus voltage and saturates at 12-14 V. The m_2 wave also increases in amplitude with increasing stimulus voltage and is saturated by a stimulus of 20 V. See figure 5:4 for graph of results. Time and voltage scales are indicated in each record. In all records, positive polarity is upward. The figures below the traces are the voltages applied.

5·3

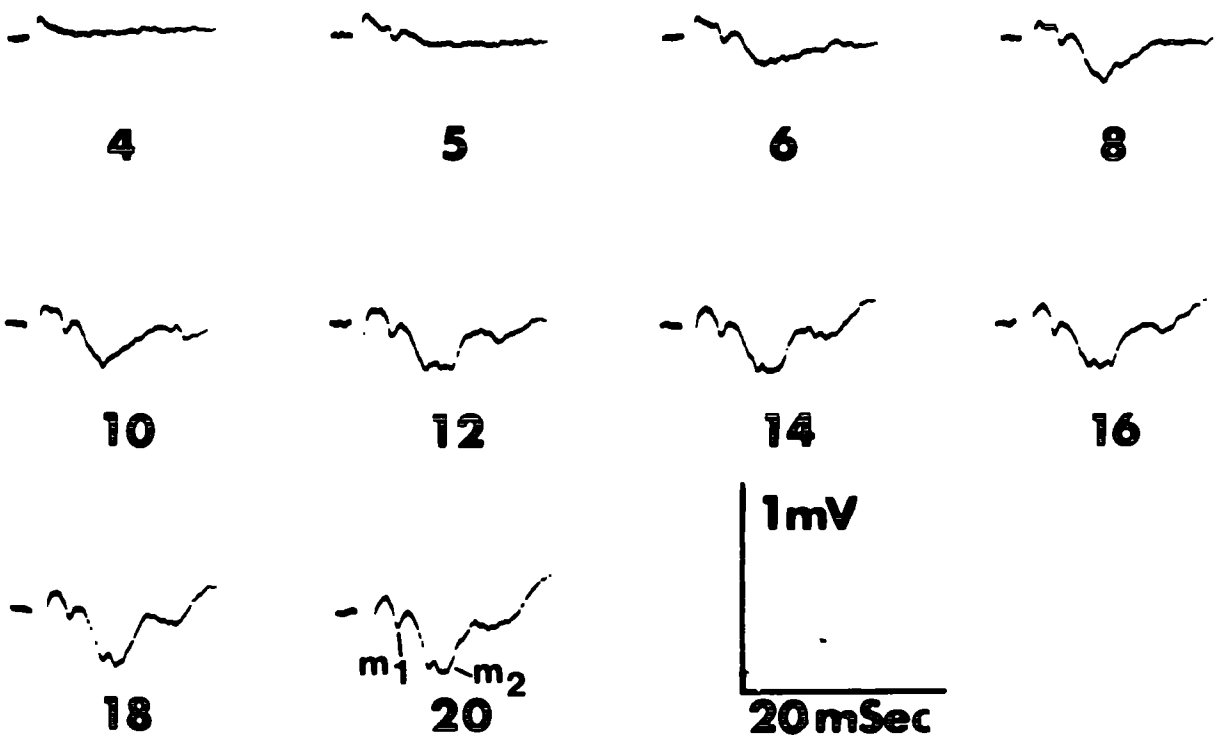

Fig. 5:4 Graph of stimulus strength - tectal response characteristics

The traces from which measurements have been taken for the graph are shown in figure 5:3 (m_1 and m_2 waves) and figure 5:5 (u_1 and u_2 waves). The threshold of the m_1 wave is 5 V, with increasing voltage the wave increases in amplitude and becomes maximal at 12-14 V. The threshold of the m_2 wave is slightly higher (6 V). With small increments of stimulus voltage the amplitude of the m_2 wave increases rapidly and is saturated with a stimulus of 20 V. The 'u' waves are evoked by higher voltages. The u_1 wave can be evoked by 10 V stimulus, and the u_2 wave by a stimulus of 13 V. Both waves increase in amplitude rapidly with small increases (1 V) of stimulus intensity. The u_2 wave is saturated by a stimulus of 20 V. However, the u_2 wave continued to increase in amplitude and is saturated with a stimulus of about 40 V.

While varaitions in the voltage level at which thresholds and saturation are evident in different experiments, the relative voltage values for threshold and saturation are constant.

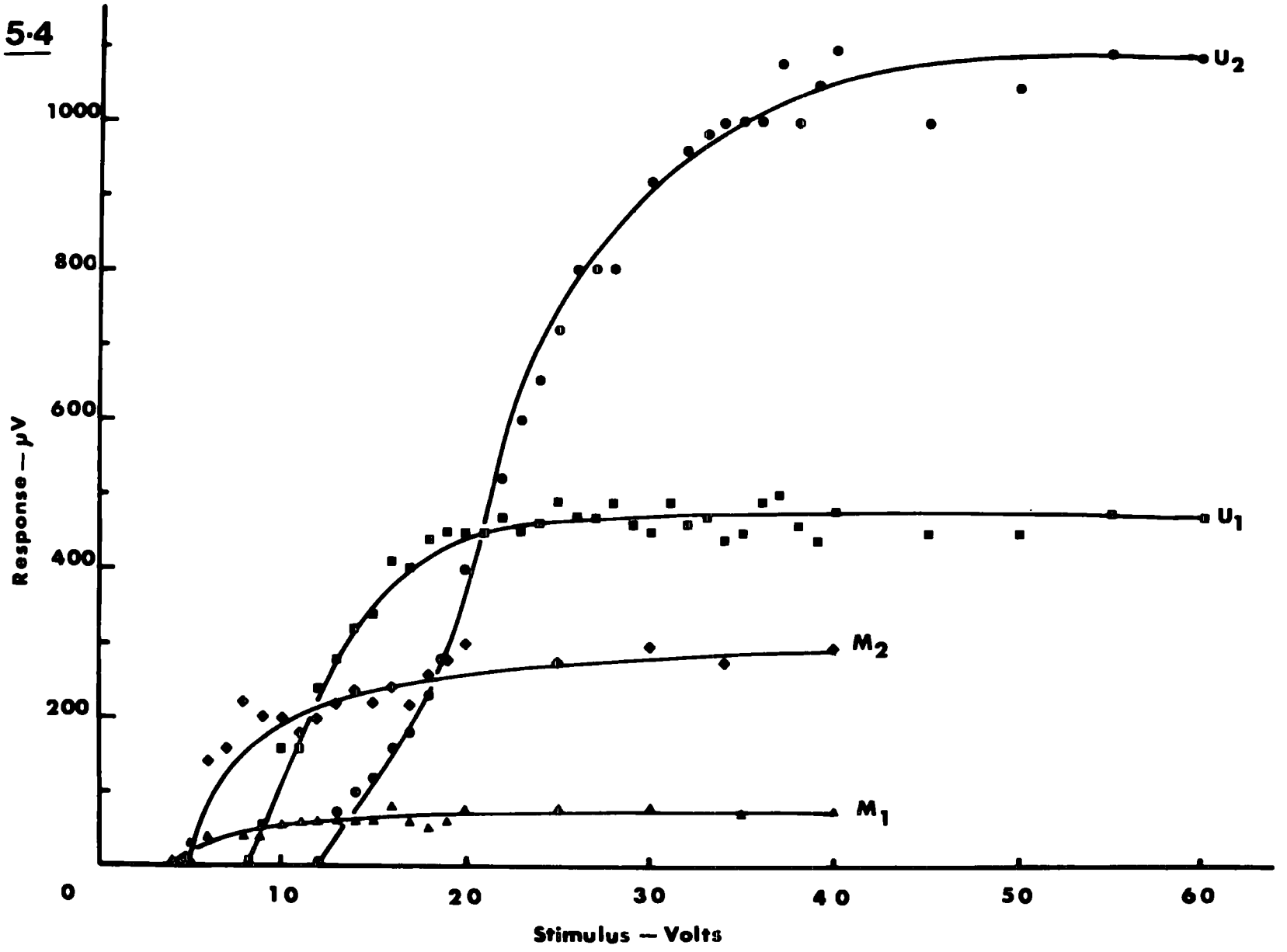
5·4
1000
800
600
400
200
0
Response — μV
10
20
30
40
50
60
Stimulus — Volts
U2
U1
M2
M1

Fig. 5:5 Stimulus voltage - tectal response characteristics 'u' waves

The effect of increasing stimulus voltage on the tectal response was recorded at the surface of the contralateral tectum. A 10 V stimulus evokes a u_1 wave, and a stimulus of 18 V evokes also a longer latency u_2 wave which is superimposed on the tail of the u_1 wave. The u_2 wave was saturated by a stimulus of 20 V. The u_1 wave continued to increase in amplitude with increasing stimulus voltage until a stimulus of 40 V at which saturation occurred. See figure 5:4 for graphical representation of the results. Time and voltage scales are indicated in each record. In all records, positive polarity is upward. The figures below the traces are the voltages applied.

5·5

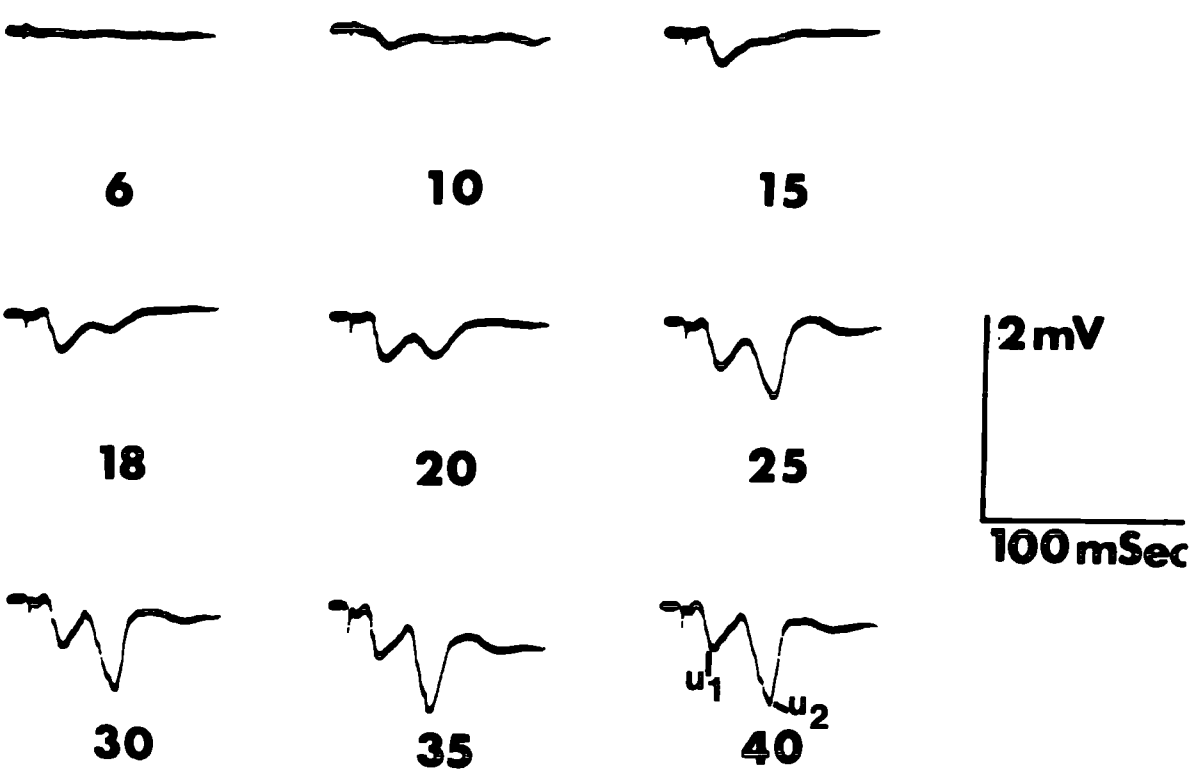

continued to increase in amplitude until a stimulus of 40 V at which amplitude saturation occurred. The results presented here while not quantitatively applicable to all experiments, since stimulating and recording conditions vary, are qualitatively similar. With increasing stimulus intensity the m_1 wave always appeared prior to the m_2, and both of these waves had lower threshold characteristics than the 'u' waves. The u_1 wave was always activated by lower voltage than the u_2 wave.

Analysis of Presynaptic and Postsynaptic Events

The m_2, u_1 and u_2 waves were often preceeded by brief monophasic, diphasic or triphasic wave forms. These low amplitude deflections were usually recorded at a tectal depth for which evoked waves had their maximum amplitude. An example of a triphasic waveform preceeding the m_2 wave is exhibited in figure 5:6 a. This brief wave has a latency of 2 msec, a duration of 0.8 msec and the differences between the latencies of this wave and the peak of the large monophasic negative wave is 4 msec. Figures 5:6 b and 5:6 c show similar small waveforms which preceed the large negative deflections. The latency, duration and difference in the latencies are 6, 2 and 8 msec for the u_1 wave and 25, 2 and 10 msec for the u_2 wave.

Fig. 5:6 (a) A triphasic, short latency (2 mSec), short duration (0.8 mSec) deflection (labelled with an open triangle) preceeding an m_2 wave.

(b) A u_2 wave preceeded by a brief (2 mSec duration) negative-going deflection (labelled with an open triangle).

(c) A u_1 wave preceeded by a brief (2 msec duration) diphasic waveform (open triangle).

(d) and (e) Records of a u_1 wave preceeded by a diphasic spike potential (open triangle in (d)). The recordings in (e) were taken at 1, 3, 5 and 8 seconds after the start of a stimulus pulse train at a frequency of 20 Hz and 12 seconds duration. Note that while the u_1 wave decreases in amplitude throughout the duration of the pulse train the diphasic potential shows little variation in amplitude. Record (d) is the control response to a single stimulus recorded before the application of the twelve second stimulation period. The u_1 wave amplitude has almost recovered its control value. A curious feature, however is the slight increase in the diphasic waveform amplitude, record (f) is the response of the u_1 wave recorded three seconds after the end of the twelve second stimulation period.

5·6

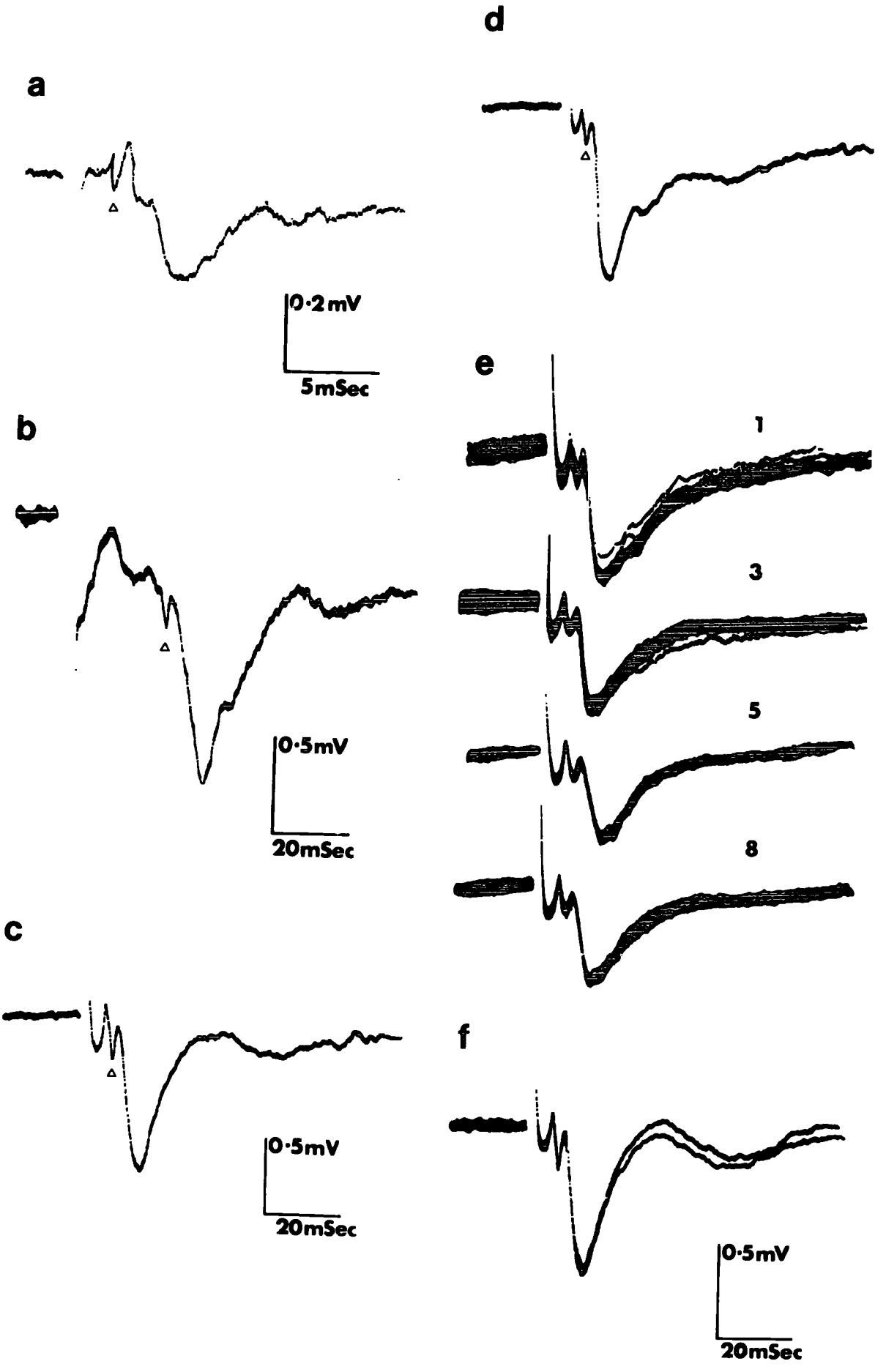

The properties of these small waveforms were investigated in conjunction with the larger, longer latency evoked waves, using double stimulus pulses and tetanic trains of stimuli. Recordings of the u_1 wave in response to a stimulus consisting of a pulse train at a frequency of 20 Hz for a period of 12 seconds is illustrated in figure 5:6 e. A control response for a single stimulus is shown in figure 5:6 d for comparison. Responses were recorded 1, 3, 5 and 8 seconds after the start of the pulse train and show a progressive decrease in amplitude of the large u_1 wave. At 3 seconds after the end of the 12 second stimulating period the u_1 wave amplitude had recovered to control levels (fig. 5:6 f). However, note that the small negative wave has a constant amplitude in all records. The susceptibility of the u_1 wave to repetitive stimuli suggests that it may be a postsynaptic component. It is possible that the preceeding small negative wave in figure 5:6 d is a presynaptic component and may be regarded as a synchronous impulse volley transmitted by afferent fibres. This conclusion is based on the evidence that this wave follows, without decrement of amplitude, a high frequency stimulus.

Further evidence for the postsynaptic nature of the large monophasic waveforms was obtained by applying double stimuli to the optic nerve. Such a record is shown in figure 5:7 (e.g. 6 msec record), where the amplitude of the evoked wave, for stimuli of constant intensity, increases on presentation of a second stimulus which rapidly follows an initial stimulus. This potentiation of the m_1 wave is expressed in terms of a percentage increase in amplitude relative to that of a control wave recorded in response to a single stimulus (fig. 5:7 a, b). No potentiation occurs with an interstimulus interval of 1 msec, but with intervals of between 2 and 6 msecs, the amplitude of the second wave rapidly increases over the control to give a potentiation of 140% (fig. 5:7 b). With interstimulus intervals greater than 6 msecs, the amplitude decreases to produce a 20% potentiated response at an interstimulus interval of 20 msecs. This degree of potentiation is maintained up to intervals of 70 to 80 msecs.

The percentage increase in the amplitude of the m_2 wave is calculated relative to the amplitude when only a single stimulus is applied (fig. 5:8 a). An interstimulus interval of 5 msecs has no effect on the amplitude of the m_2 wave, but note at this interval the potentiated response of the m_1 wave, as expected from the results above (fig. 5:7 a, b). A 10 msec interval produces a

Fig. 5:7 Effects of paired stimuli on the m_1 wave

(a) Records to show the change in amplitude of an m_1 wave to double stimuli at varying intervals. Figures below the traces indicate the interval between two pulses. The second wave in the 2 msec interval record is clearly larger than the control (o). The m_1 wave is potentiated further with increasing stimulus intervals, until a maximal second response is obtained with intervals of 5-6 msec. Thereafter the potentiated wave decreases in amplitude to control levels. Dots above traces indicate the stimulus and the calibration is as indicated.

(b) Graphical representation of the results obtained from the records illustrated in (a). The percentage increase in amplitude is plotted against the interval in msecs. Maximal potentiation (140%) occurs at an interval of 5-6 msec.

In all records positive polarity at the recording electrode is upwards.

5·7

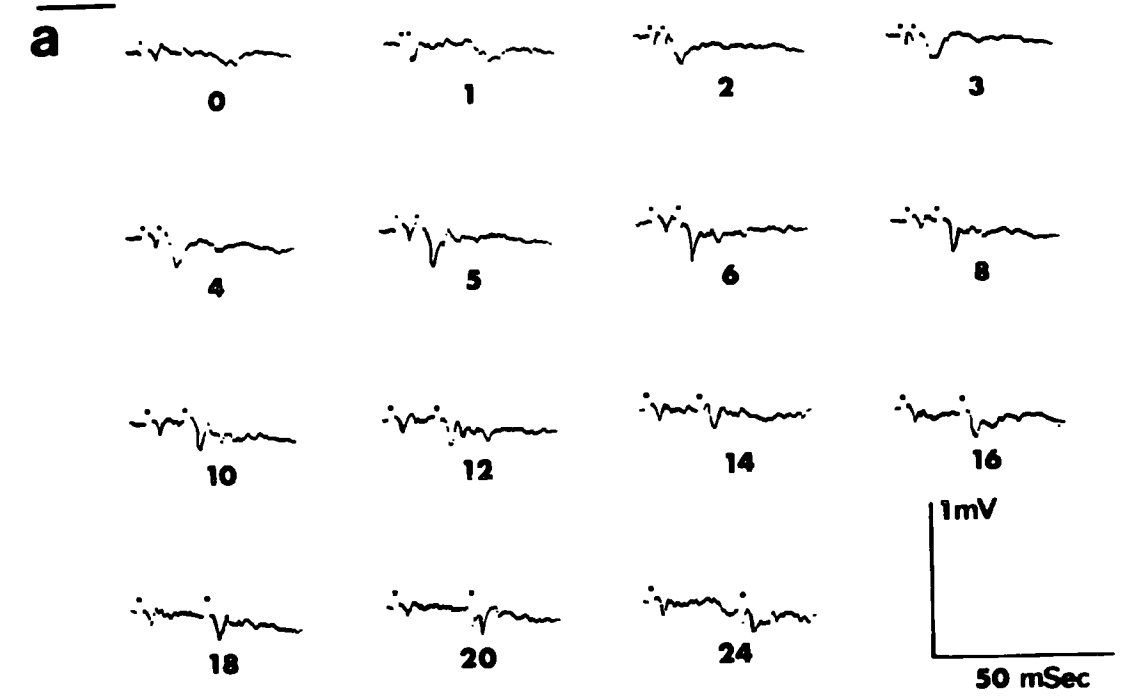
a
0
1
2
3
4
5
6
8
10
12
14
16
18
20
24
1mV
50 mSec

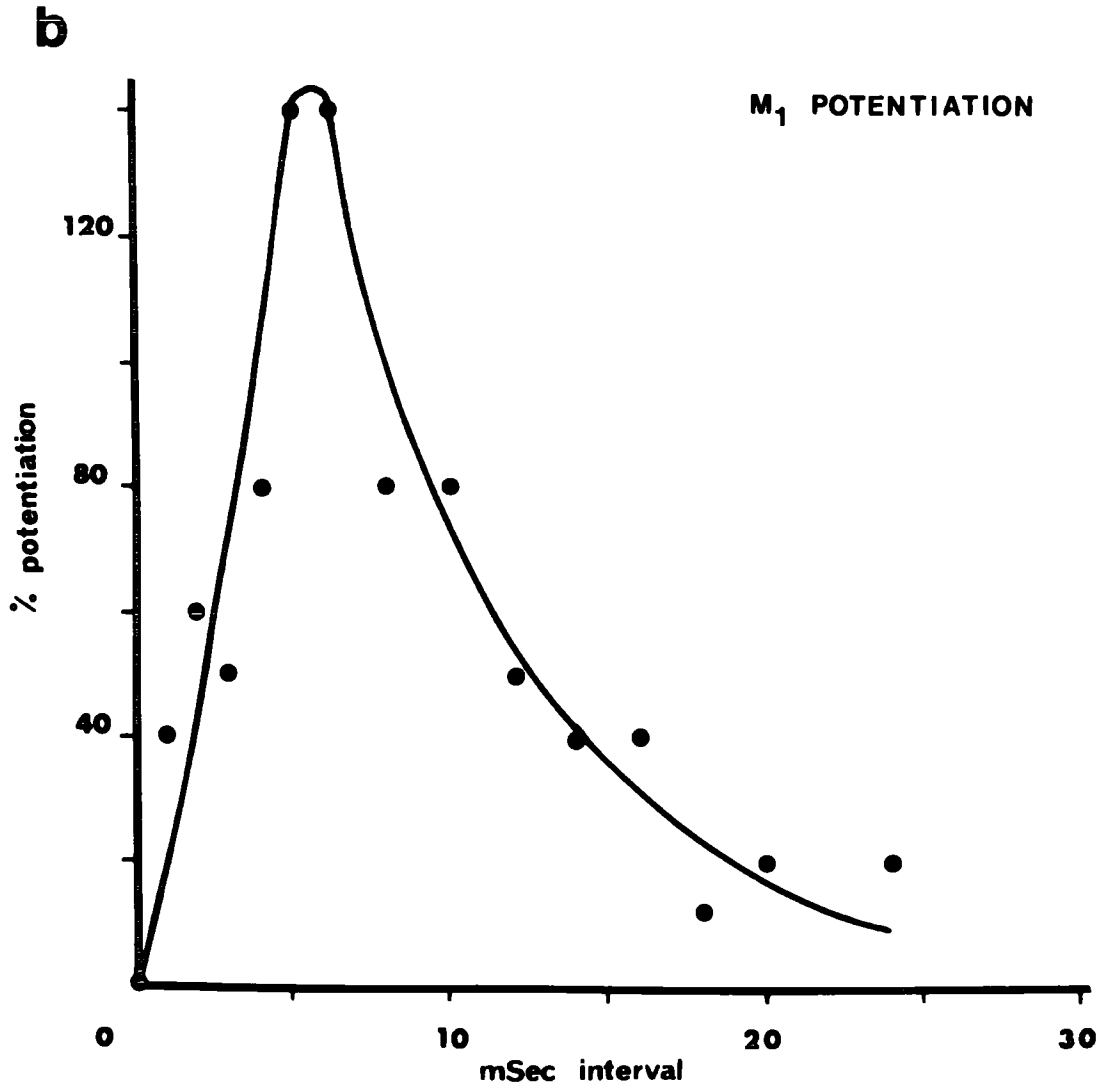
b
M1 POTENTIATION
% potentiation
120
80
40
0
10
20
30
mSec interval

Fig. 5:8 Potentiation of the m_2 wave

(a) Typical records showing m_2 wave potentiation. Figures below the traces indicate the interval in msecs between two stimuli. With an interval of 5 msec no m_2 wave potentiation is produced. A delay of 10 msec between pulses potentiates the second response maximally (50% increase in amplitude). Increasing the interval further, leads to a decline in the effectiveness of the first stimulus, until at intervals 50 msecs the secondary response is at an amplitude comparable to the initial response. Note the different time calibration marks. The 50 msec scale refers to traces 0, 5, 10, 15 and 20. Dots above traces indicate the stimuli.

(b) Graphical representation of the results illustrated above. Percentage potentiation is plotted against interstimulus interval. The m_2 wave is maximally potentiated by an interstimulus interval of 10 msec.

In all records positive polarity of the recording electrodes is upwards.

5·8

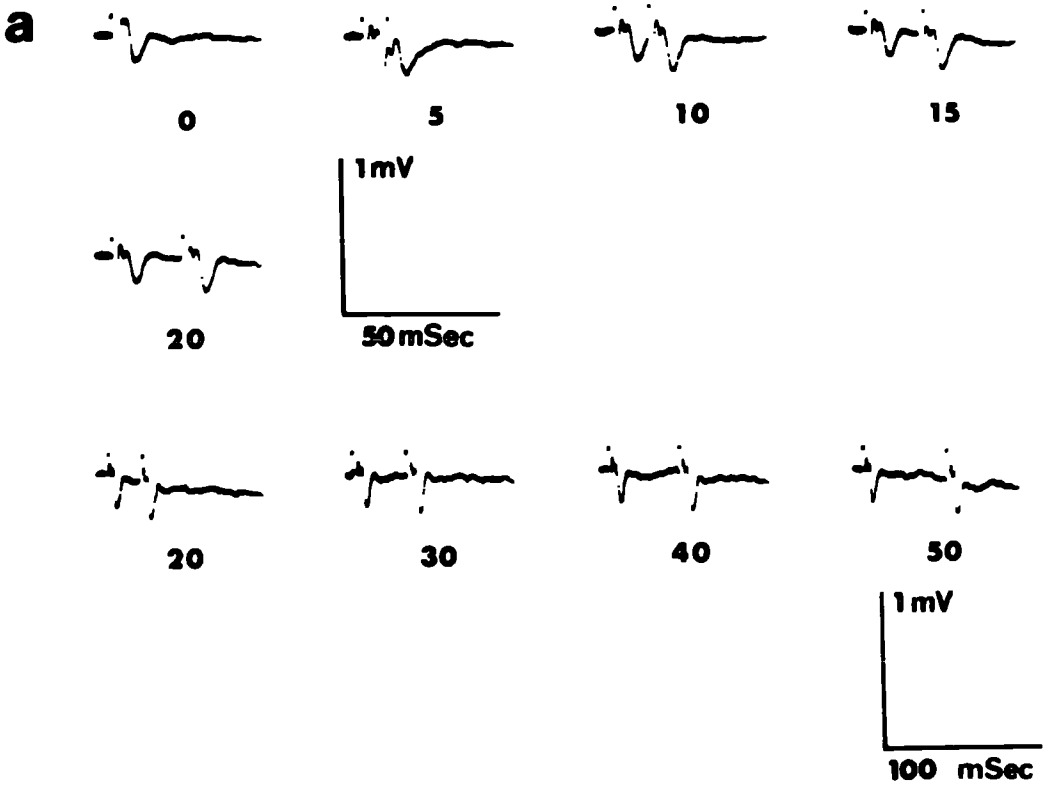
a
0
5
10
15
1mV
20
50mSec
20
30
40
50
1mV
100 mSec
b
M2 POTENTIATION
60
40
20
0
% potentiation
20
40
60
mSec interval

maximally potentiated m_2 wave, which has increased in amplitude by 50%. Intervals greater than this are less effective and the degree of potentiation is only 5% when the second stimulus is delivered 50 msecs after the first. These results are summarized in the graph in figure 5:8 b.

Figure 5:9 b shows the conditioning and potentiated responses of the u_1 wave to double stimuli with an interstimulus interval of 30 msecs. The effects of varying the interval are shown graphically in figure 5:9 a where it can be seen that the u_1 postsynaptic wave may be potentiated by double stimuli, providing the interstimulus interval is not greater than 150 msecs. Maximum potentiation (50%) occurs with intervals of 40 to 50 msecs. Figure 5:9 a summarizes the data of potentiation of the u_2 wave.

The limits of the potentiating stimulus intervals are similar to that of the u_1 wave. However, the maximal potentiation of the u_2 wave occurs at a longer interstimulus interval (60 msecs) than for the u_1 wave (40 - 50 msec). Figure 5:9 c shows an inverted potentiated u_2 wave which is the recorded deep in the tectum at 380 μm from the surface.

In summary, all four postsynaptic waves may be potentiated, with the most effective interstimulus intervals being 7 msecs for the m_1 wave, 10 msecs for the m_2 wave, 45 msecs for the u_1 wave and 60 msecs for the u_2 wave.

Fig. 5:9 Potentiation of 'u' waves

(a) Summary of the amplitudes of u_1 and u_2 waves evoked in response to double stimuli applied with various interstimulus intervals. The ordinate is the percentage increase in amplitude of the response to the second pulse of the paired stimulus compared with the amplitude of a control response to a single stimulus. Maximum potentiation of u_1 and u_2 waves occur at interstimulus intervals of 45 and 60 msecs respectively.

(b) An example of potentiation recorded in a u_1 wave with an interstimulus interval of 30 msecs.

(c) An example of potentiation recorded in a u_2 wave. In this record the polarity of the evoked wave is reversed as a consequence of the depth in the tectum from which the responses were recorded.

In all recordings positive polarity is upwards.

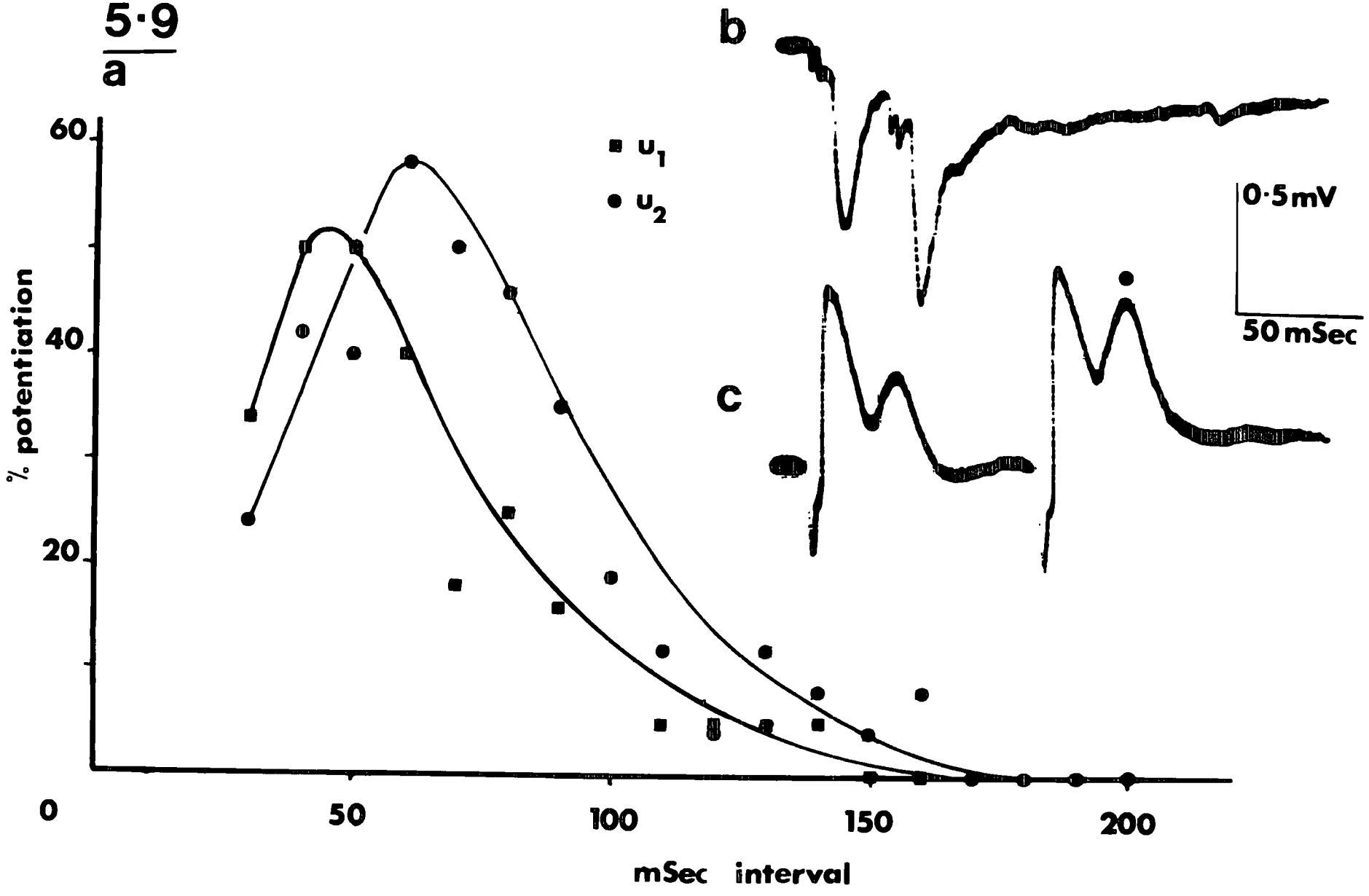
5·9
a
b
c
60
40
20
0
% potentiation
u_1
u_2
0·5mV
50 mSec
50
100
150
200
mSec interval

Depth Profiles and Current Source Density Analysis

Depth profiles of evoked wave amplitudes were determined and from these the second spatial derivatives were calculated. Comparisons between the responses obtained from different preparations and even from different electrode penetrations in the same preparation were difficult to make because of the variations in the thickness of the tectum. The results reported below are derived from single electrode penetrations in order that comparisons of the different waveforms may be made.

The M_2 wave

The m_2 wave is usually observed in records from the most superficial part of the tectum appearing as a small negative wave preceeding both the u_1 and u_2 waves (fig. 5:2 a, b). The latency of the presynaptic potentials usually associated with $^{M}u_2$ waves indicate an approximate conduction velocity of 1.1 to 1.3 $msec.^{-1}$

In figure 5:10 a, the m_2 wave is not readily apparent in the responses obtained from the first 50 μm of the microelectrode penetration, as it is obscured by the negative going edge of the u_1 wave. At 100 μm, the u_1 wave is decreasing in amplitude and the m_2 wave is beginning to appear as an inflexion on the negative going phase of this wave (fig. 5:10 a). At a depth of

Fig. 5:10 Current density analysis of Xenopus tectal m_2 waves

(a) Samples of evoked waves recorded at various depths in the tectum. The uppermost record is from the tectal surface, subsequent records are taken at successive 50 μm depth increments. The solid dot in the first record marks the time at which the contralateral optic nerve was stimulated. The solid vertical line represents the constant latency at which m_2 wave amplitudes, at the various depths, were measured.

(b) M_2 wave amplitude-depth distribution (solid circles) and its second derivative (open circles) for the potential records, some of which are illustrated in (a). The abscissa is scaled in millivolts for the amplitude-depth distribution and is also a relative scale for the second derivative. The negative quadrant represents negative polarity at the recording electrode for the amplitude-depth curve and also current sinks for the second spatial derivative. Positive values in the second spatial derivative are current sources. The depth oridinate is scaled in μm (microelectrode depth) and is also marked with a solid triangle labelled D, corresponding to the depth at which the amplitude of the negative m_2 wave was a maximum and at which a dye spot was deposited by the microelectrode Histological examination of this tectum (fig. 5:13 a) locates this spot in tectal layer 9.

5·10

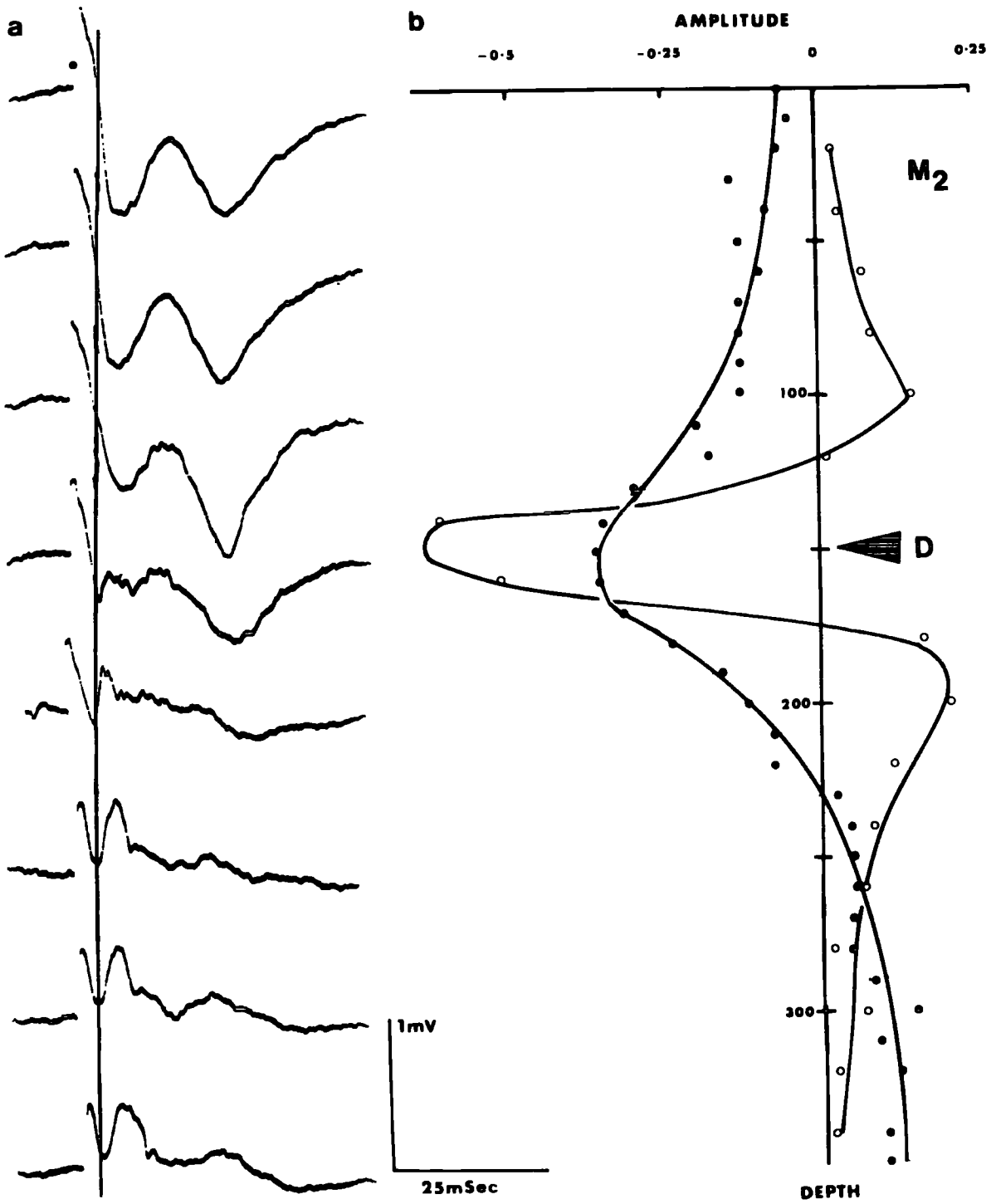

150 μm, the m_2 wave negativity is prominent and appears to increase as the u_1 postsynaptic wave inverts at 190 μm (fig. 5:10 a, b). At 300 μm, the amplitude of the m_2 wave decreases to the base line zero, although it still appears to be prominent due to the presence of the stimulus artifact.

Calculation of the second spatial derivative indicates a maximum net inward current located at a depth of 150 μm (fig. 5:10 b). This current sink was flanked both dorsally and ventrally by current sources, whose maxima lay at 100 and 200 μm, the latter being somewhat more prominent.

At a depth of 150 μm (the maximum amplitude of the m_2 wave) a dye spot was deposited, histologically recovered and illustrated in figure 5:13 a. The location of the dye spot at the maximum negativity of the depth profile corresponds to the location of the maximum current sink on the second spatial derivative. Knowledge of the depth in the tectum of any one point on the depth profile enables all other positions on the profile to be equated with a particular tectal depth. It may be assumed that shrinkage of the tissue occurred during histological processing and was constant throughout the thickness of the tectum. Therefore from figure 5:10 b it may be determined that the maximum current sink is located in layer 9 of the tectum. The location of the deep current source at 200 μm corresponds to the location of the cell bodies. A current source is also located more superficially then the current sink.

Since it is known that the cell bodies of layer 8 extend their apical dendrites into layer 9 it may be assumed that the synaptic sink occurs on the ascending dendrites of these cells and the current is distributed to the more superficial portions of the dendrites and deeper to the cell bodies.

The U_1 wave

The u_1 wave is a prominent monophasic negative potential recorded at the surface of the tectum. The conduction velocity of the afferent fibres determined from the latency of the presynaptic potential usually associated with the u_1 wave indicates an approximate conduction velocity of 0.6 $msec.^{-1}$ As the electrode penetrates the tectum in a direction perpendicular to the surface, the evoked potential is of constant amplitude for the first 50 µm of the penetration. The amplitude decreases with further penetration and finally inverts to a positive value at 170 µm (fig. 5:11 a, b). As the electrode continues to penetrate the tectum the positive inverted wave continues to increase amplitude.

Calculation of the second spatial derivative of the depth profile indicates a large current sink which is maximal 70 µm below the surface. A single current source is present, the maximum of which is located at a depth of 150 µm (fig. 5:11 b). The dye deposited during the penetration (fig. 5:13 a) localizes the current sink as being the most superficial in the tectum. The maximum current

Fig. 5:11 Current density analysis of Xenopus tectal u_1 waves

(a) Samples of evoked waves recorded at 50 μm depth increments in the optic tectum. The solid dot in the first record marks the time at which the contralateral optic nerve was stimulated. The solid vertical line represents the constant latency at which u_1 wave amplitudes, at each depth, were measured.

(b) U_1 wave amplitude-depth distribution (solid circles) and its second derivative (open circles) for the records, some of which are illustrated in (a). The scales and remarks concerning the abscissa and ordinate of this graph are the same as in figure 5:10 b. The dye spot position, marked D, when recovered histologically (fig. 5:13 a) allows comparison of the locations of the current sink and sources with the depths of cell, and synaptic layers (see text).

5·11

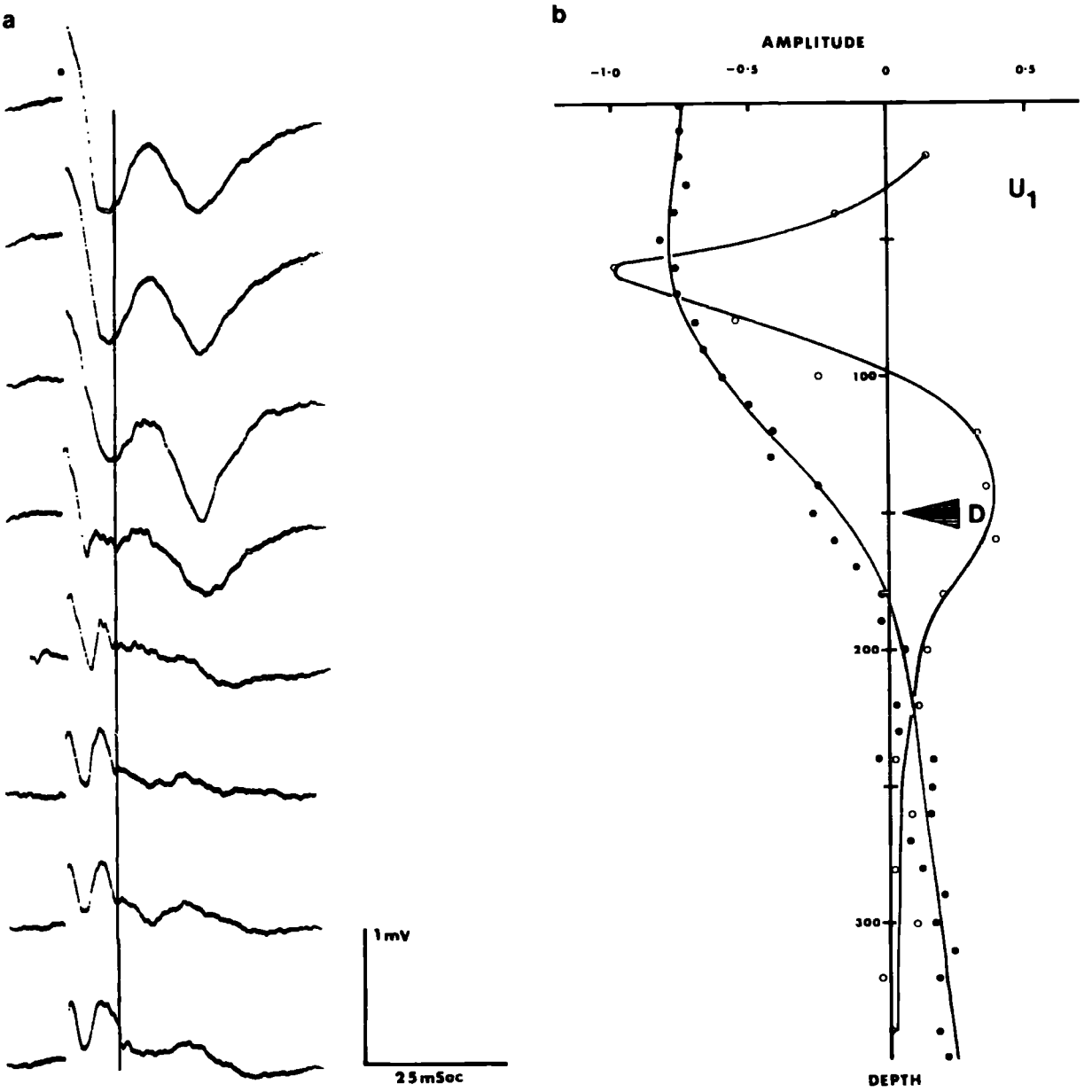

source can be localized to a region just superficial to the cells of layer 8, and this corresponds to the main apical shafts of the dendrites which originate from these cells.

The U_2 wave

The u_2 wave is a prominent negative deflection when the recording electrode is at the surface of the tectum. The latency of the presynaptic potentials usually associated with u_2 waves indicate an approximate conduction velocity of 0.2 $msec.^{-1}$

For a constant stimulus strength the amplitude of the u_2 wave increases as the electrode is advanced radially into the tectum, down to a depth of 100 μm from the surface (fig. 5:12 a, b). With further penetration the wave decreases in amplitude and eventually reverses polarity at a depth of 250 μm. When the second spatial derivative of the depth profile is calculated, the results indicate three peaks; a small positive maximum very close to the surface, a large negative minimum at a depth of 100 μm and a positive maximum at 180 μm. Since the dye spot deposited during the penetration at a depth of 150 μm was recovered (fig. 5:13 a), the location of the deep current source at 180 μm may be identified as the cells of layer 8. The prominent current sink is located superficially in layer 9, however it is located at a level slightly deeper than the location of the maximum u_1 sink.

Fig. 5:12 Current density analysis of Xenopus tectal u_2 waves

(a) Samples of evoked waves recorded at various depths in the tectum (for details see legend to fig. 5:10 a). The solid vertical line represents the constant latency at which u_2 wave amplitudes, at successive depths, were measured.

(b) U_2 wave amplitude-depth distribution (solid circles) and its second derivative (open circles) for the records illustrated in (a). Interpretation of abscissa and ordinate as in figure 5:10 b. The position of the deposited dye spot marker is indicated by a solid triangle labelled D.

5·12

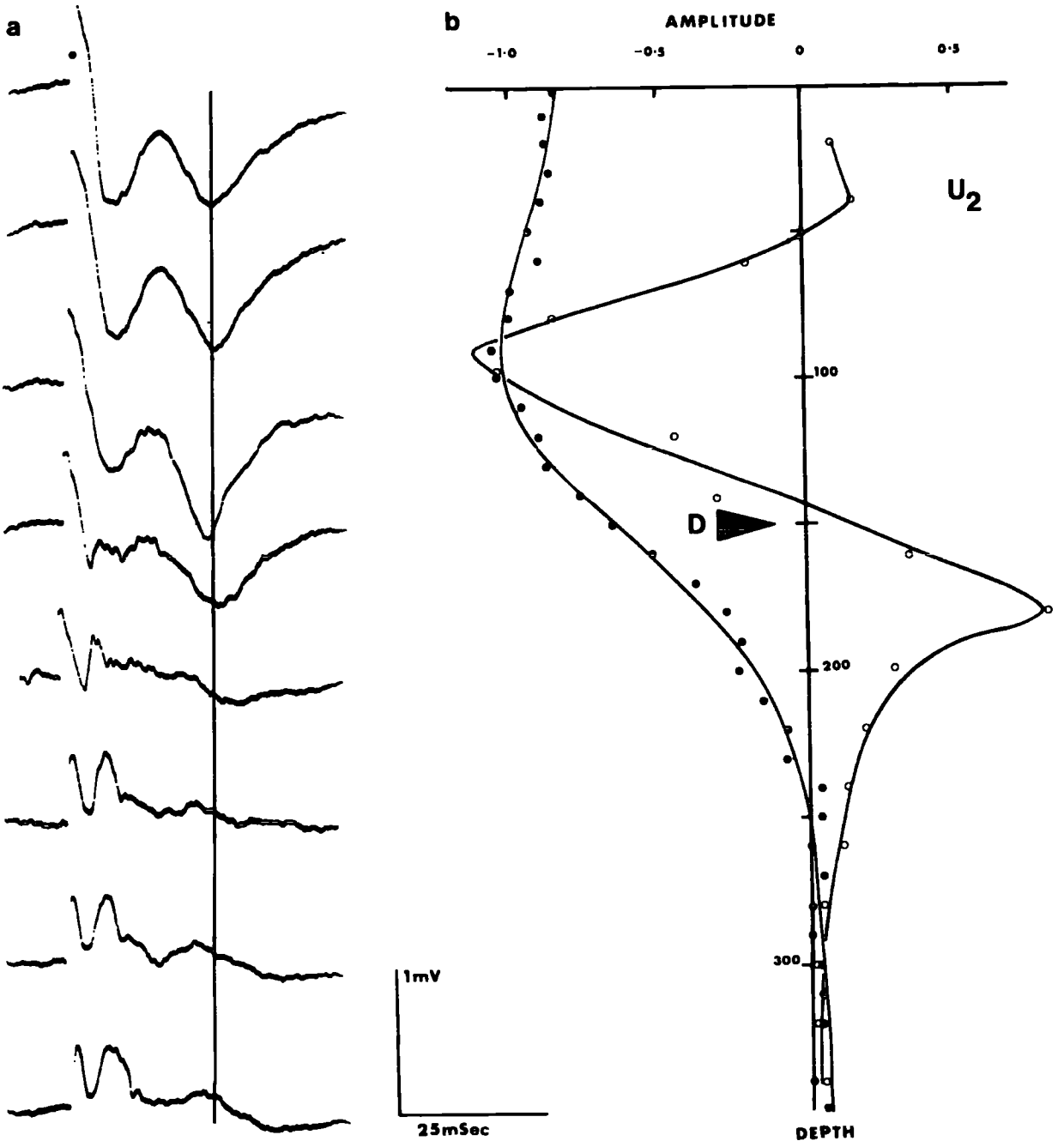

Fig. 5:13 Light micrographs to show deposited dye spots.

In all figures the figure '8' indicates layer 8 of the tectum and 'D' indicates the dye spot.

(a) A dye spot is indicated which was deposited during the penetration from which the previous depth profiles were calculated (figs. 5:10, 5:11 and 5:12). The spot was deposited at the site of maximum negativity of the m_2 wave (1.5 μm). This site is located above layer 8 and corresponds to the location of maximum inward current of the m_2 wave.

(b) The dye spot indicates the location of maximum negativity of an m_1 wave during a penetration of the tectum with a microelectrode. The spot is located immediately beneath the cell bodies of layer 8.

(c) The dye spot (at a microelectrode depth of 120 μm) indicates the location of the postsynaptic neuron whose activity was superimposed on the m_2 wave. The records of the activation and the effects of a stimulus pulse train are shown in figures 5:19 e, f and g.

(d) Dye spot marking the location of deep neuron (see fig. 5:20 a, b, c) whose activity could be recorded over a distance of 50 μm (fig. 5:20 a, b, c). The cell is located in layer 2 of the tectum.

5·13

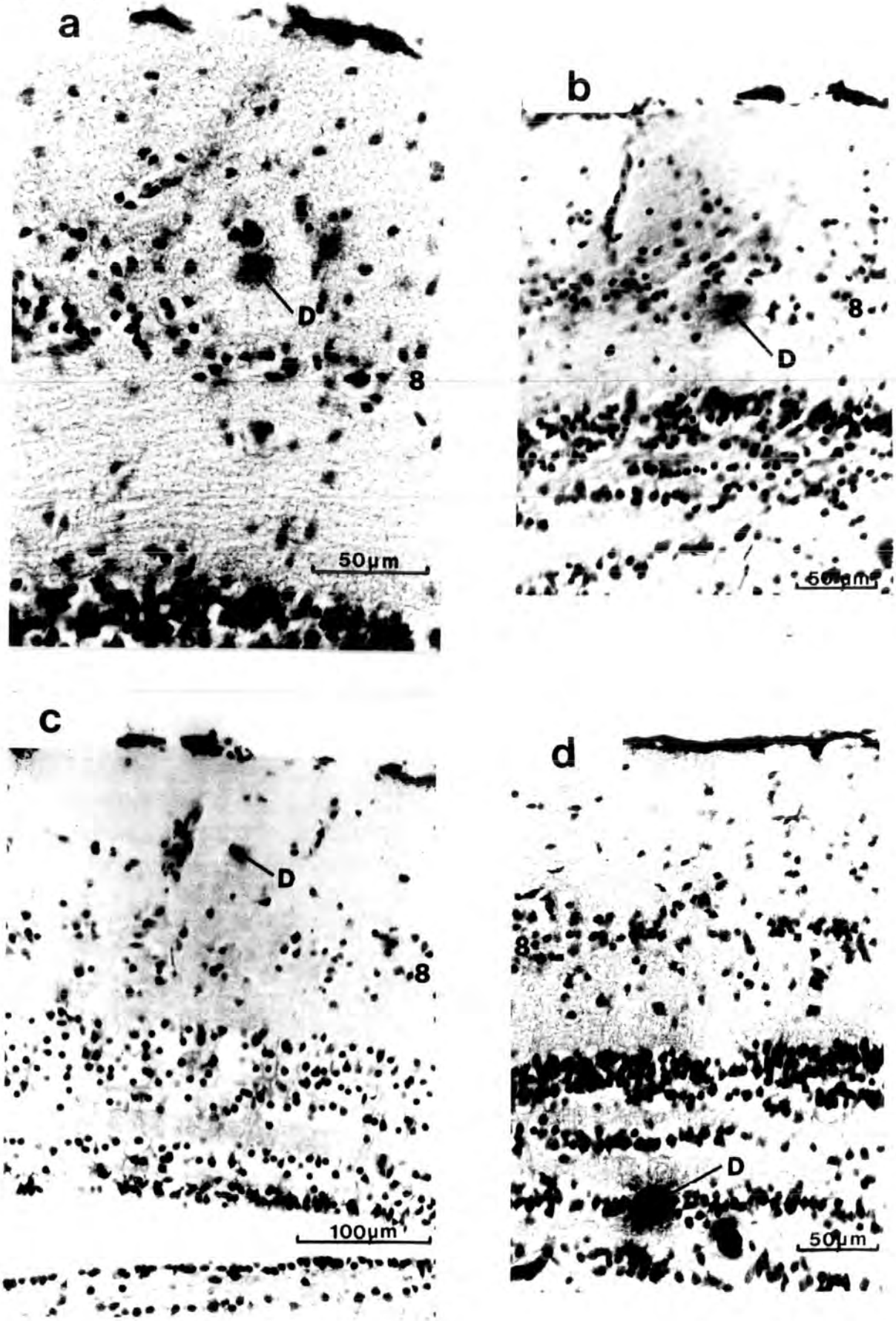

The M_1 wave

The conduction velocity of the afferent fibres of the m_1 wave could not be determined since it is rarely preceeded by a presynaptic component. No depth profile could be determined for the m_1 wave in Xenopus since the amplitude of the wave was too small to be recorded at a number of depths thus preventing construction of an adequate depth profile. However, in the penetration described above for the m_2, u_1 and u_2 waves, the m_1 wave exhibited a maximum negativity at a depth 240 μm and is shown in figure 5:17 a. From the deposition of the dye spot this indicates that the locus of maximum negativity is located deeper than the cell bodies of layer 8. Indeed, in another penetration where dye was deposited at the maximum negativity of the m_1 postsynaptic wave, it was recovered beneath the cell bodies of layer 8 (fig. 5:13 b).

Field Potentials in Rana

The field potentials evoked from the frog contralateral optic tectum in response to an electrical stimulus of the optic nerve are qualitatively similar to those obtained from Xenopus. However, they do differ quantitatively with respect to the location of their sources and sinks.

The U_2 wave

The u_2 wave, as in Xenopus is recorded as a prominent negative potential at the surface of the tectum. With increasing electrode depth, the amplitude of the wave increases slightly to give a maximal response at about 100 μm (fig. 5:14 a, b). On further penetration the wave decreases in amplitude and reverses its polarity at 320 μm after which the amplitude of this reversed polarity wave starts to increase again.

The second spatial derivative indicates a maximum current sink at a depth of 100 μm and a maximum current source at 360 μm (fig. 5:14 b). The deposition of dye spots, as carried out for Xenopus, indicate that a current sink is located superficially in layer 9 and the depth of the current source corresponds to the cells of layer 8. A second minor current source is also present at a slightly deeper position, which corresponds to the deeper cells of layer 6.

The U_1 wave

Figures 5:15 a and 5:15 b show that the u_1 wave is prominent at the tectal surface and increases in amplitude within the first 60 μm of the tectal cortex, after which the amplitude decreases. The polarity of the wave reverses at a depth of 230 μm and reaches a maximum positivity at a depth of 420 μm.

Fig. 5:14 Current density analysis of u_2 waves in Rana tectum

(a) Samples of evoked waves recorded at various depths in the tectum. The uppermost record is from the tectal surface, subsequent records are taken at successive 100 μm depth increments. The solid vertical line through all records is the constant latency at which u_2 wave amplitudes were measured.

(b) U_2 wave amplitude-depth distribution (solid circles) and its second derivative (open circles). Scales for the amplitude and second derivative curves are explained in figure 5:10 b, but note the greater depth to which penetrations are made in the tectum of Rana (to 600 μm) compared with that in Xenopus (to 350 μm). The solid triangle labelled D corresponds to the location of a dye spot that was used to correlate source-sink location with specific tectal layers (see text).

5·14

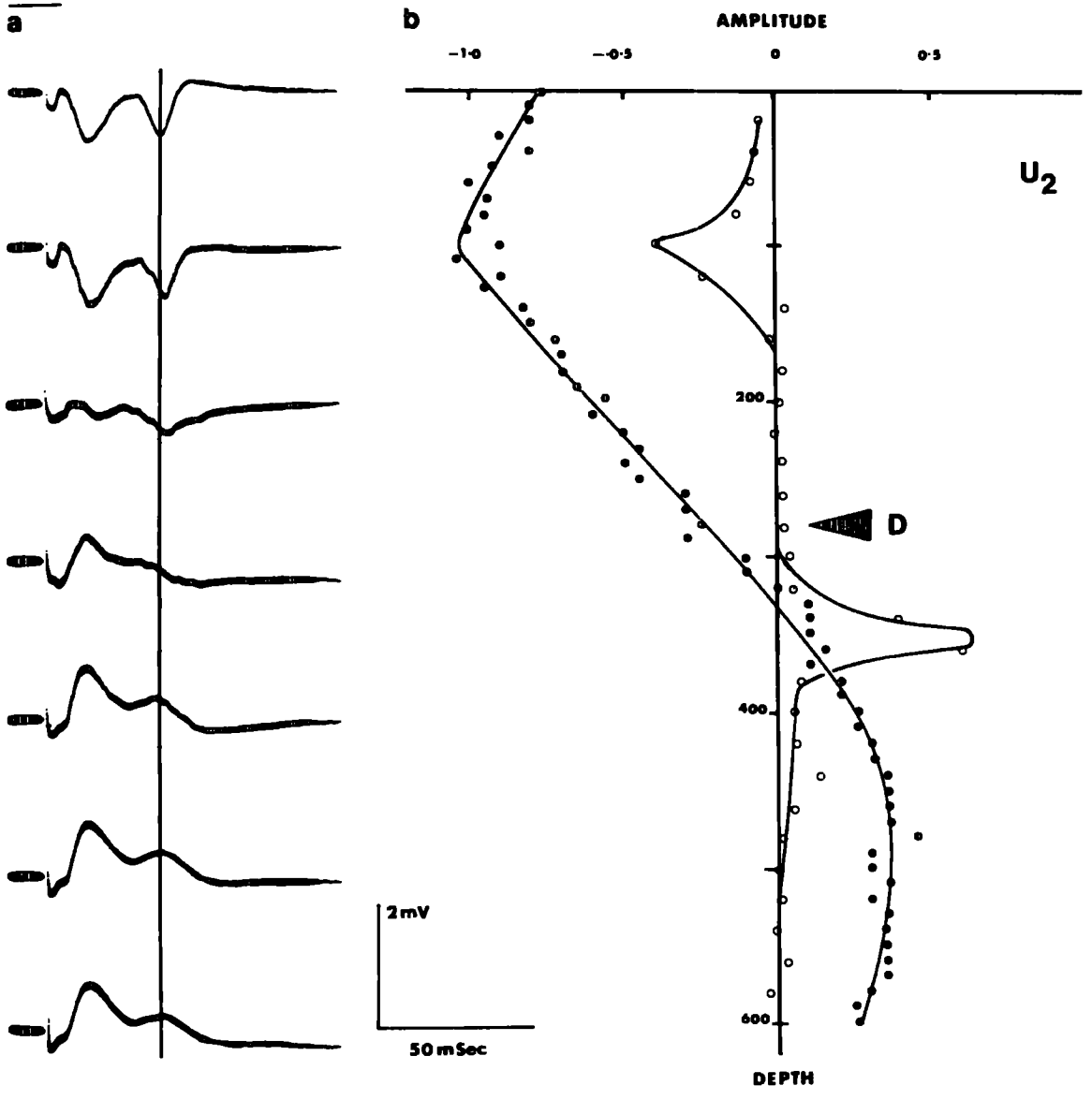

Fig. 5:15 Current density analysis of u_1 waves in Rana tectum

(a) Samples of evoked waves recorded at various depths in the tectum. The uppermost record is taken from the tectal surface, subsequent records are taken at successive 100 μm depth increments. The solid vertical line through all records is the constant latency at which u_1 wave amplitudes were measured.

(b) U_1 wave amplitude-depth distribution (solid circles) and its second derivative (open circles). Explanation of scales as in figure 5:10 b and figure 5:14 b. The position of the microelectrode deposited dye spot was used to correlate source-sink locations of the second derivated with specific tectal layers (see text).

5·15

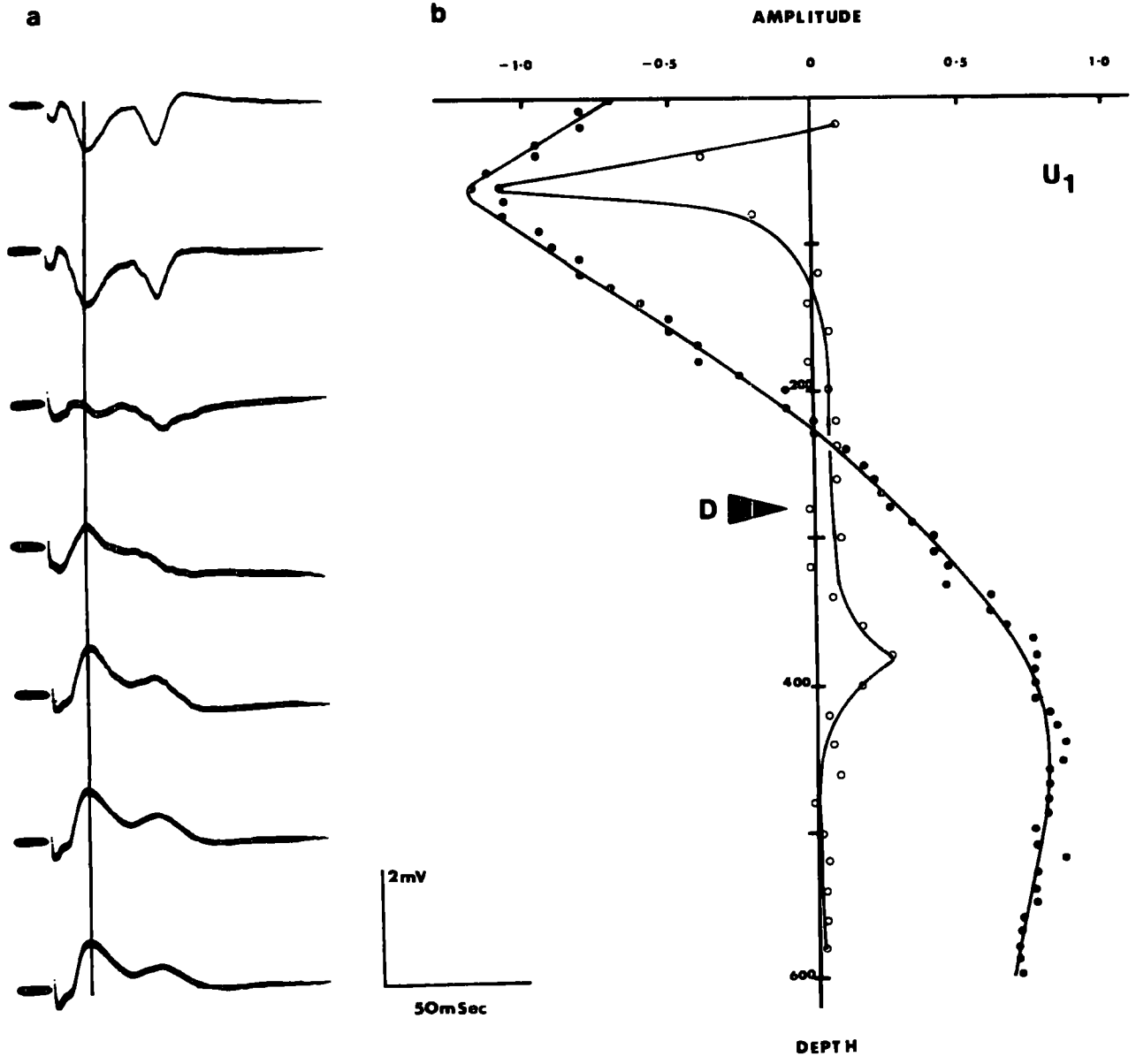

The second spatial derivative (fig. 5:15 b) indicates a sharply localized current sink at a depth of 60 μm, the source of which is located at 380 μm (fig. 5:15 b). The deposited dye spot of this penetration indicates that the current sink is located more superficially than the u_2 sink and that the current source can be localized to the somata of layer 8.

The M_2 wave

The depth profile for the m_2 wave is shown in figure 5:16 b and is derived from the traces shown in figure 5:16 a. This negative wave has a small amplitude from the tectal surface down to a depth of 150 μm. On further advancement of the microelectrode, the wave increases dramatically to become maximally negative in the region of 270 μm from the tectal surface (fig. 5:16 a, b). On further penetration the amplitude of the wave then showed an equally dramatic decrease to an almost constant level at approximately 400 μm depth.

The current sources and sinks of the m_2 wave determined from the second spatial derivative were located in a similar position to those of the m_2 wave in the Xenopus tectum. The maximum current sink was at a depth of 280 μm and this corresponds to a position which lies half-way between the u_2 current sink and the cell bodies of layer 8. This sink is flanked both dorsally and ventrally by current sources, the deeper of which corresponds to the deeper cell bodies of layer 8.

Fig. 5:16 Current density analysis of m_2 waves in Rana tectum

(a) Samples of evoked waves recorded at various depths in the tectum. The uppermost record is taken from the tectal surface, subsequent records are taken at successive 100 μm depth increments. The solid vertical line through all records is at a constant latency from the application of the stimulus to the contralateral optic nerve and is the time at which m_2 wave amplitudes were measured.

(b) M_2 wave amplitude-depth distribution (solid circles) and its second derivative (open circles). Explanation of scales and significance of dye spot (marked D) as in figure 5:10 b and figure 5:14 b.

5·16

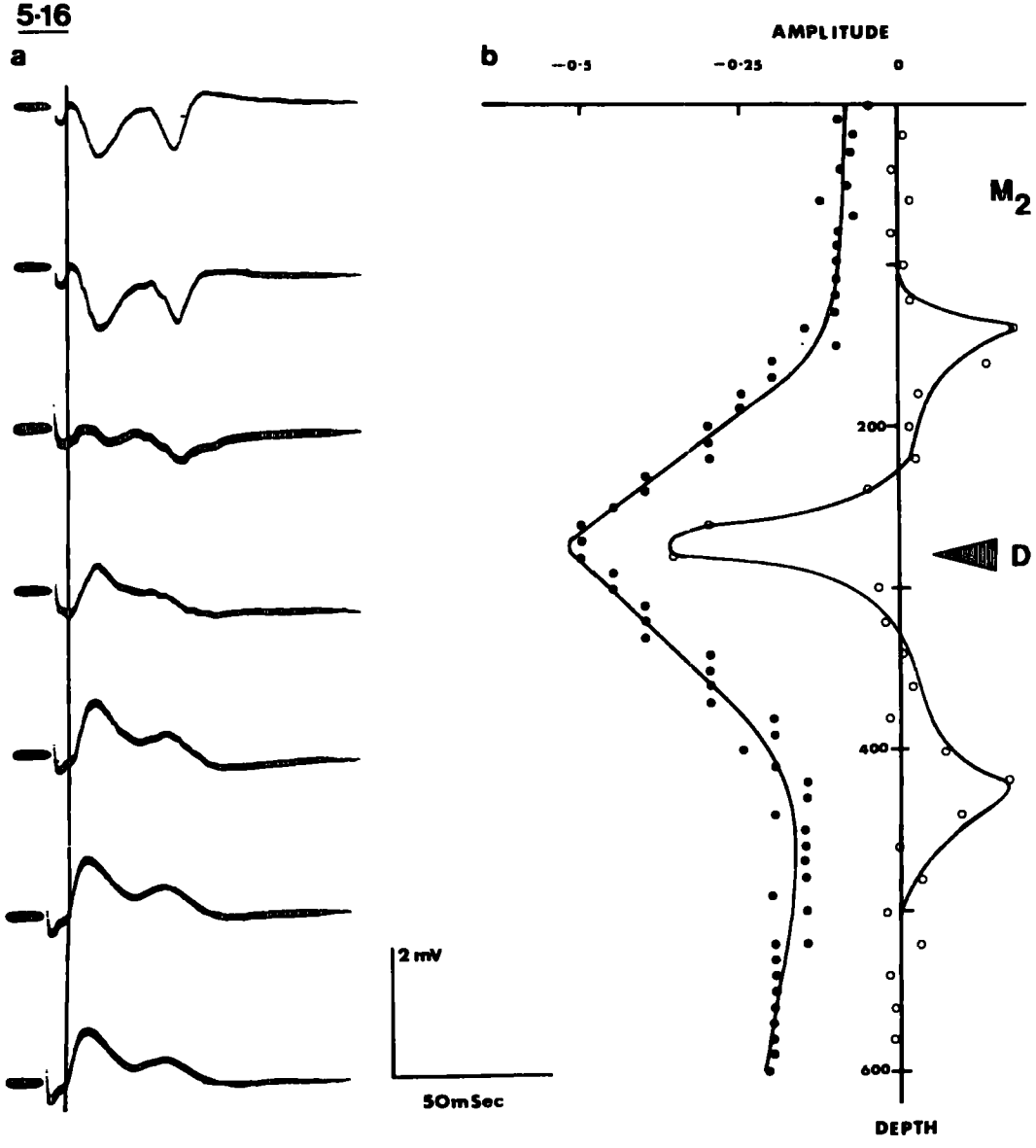

The M_1 wave

As in Xenopus, current source density analysis could not be carried out on the m_1 wave, since the encroachment of the stimulus artifact on the wave prevented accurate measurement of its amplitude. Dye spots at the site of maximum negativity were found at the junction between layers 7 and 8.

Other postsynaptic events in Xenopus tectum

During the course of studying the field potentials evoked in the contralateral tectum by electrical stimuli applied to the optic nerve, a number of other events were observed which could be regarded as being a direct consequence of the application of a stimulus to the nerve.

As the electrode penetrated the tectum, small negative deflections could be observed on the negative going phase of the u_2 wave in layer 9 (fig. 5:17 b). As the electrode penetrated further and the 'u' waves started to decline in amplitude or reverse in polarity brief monophasic positive deflections could be observed to be superimposed on these waves at a depth of 230 μm (fig. 5:17 c) and could be recorded over many microns. The response illustrated in figure 5:17 d was recorded at a depth of 250 μm. It is possible that these spikes

Fig. 5:17 (a) M_1 wave recorded at a depth of 240 μm at which it exhibited maximum negativity. Dye spot deposition indicated that the locus of m_1 maximum negativity was beneath cell bodies of layer 8 neurons (fig. 5:13 b and text).

Figs. 5:17 b, c, d, e, f and g Monophasic potentials associated with u_2 waves

(b) U_2 wave recorded in layer 9 of the tectum with an associated brief potential deflection on its rising (negative-going) edge.

(c) The U_2 wave of (b) recorded at a deeper location (230 μm). The u_2 wave in this region has a smaller amplitude and has superimposed on it a brief, monophasic positive potential.

(d) and (e) The u_2 wave of (b) and (c) recorded at a depth of 250 μm. The presence of brief monophasic positive potentials in records (c), (d) and (e) are suggestive of action potentials originating from the somata of layer 8 neurons.

(f) and (g) The u_2 wave of records (b) to (e) recorded in tectal depths in which polarity reversal is taking place. Small monophasic negative potentials are superimposed on the low amplitude u_2 wave.

5·17

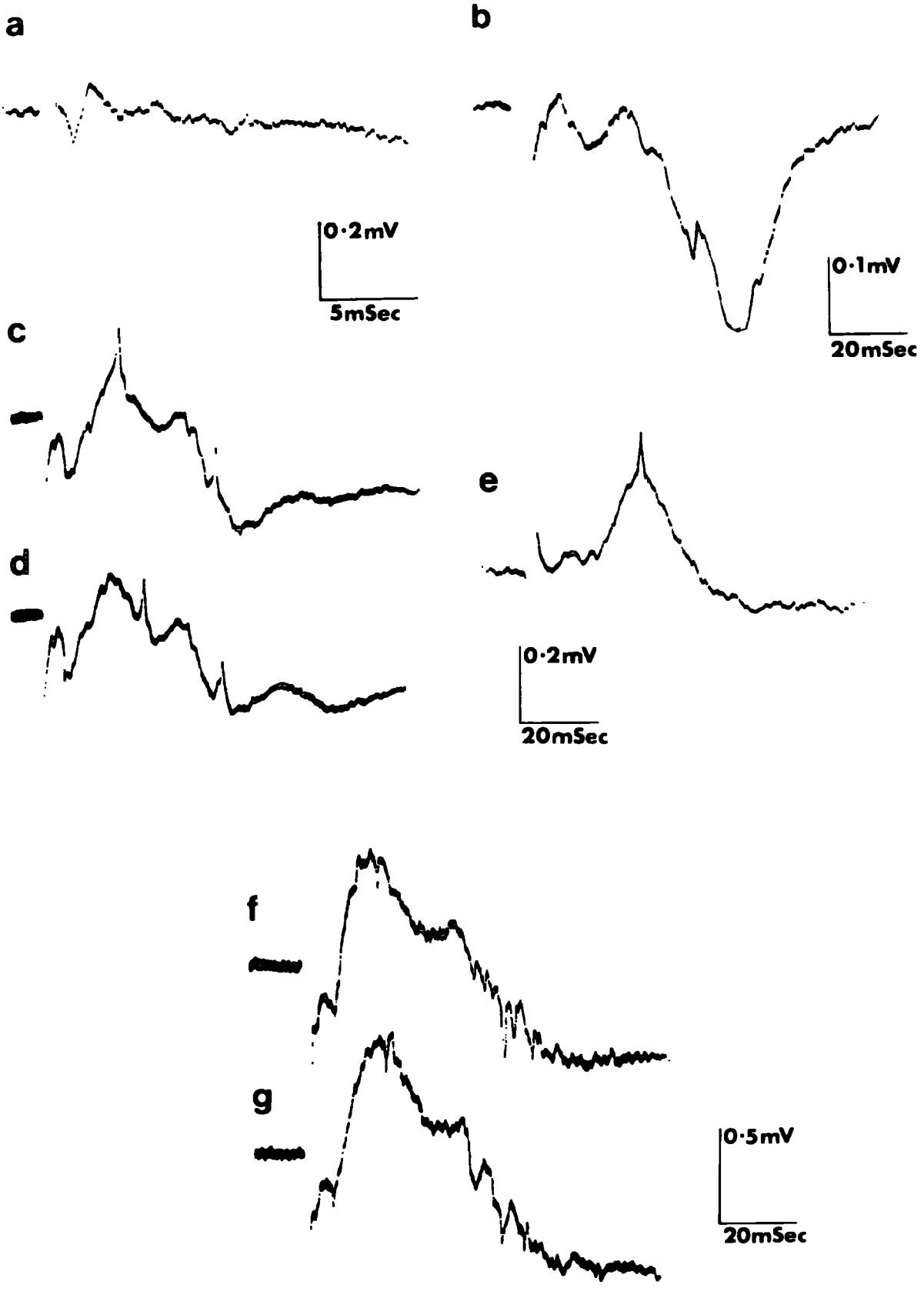

may have originated from the somata of layer 8 neurons. These spikes occurred either singly (fig. 5:17 e) or occasionally in multiples (figs. 5:17 c, d). In addition at slightly deeper positions, small monophasic potentials were superimposed on the inverted 'u' waves (figs. 5:17 f, g). These small waves are indicative of an action potential passing close to the tip of the microelectrode.

At depths in which the u_2 wave is inverted diphasic spikes can occasionally be seen to be superimposed on this 'u' wave. These diphasic spikes may have originated from a cell in layer 8 or from deeper laminae. The examples shown in figures 5:18 a, b and c were recorded deep in the tectum. The latency of the prominent spike was variable.

Action potentials were regularly recorded in association with the m_2 postsynaptic wave (fig. 5:18 d). These action potentials were often much larger than those superimposed on the u waves (fig. 5:17 c, d, f, g). The response illustrated in figure 5:18 d was recorded at a depth of 210 μm. The synapse had a fairly high safety factor, since it was only at stimulus frequencies higher than 20 Hz that spike initiation failed (fig. 5:18 d, e). Action potentials superimposed on m_2 waves were not adversely affected by double stimuli of 15 msec interval and, in figure 5:18 f, a small diphasic deflection is present at a much longer latency.

Fig. 5:18 (a), (b) and (c) Sample responses of diphasic potentials recorded in association with an 'inverted' u_2 wave. The depth of the tectum at which the records were taken was below layer 8. The latency of the prominent diphasic response, illustrated by these records was found to be variable.

Fig. 5:18 (d), (e) and (f)

(d) Diphasic potential recorded with a latency similar to that of an m_2 wave. The tectal depth from which this record was taken was 210 μm.

(e) Successive, superimposed responses of the diphasic potential recorded in (d), with a stimulus frequency of 20 Hz.

(f) The responses of the diphasic potential, recorded in (d) and (e), to two stimuli separated by 15 msecs.

In addition to the two responses of the diphasic potential an additional, lower amplitude diphasic potential is noted having a greater latency.

5·18

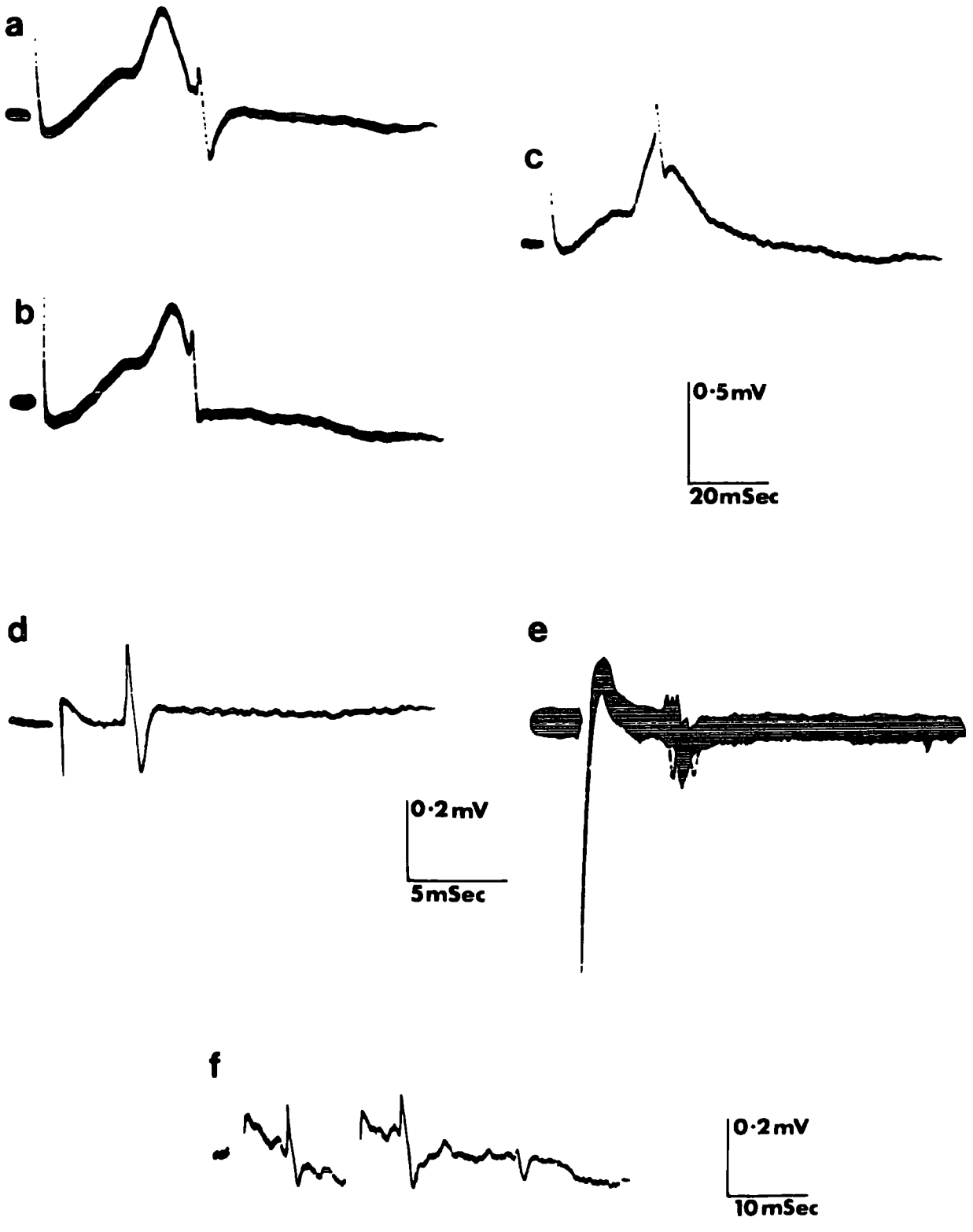

At a depth of 200 μm, in addition to a prominent m_2 wave, presynaptic and postsynaptic potentials that have long latencies (200 msec) could be evoked (figs. 5:19 a, b). These long latency potentials are reproduced on an expanded time scale in figures 5:19 c and d.

It can be seen in figure 5:19 a that the long latency evoked potential has an amplitude about half of that of the m_2 wave. Comparison of the latencies of these small waves show they vary by little more than 1 msec. Figures 5:19 c and d show clearly a 1 msec presynaptic and a 20 msec postsynaptic component. The postsynaptic component can be conditioned by an initial impulse and potential by a second impulse, if this arrives shortly afterwards (fig. 5:19 d). In this particular case, the potentiation amounts to a 70% increase with an interspike interval of 14 msecs, and the amplitude of the postsynaptic wave is almost as large as that of the m_2 wave.

A curious result was obtained at one electrode site and is exhibited in figure 5:19 e, f. A monophasic negative spike superimposed on the m_2 wave was recorded at a depth of 120 μm in the tectum. The spike had a constant latency, but failed when tetanic stimuli were applied briefly at 100 Hz (fig. 5:19 g). The location of the electrode tip at the time of recording was confirmed by dye deposition and was found to be situated next to a superficially located neuron in layer 9 of the tectum (fig. 5:13 c).

Fig. 5:19 Long latency waves

(a) and (c) Long latency wave recorded at a depth of 200 μm. The time calibrations are 100 msec and 20 msec for (a) and (c) respectively. The record at a faster sweep speed reveals that this long latency wave is composed of two components, a brief duration (1 msec) possibly presynaptic potential (open triangle), and a longer duration (20 msec) postsynaptic component.

(b) and (d) Illustrate potentiation occurring in the postsynaptic component when two presynaptic potentials (open triangles) occur at an interval of 14 msec. The amplitude of the second postsynaptic (e) wave is potentiated by 70%. The time calibration in (b) is 100 msec, in (d) it is 20 msec.

Short latency waves

(e) and (f) Records of a short latency, monophasic negative potential superimposed on an m_2 wave recorded at a depth of 120 μm. Tetanic stimuli of 100 Hz applied briefly (record g) result in failure of this potential. The electrode was located in layer 9 (fig. 5:13 c).

5·19

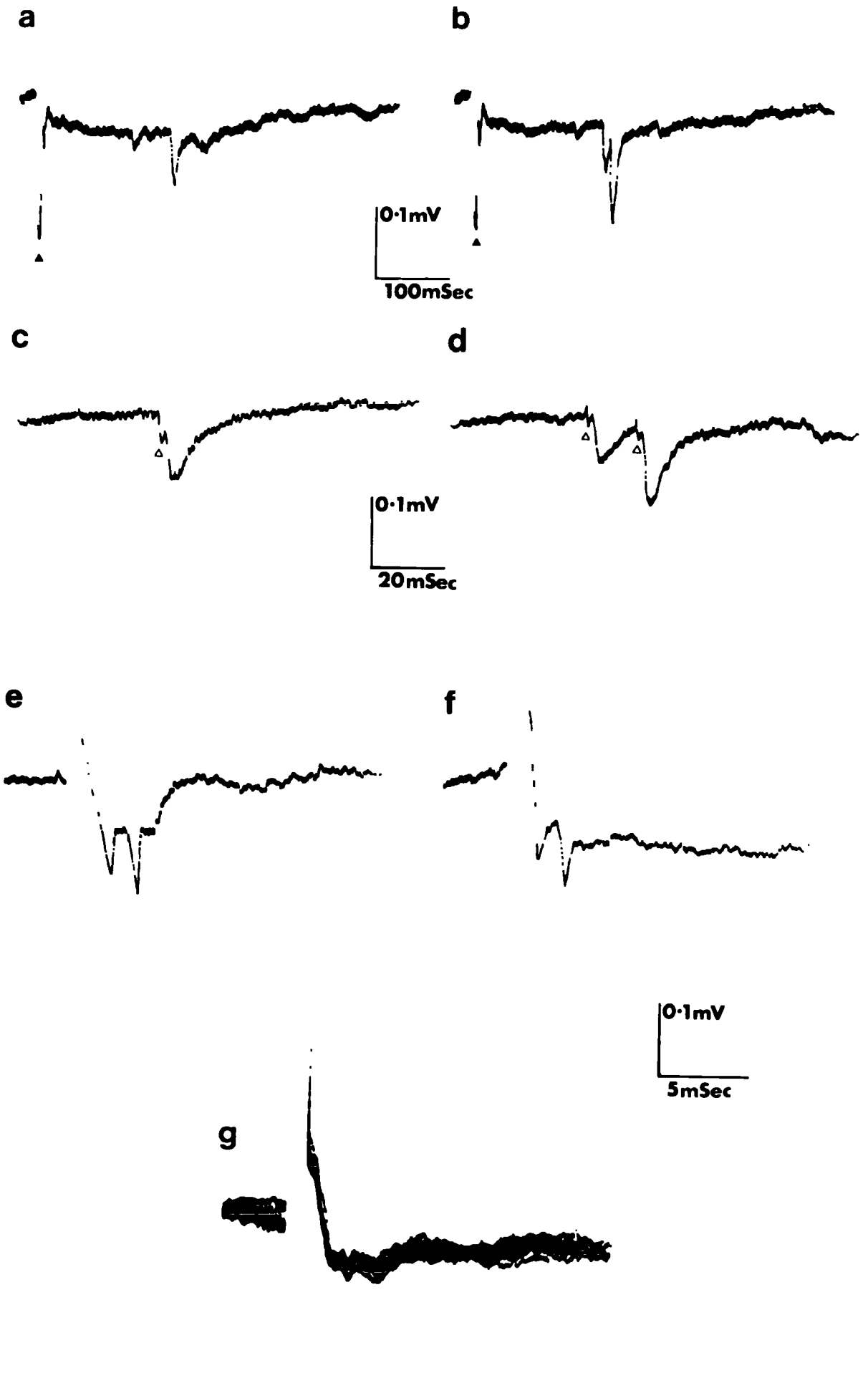

Neurons in the deep layers which were activated to produce spikes were found occasionally. An example is shown in the series in figure 5:20. A monophasic negative wave was recorded in the ascending phase of a positive wave, at a depth of 360 μm (fig. 5:20 a). The latency of the spike was comparable to that of an m_2 wave. As the electrode penetrated further, the spike could be recorded with a purely positive component at a depth of 400 μm (fig. 5:20 b). As the electrode advanced a further 10 μms, a large typical diphasic extracellular soma spike was recorded at a lower gain in figure 5:20 c. The position of the spike-producing structure was localized to layer 2 of the tectum by depositing a small dye spot (fig. 5:13 d).

B. MORPHOLOGY

Electron micrographs of the optic tectum reveal layer 8 to comprise a band of somata enmeshed in axons and dendrites. More superficial to layer 8, there is a dense network of axonal and dendritic profiles, with the occasional cell soma. Synaptic glomeruli (Székely et al, 1973) are also evident in layer 9.

Synapses are readily apparent in layer 9 (fig. 5:21 a). Figure 5:21 b illustrates a presynaptic terminal in greater detail. It is an unmyelinated fibre terminal located at a

Fig. 5:20 (a) A monophasic brief negative wave superimposed on a slower 'inverted' wave recorded at a tectal depth of 350 μm. The latency of the brief negative wave is similar to that of an m_2 wave. With further penetration of the microelectrode to 400 μm depth the brief wave inverted in polarity and a monophasic positive potential was recorded (b). With an additional microelectrode advance of 10 μm a large, typical diphasic extracellular soma spike was recorded.

The rapid potential changes in these records have been retouched for clarity.

5·20

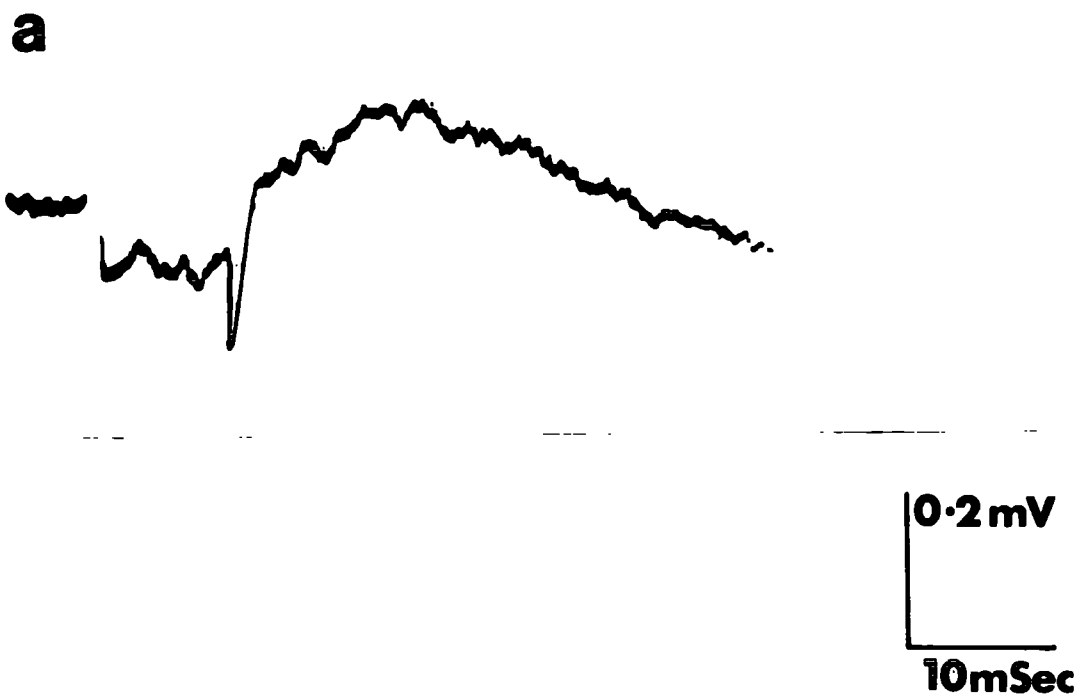

Fig. 5:21 Synapses in the superficial part of layer 9 in Xenopus tectum

(a) Numerous synapses (S) are located in the most superficial part of the tectum and are formed between an axon and a dendrite (for example S_1) or between two dendrites (for example S_2). An unmyelinated fibre which ends in terminal (large S) forms a synapse with a dendritic spine and is enlarged in figure 5:21 b.

(b) An unmyelinated fibre (U) containing microfilaments has a terminal swelling (T) which is filled with synaptic vesicles and the occasional dense core vesicle (arrow). An assymmetrical synapse is formed with a small (0.28 μm) diameter dendritic spine (S). The dendrite (D) contains microtubules. The synaptic membranes are assymmetrical, the postsynaptic membrane is thickened on the cytoplasmic face. The morphology suggests a Type 1 terminal of Szekely et al (1973).

(c) Five terminals are illustrated (1 a-d and 3 D). Terminals 1 a and 1 c are filled with synaptic vesicles and 1 a forms a synapse (s) with the profile 3 D. Terminal 1 b is also filled with synaptic vesicles and has a lightly stained mitochondrion (M). Terminal 1 d forms an en passant synapse with the profile 3 D prior to a terminal swelling T. The characteristics of terminals filled with vesicles and the presence of lightly stained mitochondria are indicative of optic afferents. (Type 1 terminals of Szekely et al, 1973) Terminals 1 a, 1 b and 1 d form assymmetrical synapses with profile 3 D. Profile 3 D contains a moderate number of synaptic vesicles and has a lighter background matrix than the type 1 terminals. This profile corresponds to a type 3 dendritic terminal of Szekely et al (1973).

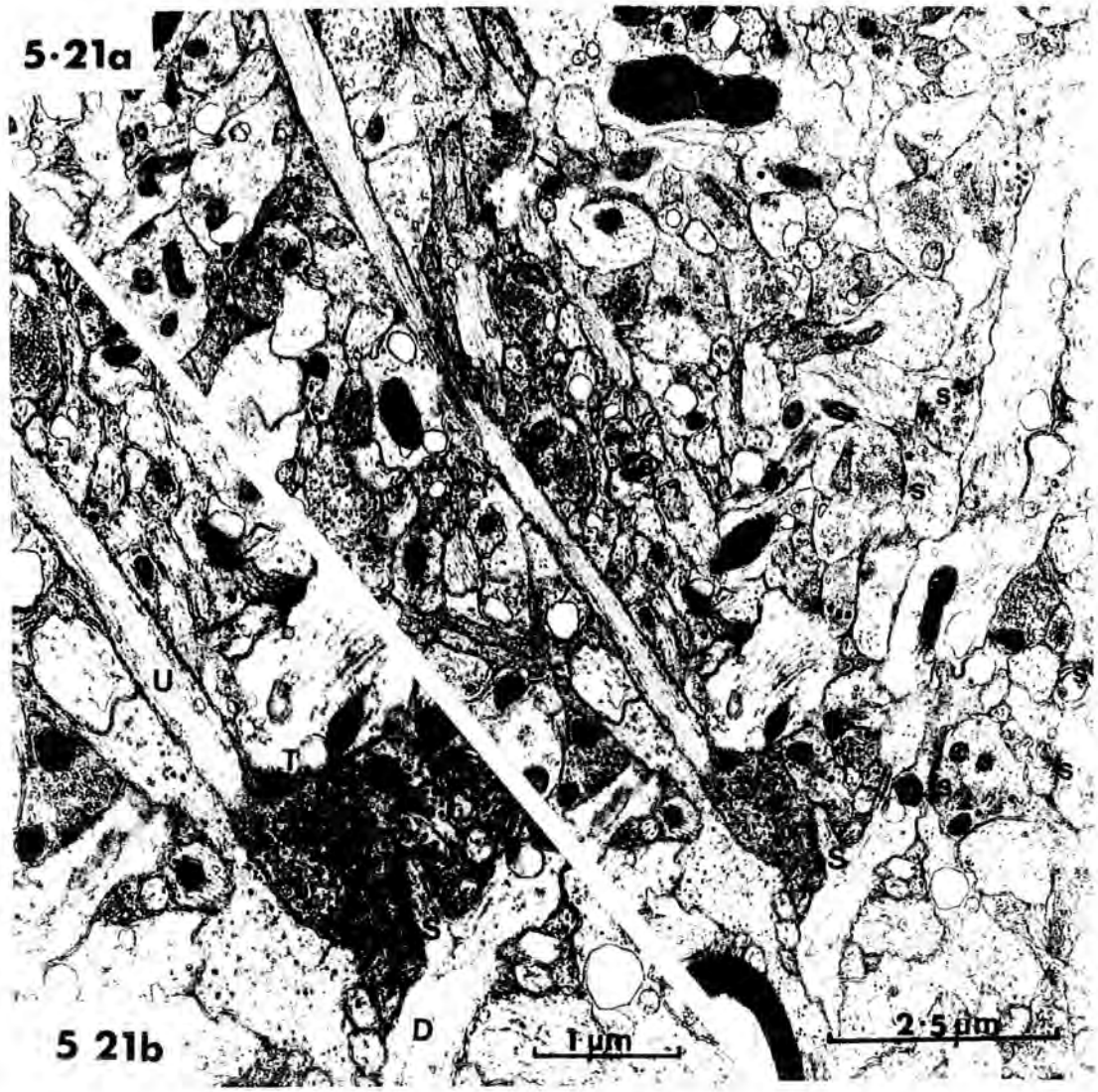
5·21a
U
T
S
S
S
S
S
S
S
S
S
5 21b
D
1 µm
2·5 µm

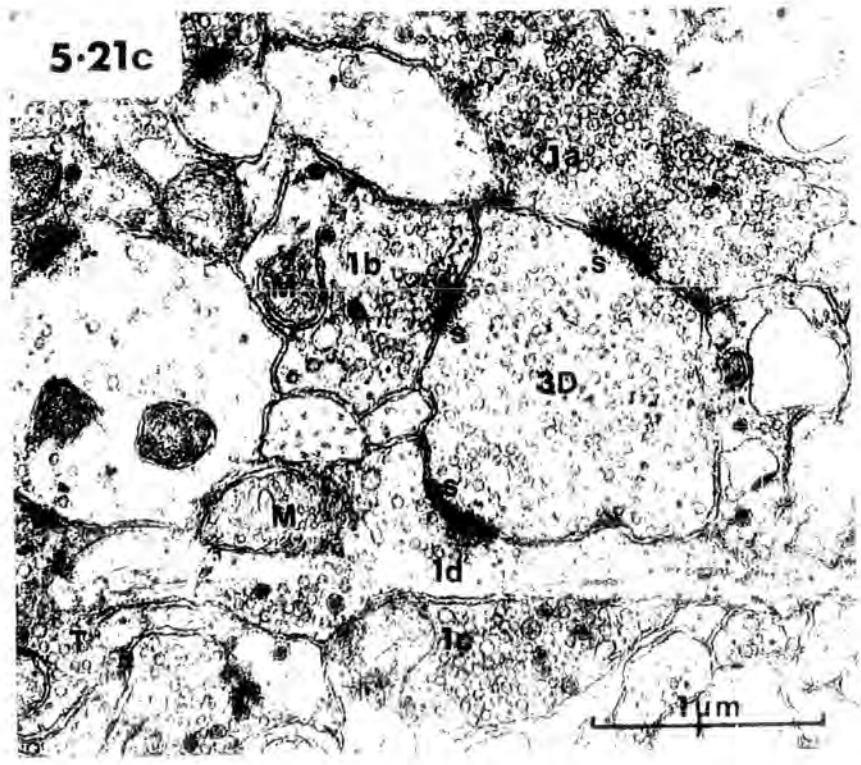
5·21c
1a
1b
S
3D
M
S
1d
T
1c
1 µm

depth of 49 μm from the surface. The axon contains microfilaments and microtubules and the terminal is densely packed with synaptic vesicles of different sizes. Two dense core vesicles are also evident (fig. 5:21 a, b). The synapse is formed with a small (0.28 μm diameter) dendritic appendage. The synapse is asymmetrical with an accumulation of dense material on the cytoplasmic side of the postsynaptic membrane. The morphology of this terminal suggests that it may be classified as Type 1, according to the terminology of Székely et al (1973), who regard these terminals as originating from optic afferents.

Figure 5:21 c shows a small group of terminals which are filled with synaptic vesicles and form a number of synaptic interconnections. These are Type 1 optic terminals (Székely et al, 1973). In the figure, four Type 1 profiles are present. Terminals 1a and 1c are full of vesicles and terminal 1a forms a synapse with a larger profile (3D). Terminal 1b similarly is packed with vesicles and has a lightly stained mitochondrion, which is also indicative of an optic afferent terminal (Székely et al, 1973). This optic terminal forms a synapse on to profile 3D. Profile 1d contains a lightly stained mitochondrion and forms en passant synapses with profile 3D. The beginning of a terminal swelling can be seen (T).

Profile 3D contains a moderate number of synaptic vesicles and has a lighter background than the Type 1 terminals. This profile corresponds to a Type 3 dendritic terminal (Székely et al, 1973). This Type 3 terminal is postsynaptic to terminals 1a, 1b and 1d, and is presumably presynaptic to a profile not apparent in this plane of sectioning. Note that the synapses formed by terminals 1a, 1b and 1d have a thickened postsynaptic membrane.

Figure 5:22 a shows an ascending, branching, layer 8 cell dendrite with abutting terminals, two of which are of optic afferent origin. One of these terminals forms a synapse on to the dendritic shaft. The vesicles in this synaptic terminal are fewer than in the other optic terminal present, but the mitochondria are not as heavily stained as in the other processes in the neuropil.

Figure 5:22 b is a low power micrograph of part of a layer 8 cell. A number of terminals are present, of which five form synapses with the base of the dendrite and one of these is of optic afferent origin. This terminal is shown in more detail in figure 5:22 c. It is densely packed with vesicles and has a postsynaptic membrane thickening with a mitochondrion present.

Optic afferents form synapses with layer 8 neurons (fig. 5:23 a, b). They are densely packed with vesicles and appear electron dense. Their synaptic membrane

Fig. 5:22 Optic terminal synapses on to the bases and shaft dendrites of layer 8 cells

(a) An ascending branching layer 8 cell dendrite with a butting terminals (T, OT). Terminal 'T' is full of synaptic vesicles but to synapses. Terminal 'OT' contains numerous vesicles and a lightly stained mitochondrion (M). The terminal forms a synapse (arrow) with one of the dendritic branches.

(b) A layer 8 cell body (L8) has five synapses on to the base of an ascending dendrite. Of these synapses (T) one is of optic origin (OT) and is shown in more detail in figure 5:22 c.

(c) Detail of the optic terminal (OT) of (b) above. Abundant synaptic vesicles are present, a mitochondrion (M) and a well developed post ynaptic membrane thickening to produce an assymmetrical synapse on to the base of the layer 8 cell dendrite.

5·22

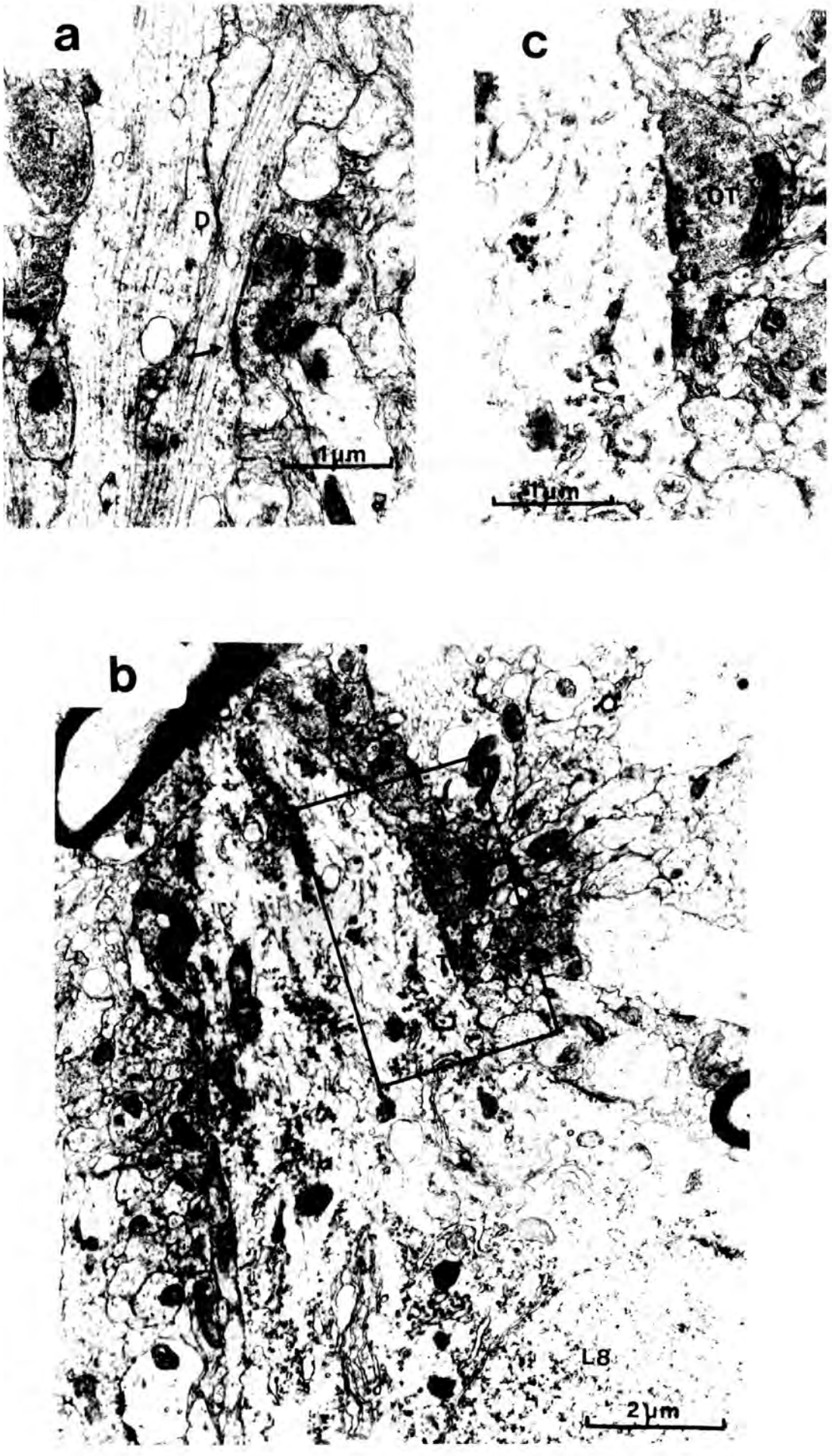

Fig. 5:23 Synapses on to the cell bodies of layer 8 cells

(a) A terminal (1) is filled with vesicles in a dense matrix. A synapse (arrow) is formed between this terminal (and the soma of a layer 8 cell. The terminal has the characterisitcs of a type 1 optic terminal (Székely et al, 1973).

(b) Two synapses on to a layer 8 cell body are evident (arrows). Terminal 1 is filled with vesicles within a dense matrix, and the synapse has a post-synaptic membrane thickening. This is a type 1 of Szekely et al (1973). In contrast the second terminal (X) has fewer vesicles which are in a lighter background matrix. The preterminal region is evident and is characteristic of a dendrite. This terminal may be a type 3 (Székely et al, 1973).

(c) The terminal 3 contains distributed synaptic vesicles. The terminal forms a symmetrical synapse (arrow) with a layer 8 cell body. This terminal may be characterized as a type 3 (Székely et al, 1973).

5·23

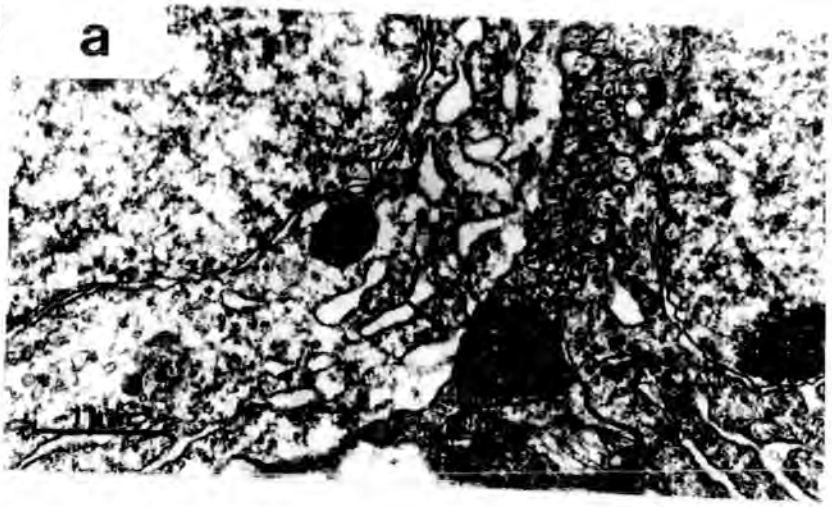

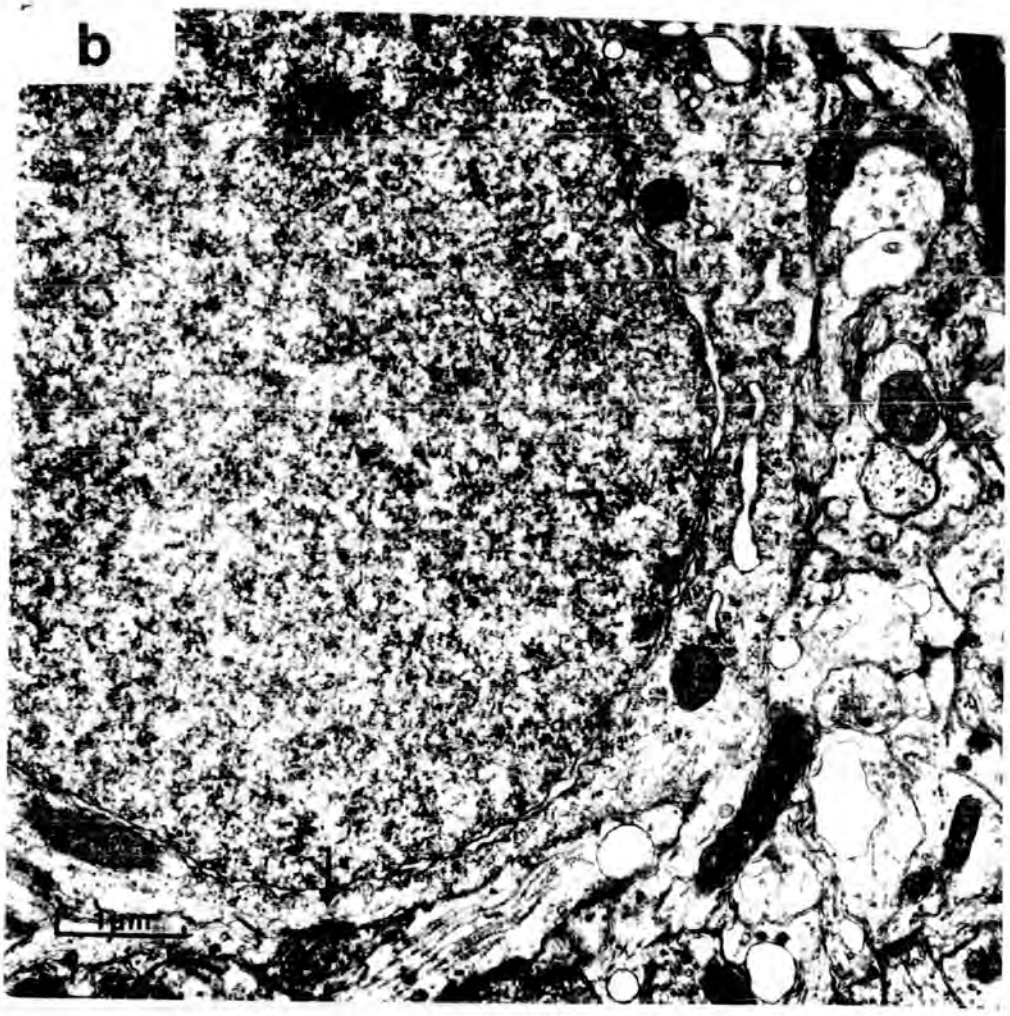

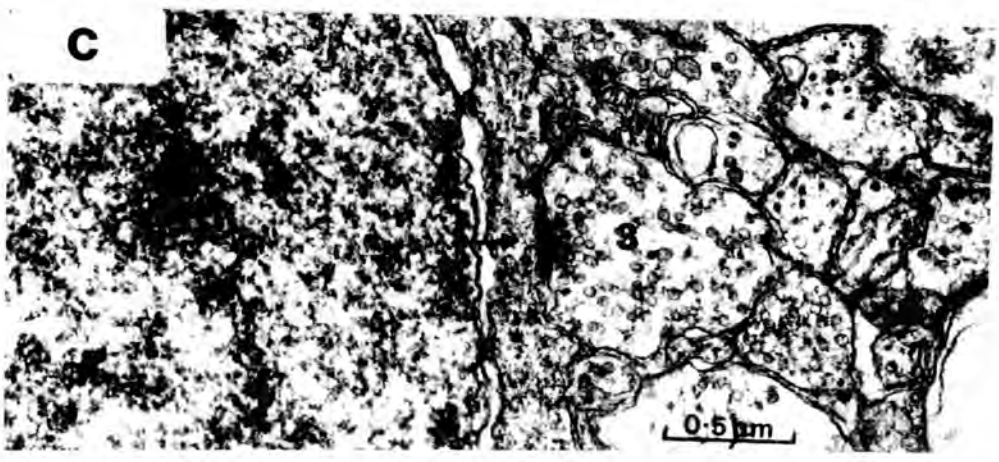

specialization is small (0.5 μm in figure 5:23 a) and 0.2 μm in figure 5:4 b) and densely stained. The terminal in figure 5:23 c, with its synapse on to a layer 8 soma, is different to those illustrated in figures 5:23 a and 5:23 b. Although the synaptic specialization is of a similar size to that of the previous examples (0.2 μm), it is symmetrically thickened and has only a few vesicles within a lightly stained matrix. This is a Type 3 terminal and is considered by Székely et al (1973) not to be an optic afferent.

DISCUSSION

The field potentials produced by a group of cells reflect, indirectly, changes in membrane current that occur in unison whether these be synaptic or action currents. A study of such potentials gives invaluable information concerning the average activity of the cells in a group and is a basic prerequisite for the understanding of the physiological characteristics of any neuronal assembly. When the anatomical arrangement of a neuronal group is well understood, the activity of the group as a whole can often be treated as if it were generated by a small number of "ideal" elements, with each element representing the activity of the particular cells which are activated synchronously from specific sites of stimulation (Hubbard et al, 1969).

A cell whose membrane potential is changed non-uniformily, so that one part of the membrane is depolarized more than another, will have cytoplasmic current flow. Together with this intracellular current, there is by necessity a corresponding flow of current in the extracellular medium, whereby the current path is completed. Since the conductivity of the extracellular field is finite, the current field is associated with an

extracellular potential field, the potential gradient at any point being proportional to the current flow. The extracellular field potentials generated from the transmembrane currents of a number of cells will summate linearly and algebraically at every point in space concerned. Thus cancellation of fields can occur (Lorente de Nó, 1947 a; Llinás and Nicholson, 1974; Nicholson and Freeman, 1975). The site of maximum amplitude of the extracellular potential is not necessarily the site of the maximum current sink. This is because a synchronous depolarization of a part of a neuron will not be detected by a microelectrode if the area activated is large with respect to the electrode tip, even if it is recording at the site of maximum activity. Since the whole neural surface near the recording site is at a new potential level, little or no current will flow between adjacent points of the membrane. Therefore only small potential differences will arise between the microelectrode and the reference zero electrode. On the other hand if the electrode is moved to a new recording site where the current distribution is not uniform, large potentials will be recorded at the new site (Hubbard et al, 1969).

In order to reconstruct transmembrane currents in any medium, it is necessary to measure the potential value from different sampling points at exactly the same moment in time after a stimulus since current flow is essentially instantaneous.

Evidence suggests that extracellular current produced by a particular neurone does not flow through the cell membranes of adjacent cells (Nicholson, 1973) since all membranes have a large capacity and high resistance. The distribution of transmembrane current results in a system of sources and sinks of current. On simultaneous activation of a densely packed ensemble of cells, the sources and sinks are numerous, dense, and may be regarded as being continuously distributed within a finite volume defined by the ensemble of active cells (Nicholson, 1973).

Synchronous activation of optic afferents produces synchronous depolarization of the tectal dendrites. Current flow into the dendrite at the postsynaptic membrane is distributed passively to the remainder of the cell. Intracellular current flow in the dendrite results in a small component of outward current flow across the dendritic membrane. However, the majority of the current reaches the cell soma and, since it is in this region that the space constant decreases abruptly (Katz, 1966), the current passes through the cell membrane to the extracellular space. Since the cells in the tectum have an arrangement of long ascending apical dendrites, the neuronal population is of the open field type (Lorente de Nó, 1947 a) and can be represented by a single pyramidal cell. Thus depolarization of the dendrite will produce a

dipole of inward current at the synapse and a distributed outward current passively extruded principally at the cell soma. Since the extracellular current passes through a medium of finite conductivity, a potential gradient is produced. The potential so produced can be recorded and is proportional to the transmembrane current (Llinás and Nicholson, 1974; Nicholson and Freeman, 1975).

A singe cell activated by afferent input generates an extracellular potential gradient in the microvolt range (Klee and Rall, 1977). Since the extracellular current arises from a system of sources and sinks resulting from the passage of current through the membranes of a number of individual neuronal elements, the resultant extracellular potential may be in the millivolt range. Klee and Rall (1977) carried out a theoretical analysis of extracellular field potentials in an attempt to explain the results obtained by Rall and Shepherd (1968), Shepherd and Haberly (1970) and Haberly and Shepherd (1973) in their studies on the olfactory bulb and prepyriform cortex. They have shown that a truely spherical cortical population of neurons generates an extracellular field potential which cannot be recorded outside the population. They also show that once a puncture has been made in the sphere and an open field cortical population has been produced, extracellular currents generated by the active cortical population may flow along one of two pathways, thus primary and secondary extracellular currents are produced (Rall and Shepherd, 1968). The primary current

flows within the cortical region and remains essentially radial. The secondary current flows from the inner cortical surface out through the puncture and in the region of the indifferent electrode to the outer cortical surface. This secondary current is responsible for two effects, a current shunt and a potential shift. By shunting some of the primary current a reduction in the potential difference generated across the cortex occurs to an extent of 5 to 15%. However, even if the potential difference generated across the cortex is decreased by 15% in this way, the effect is only on the magnitude of the depth profile, not on its shape. A second consideration in an open field situation is that since a zero isopotential line, with respect to a distant electrode, extends ad infinitum (Hubbard et al, 1969) the total parallel resistance of the secondary current path is divided into an outer and an inner secondary resistance, which are in series with each other. This pair of resistances divides the potential generated across the cortex and shifts the potential values within the cortex relative to a reference electrode. Therefore, while the locus of the zero potential of the depth profile may vary, the shape of the depth profile and hence the second derivative are not altered.

Before current source density analysis can be undertaken, four assumptions must be made if an ideal situation is to be realised.

(i) The synaptic and cell body layers should be well laminated.

(ii) The tectal cortical layers should be perfectly planar and have no structural gradients or electrical inhomogeneities.

(iii) Synchronous activation over a large area of the tectum is required.

(iv) The penetration of the recording electrode must be normal to the surface.

Under these conditions intracortical extracellular current flow generated by radially oriented cells is strictly perpendicular to the tectal surface.

However, these four assumptions can be regarded as being partially valid in the Xenopus tectum. Firstly, the cell body layers are not ideally laminated (fig. 5:13 a, b) and it is not known to what degree the synaptic layers are laminated. Secondly, while the tectal layers are not planar, they do run parallel to each other across the whole curvature of the tectum. Structural gradients do exist, such as between the plexiform and cellular layers, but it is not known whether these create extracellular electrical inhomogeneities. If the radial conductivities are not constant or are not known, the potential gradient

may not reflect accurately the magnitude and direction of the transmembrane current (Freeman and Stone, 1969; Haberly and Shepherd, 1973). Thirdly, synchronous activation by myelinated fibres is likely to occur within a given area of the tectum, since the latencies of myelinated fibre input show little variation. The situation is slightly different for unmyelintted fibres since it is known that the conduction velocities of these fibres are part of a broad spectrum (Chapter 3), which coupled with the conduction distance, indicates that the CAP is permitted to fractionate leading to non-synchronous activation of tectal cells. Non-synchronous activation of tectal neurons could lead to substantial horizontal current pathways and hence horizontal voltage gradients which would affect the depth profiles. Klee and Rall (1977) suggest that lack of synchrony and spatial register can be treated by modifying the population source currents. At any instant in time, the source densities can be thought of as the sum of the currents produced by the synchronous cells plus the time shifted currents produced by the leading and lagging neurons. Similarly, the current densities at any level will be derived from those cells in register plus shifted values from those above or below the main population. Fourthly, it is unknown whether the electrode penetrates the tectum normal to the surface. Even if this were the case, many neurons and their dendrites may not be arranged

perfectly perpendicular to the pial surface. However, the fact that the spatial distribution of current sources and sinks can be correlated with the known distribution of optic nerve terminals and cell bodies suggests that whatever departures from the above criteria occur, they have little significant effect on the conclusions drawn from the data.

Interpretation of current source density analysis results

The second derivative of the depth profile indicates that the u_2 current sink is localized in a region of the tectum about 100 μm from the surface (fig. 5:12 b) and has a small current source superficial to the sink and a much larger current source deeper in the tectum. The sink/source distribution corresponds to the dendrites and cell bodies of layer 8 neurons with respect to the second spatial derivative. A similar pattern is exhibited by the second spatial derivative of the m_2 postsynaptic depth profile (fig. 5:10) with a sharply localized current sink at a depth of 150 μm, bounded more superficially and deeply by two equally prominent current sources. This similar pattern of the second derivatives obtained from the u_2 and m_2 depth profiles in the tectum indicates that a region of inward current flow at an excitatory synapse draws current from regions which are located proximal and

distal to the synapse. The synapses can be regarded as being located on the main shaft of the apical dendrites of layer 8 neurons (fig. 5:10).

A slightly different distribution occurs for the u_1 postsynaptic wave. The second spatial derivative has one sink and one source which are located at 70 and 150 μm respectively. The prominent current source is located in the region of the layer 8 cell somata and the bases of their ascending apical dendrites. These results suggest that u_1 synapses are located at the apices of the tectal dendrites, since a more superficial current source is absent.

Since second spatial derivatives are highly sensitive to small changes in the depth profile and calculations are based on the rate of change of potential, the indicated location of the maximum inward current sink may be subject to error. In u_1 waves the wave amplitude alters only slowly for the first 50 μm of penetration. As a result the location of the superficial sink may in fact be as far as the extreme terminals of the apical dendrites at the pial surface and not as a discrete band as suggested by the second spatial derivative.

A source-sink distribution could not be determined for the m_1 wave in Xenopus or Rana, although the location of the dye spot indicates that the synapses are located below layer 8. However, the present study provides no data on the location of the postsynaptic neurons. Chung,

Bliss and Keating (1974) have evidence that the m_1 post-synaptic cell bodies are located in layer 8.

Comparison with other studies of tectal field potentials

The optic tecta of non-mammalian vertebrates have often been the subject of investigations to determine the response of tectal components to an electrical stimulus applied to the optic nerve. These studies have been carried out principally on fish (Motokawa et al, 1958; Konishi, 1960; Sutterlin and Prosser, 1970; Vanegas, Essáyag-Millán and Laufer, 1971; Vanegas et al, 1974) or birds (Cragg et al, 1954; Holden, 1968 a, b; Stone and Freeman, 1971; Mori, 1973; Rager, 1976 b). Only two studies have been reported for reptiles (Heric, 1964; Heric and Kruger, 1966) and only three for amphibians (Peretz, 1969; ter Keurs, 1970; Chung, Bliss and Keating, 1974). The responses evoked from the tectum are complex in all non-mammalian species studied.

An interesting feature of all these studies is that, as in Xenopus, the tectum is innervated by afferent ganglion cell axons which have different conduction velocities (Holden, 1968 b; Stone and Freeman, 1971; Vanegas, Essayag-Millan and Laufer, 1971; Mori, 1973; Chung, Bliss and Keating, 1974; Vanegas et al, 1974; Rager, 1976 a, b).

Ipsilateral responses

All studies on the retinotectal projection using anterograde degeneration, autoradiography and horseradish peroxidase transport, have shown that the retinotectal projection in amphibia is totally crossed (Székely and Lázár, 1976; review by Scalia, 1976). However, Neary (1976) using autoradiographic tracing methods, obtained evidence for an ipsilateral retinotectal pathway in Rana, Bufo, Bombina and Xenopus. The results illustrated in figure 5:2 e show that activity can be recorded in the ipsilateral tectum in response to a stimulus applied to the optic nerve. The potential waveforms recorded may be elicited by four possible mechanisms:

(i) they may be an extension of the potential field generated by the contralateral tectum (Lorente de Nó, 1947 a; Hubbard et al, 1969),

(ii) they represent activity which is relayed to the ipsilateral tectum via the thalamus or the contralateral tectum,

(iii) they are produced by impulses in retinal ganglion cell axons, which arise by the synchronous current flow in fibres of the contralateral optic nerve, since the ganglion cell axons interdigitate at the chiasm,

(iv) they are produced by the activation of a direct ipsilateral retinotectal pathway, as suggested by Neary (1976), Picouet and Clairambault (1976) and Gaillard and Galand (1977).

Experiments were not performed to test these alternatives.

Contralateral responses

Potential waves have been recorded in the optic tectum of Rana (Peretz, 1969; ter Keurs, 1970; Chung, Bliss and Keating, 1974). The former two studies recorded three potential waves which correspond to the m_2, u_1 and u_2 waves reported here. In agreement with the present results for Xenopus, Chung, Bliss and Keating (1974) reported four postsynaptic potential waves, two being maximally negative close to the surface and two being maximally negative deeper in the tectum.

Peretz (1969) and ter Keurs (1970) monitored field potentials at different depths in the optic tectum of Rana. Solely on the evidence of presynaptic elements, Peretz concluded that the optic afferent terminals are distributed throughout the tectal plate. Ter Keurs (1970) used the activation of single postsynaptic units as an indication of the location of the postsynaptic elements in Rana, in the same way as Holden (1968 b) has

done in the pigeon. Ter Keurs concluded that the three waves evoked in the tectum were produced by the arrival of impulses in the afferent fibres (the first wave), which depolarize layer 6 cells (the second wave) which in turn depolarize other layer 6 cells (the third wave).

Although the absolute depth values for the location of the maximum current sources and sinks are different in Xenopus and Rana for the m_2, u_1 and u_2 waves, the events appear in the same sequence during a single electrode penetration from the tectal surface.

Chung, Bliss and Keating (1974) reported typical values for the depths of the four maximal current sinks in Rana to be 90, 130, 240 and 380 μm for the u_1, u_2, m_2 and m_1 respectively. These results are in reasonable agreement with those reported here for Rana with maxima at 60, 100 and 280 μm for the u_1, u_2 and m_2 waves. Chung, Bliss and Keating (1974) recorded a depth profile for the m_1 wave which was not achieved in the present study, although typical values for the maximum negativity of the m_1 wave appears to be a good indication of the site of the synapses.

The present results for Xenopus are qualitatively similar to those for Rana. However the quantitative results are rather different. The u_1 current sink of the postsynaptic neurons is located most superficially at a depth of 70 μm in Xenopus and 60 μm in Rana. The

depths of the current sources differ greatly between the two species, with a value of 180 μm in Xenopus and 390 μm in Rana. However, current source density analysis demonstrates that the afferents impinge on to the apical dendrites of layer 8 cells. Although the depth distributions for Xenopus are quantitatively at variance with those obtained for Rana, this is a reflection of the different tectal thicknesses, hence the distribution of optic afferents in the Xenopus optic tectum may be regarded as homologous with those obtained from Rana species.

Postsynaptic activated unitary potentials

Action potentials have been recorded in the optic tectum in response to optic afferent stimulation. These action potentials cannot be ignored and have either been shown to be presynaptic (fig. 5:6) or postsynaptic (fig. 5:18 d, e). The presynaptic action potentials are usually recorded in the regions which correspond to the locations of the maximum negative amplitudes of the evoked waves. The postsynaptic action potentials are likely to be soma/axon potentials or alternatively dendritic spikes.

Negative monophasic potentials (fig. 5:19 c, d) on the negative going phase of the evoked wave are indicative of dendritic spikes (Stone and Freeman, 1971).

There have been a number of reports of dendritic action potentials in the non-mammalian central nervous system for example in the cerebellum of the alligator (Llinás and Nicholson, 1971; Nicholson and Llinás, 1971). Other workers have reported dendritic spikes in the optic tectum of non-mammalian species, in the teleost Eugerres (Vanegas, Essáyag-Millán and Laufer, 1971) in Rana (Chung, Bliss and Keating, 1974) in Necturus (Caldwell and Berman, 1977) and in the pigeon (Stone and Freeman, 1971).

Monophasic positive and diphasic waves on the negative m_2 wave and on the inverted 'u' waves were usually recorded in the region of the cell bodies of layer 8. Similar potentials have been reported by Shepherd (1962, 1963) and Haberly (1973) in the olfactory bulb and prepyriform cortex in response to synchronous afferent stimulation. The action potentials superimposed on the 'u' waves are usually smaller than those superimposed on the m_2 wave. Recordings from the latter units could usually be maintained for a longer period of time, this fact in conjunction with the larger size of the spikes may indicate that the m_2 afferents synapse on to a ~~larger~~ larger population of neurons. Unitary potentials could also be recorded occasionally in the stratum periventriculare.

The long latency unitary potentials are probably evoked as a consequence of polysynaptic activity, such as that relayed via the diencephalic visual centres.

CHAPTER VI

Sequence and distribution of optic afferent innervation to the developing tectum

INTRODUCTION

In preceeding chapters the morphogenesis of the optic nerve and the physiogenesis of ganglion cells and their axons were studied. In Chapter 5, electrophysiological methods were used to determine the location and the properties of optic afferent synapses in the Xenopus tectum. The present chapter deals with the synaptogenesis of ganglion cell axons in the tectum and the properties of these synapses.

Although the development of the optic tectum of Xenopus has been the subject of a number of investigations (Straznicky and Gaze, 1972; Lázár, 1973; Gaze et al, 1974; Scott, 1974; Scott and Lázár, 1976), only one study has been concerned with the responses of postsynaptic neurons to afferent activity (Chung, Keating and Bliss, 1974).

The optic afferent input to the optic tectum of adult Xenopus is laminated (Chapter 5) and there is good correlation between the retinal ganglion response types, their conduction velocities and their sites of termination (see General Discussion). It is known that

the first axons to appear in the optic nerve are unmyelinated and that ganglion cell responses are different from those of the adult, it is therefore important to determine whether these retinal ganglion cell afferents synapse in the tectum. The properties of these synapses were investigated and the postsynaptic potentials were correlated with the CAPs recorded in the adult tectum.

Electron microscopical analysis of the locations of synapses and their time of origin in the tectum do not produce unequivocal evidence of innervation since other afferent fibres may also be developing. However, the use of physiological methods to locate and characterize the synapses is extremely useful if carried out in conjunction with morphological studies.

Studies of the normal development of the amphibian retina (Hollyfield, 1968, 1971; Straznicky and Gaze, 1971) have shown that growth occurs by addition of cells at the ciliary margin, although this development is not truly concentric (Jacobson, 1976; Straznicky and Tay, 1977). During tadpole development the tectum grows from its rostroventrolateral pole to its caudodorsomedial pole in a curvilinear fashion, the cells being generated in a series of roughly parallel 'developmental bands' (Straznicky and Gaze, 1972; Currie, 1974). The first neurons to be generated and to differentiate are found

at the anterior pole, and the first axons to innervate the tectum are also located in this region (Currie, 1974; Currie and Cowan, 1975).

In previous studies the sequence of tectal invasion by optic nerve fibres during development has been analyzed in material prepared by various, relatively non-specific histological methods. For example, using acid haematoxylin histology Kollros (1953) described what he thought to be optic nerve fibres at the rostral pole of the tectum in Rana pipiens at embryonic Stage 23, and regarded them as having reached the caudal pole by larval stage IV (Taylor and Kollros, 1946). Straznicky and Gaze (1972) have suggested on the basis of a study of Holme's silver preparations, that many of the fibres which comprise the white matter at the rostral end of the Xenopus tectum at Stage 41 are retinal afferents. This conclusion is by no means certain since it is impossible to determine the origin of the fibres in question in this type of material. The results of Currie (1974) and Currie and Cowan (1974) who used autoradiographic tracing methods in tadpole Rana pipiens suggest that retinal ganglion cell terminals are present in the tectum from embryonic Stage 23.

Most physiological studies of the anuran optic tectum have been concerned with recording ganglion cell responses at their terminals in the tectum and not with the connexions and processing of information

by tectal neurons. Field potentials may be used to determine at what stages functional synapses are formed and to discriminate between excitatory and inhibitory actions. Information about the location of postsynaptic neurons may also be obtained.

METHOD

A. PREPARATION OF THE ANIMAL

Twenty-four tadpoles and fifteen juvenile toads were used in this study. The brains were exposed as described in section B of the General Methods. The forebrain was removed by suction and a small hole was made in the sclera of the eye to facilitate the entry of a stimulating electrode. All animals were immobilized with 0.02 to 0.05 mg d-tubocurarine (Duncan, Flockhart and Co. Ltd., London) administered by injection into the leg of young toads and behind the non-experimental eye in tadpoles (Gaze et al, 1974). Preparations were half submerged in Niu-Twitty solution and were covered with a medical wipe tissue. The Niu-Twitty solution was not permitted to come into contact with the brain in order to avoid attenuation of the evoked potentials. To avoid dessication all exposed surfaces were covered with paraffin oil.

B. ELECTRODES

Wood's Metal-in-glass or stainless steel electrodes were used to deliver stimulating pulses and were manufactured as described in the Methods section of Chapter 4.

Silver/silver chloride wires and glass micropipettes were used for recording and were manufactured by the procedure described in section B of the Methods of Chapter 5.

C. RECORDING PROCEDURE

The recording procedure for tadpoles and young toads was essentially the same as for adults, and is described in section C of the Methods of Chapter 5. However, stimulating pulses were delivered only to the optic nerve head and not to the optic nerve itself.

D. MORPHOLOGY

The morphology of single neurons within the tectum of Xenopus tadpoles was studied using the Golgi impregnation method. Details of this procedure are given in section D of the General Methods.

The optic tecta of Xenopus tadpoles were processed for electron microscopy as described in section B of the General Methods.

RESULTS

A. MORPHOLOGY

Stage 46 was the earliest tadpole stage at which potentials could be evoked from the tectum and at this stage synapses were present at the anterior pole (fig. 6:1), but were scarce in any one electron microscope section of this area. The synapse illustrated in figure 6:1 is located 9 μm from the surface of the tectum and is surrounded by many axons which are presumed to be optic afferents. Some of these afferents are very small, less than 0.1 μm in diameter, and contain only one microtubule. The synapse contains a small number of synaptic vesicles, possesses a synaptic cleft and has a thickened postsynaptic membrane. However, in other presumably terminal processes, vesicles and vesicular structures are more plentiful. The presynaptic profile is believed to be an optic afferent since it is located at the surface of the tectum and is accompanied by a multitude of axons, all of which are alined along an anteroposterior axis. It is not possible, however, to verify the nature of the postsynaptic profile since very young larval material is affected adversely by the electron microscopical preparative methods.

Fig. 6:1 A coronal section of the superficial part of a Stage 46 tadpole tectum

The terminal (T) forms a synapse (arrow) with an unidentified postsynaptic structure, which is believed to be a dendrite. The terminal contains vesicles (V) and the presynaptic membrane is more electron dense than the cytoplasm. Between the pre- and postsynaptic strucutres a synaptic cleft is present. The cytoplasmic side of the postsynaptic membrane is thickened. In an adjoining profile the numbers of vesicles is greater and the vesicles are larger (LV). The large number of axons (some labelled 'a') are present and many are smaller than 0.1 μm and only contain one microtubule (Mt).

6·1

In Stage 46 tadpole optic tectum, synapses were rarely found being limited to the marginal zone to a depth of 25 μm. It was not until Stage 50 that axosomatic synapses were observed. Synaptic profiles observed before this stage are presumably axodendritic.

The Golgi method of impregnating neurons is extremely useful for determining the form of the constituent neurons of the tectum. In figure 6:2, two Golgi impregnated cells from the tectum of a Stage 49 tadpole are illustrated. The impregnated neurons clearly indicate well developed dendritic arborizations which are not arranged perpendicular to the surface, although they have not migrated from the ventricular zone (Boulder committee, 1970). As the tectum develops, obvious radial orientation is evident at Stage 55 at the anterior pole and at metamorphosis for the remainder of the tectum. However in the major part of the tectum, where cell proliferation or cell migration is occurring, a major number of neurons are arranged such that their dendrites are not radially oriented.

B. PHYSIOLOGY

Postsynaptic events and potentials

The earliest tadpole stage from which responses could be recorded was Stage 46. Figure 6:3 a shows a recording

Fig. 6:2 Morphology of tectal neurons in a Stage 49 tadpole

The figure shows camera lucida drawings in the left hand and light micrographs of the impregnated neurons in the right hand column. The top of the figure corresponds to the dorsal surface of the animal.

The upper pair of illustrations show a cell with a pair of ascending dendrites which are oriented 45° to the surface. The ascending dendrites have small club shaped sprigs (sp) and the cell body has an axon emanating from it. The cell body is located in the middle of the cell body layer. The lower pair of illustrations show a cell body whose apical dendrite gives rise to a complex dendritic tree which is oriented almost horizontal to the surface. Some of the dendrites have small spines (spine) in contrast to the club shaped sprigs of the upper illustration. An axon (Ax) originates at the base of the cell body.

Note the slightly different calibration between the upper and lower pairs of figures.

Golgi stain.

6·2

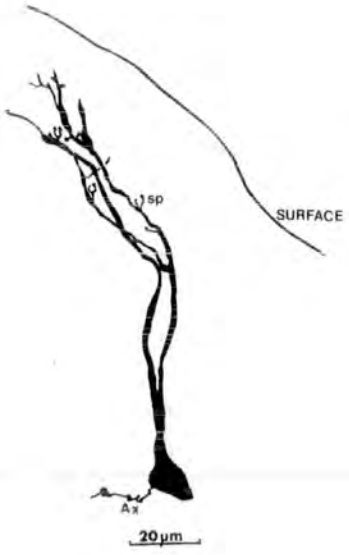

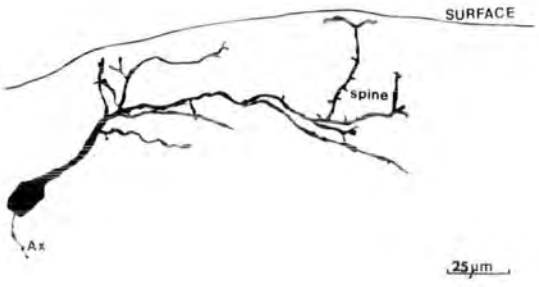

Fig. 6:3 Responses recorded in the tadpole tectum to an electrical stimulus to the optic nerve

(a) and (b) Records from a Stage 48 tadpole. Two large negative waves are present in (a) which was recorded at the surface of the tectum. Record (b) shows the response to the same stimulus recorded at depth. Note that the waves are the same except that they have inverted.

The latencies of these waves indicate that they are comparable to the u_1 and u_2 waves recorded in the adult.

(c) and (d) Similar responses from a Stage 52 tadpole to those above in (a) and (b). The surface recording (c) shows the u_1 and u_2 negative waves which invert as the electrode penetrates the tectum.

(e) Responses recorded from a Stage 59 tadpole to show the two 'u' waves and an 'm' wave which is superimposed on the stimulus artifact. The stimulus is submaximal to avoid loss of the initial 'm' wave.

Calibrations for (a) to (e) as indicated next to record (e). Electrode positivity is upward.

(f) Similar responses from a Stage 59 tadpole to that illustrated in (e). An 'm' wave and two 'u' waves are present. Calibration as indicated.

(g) Three waves are clearly evident in this record which was obtained from a two week old toad. These waves are the m_2, u_1 and u_2. A small inflexion (triangle) is superimposed on the stimulus artifact and this may be a small m_1 wave. Calibrations indicated.

6·3

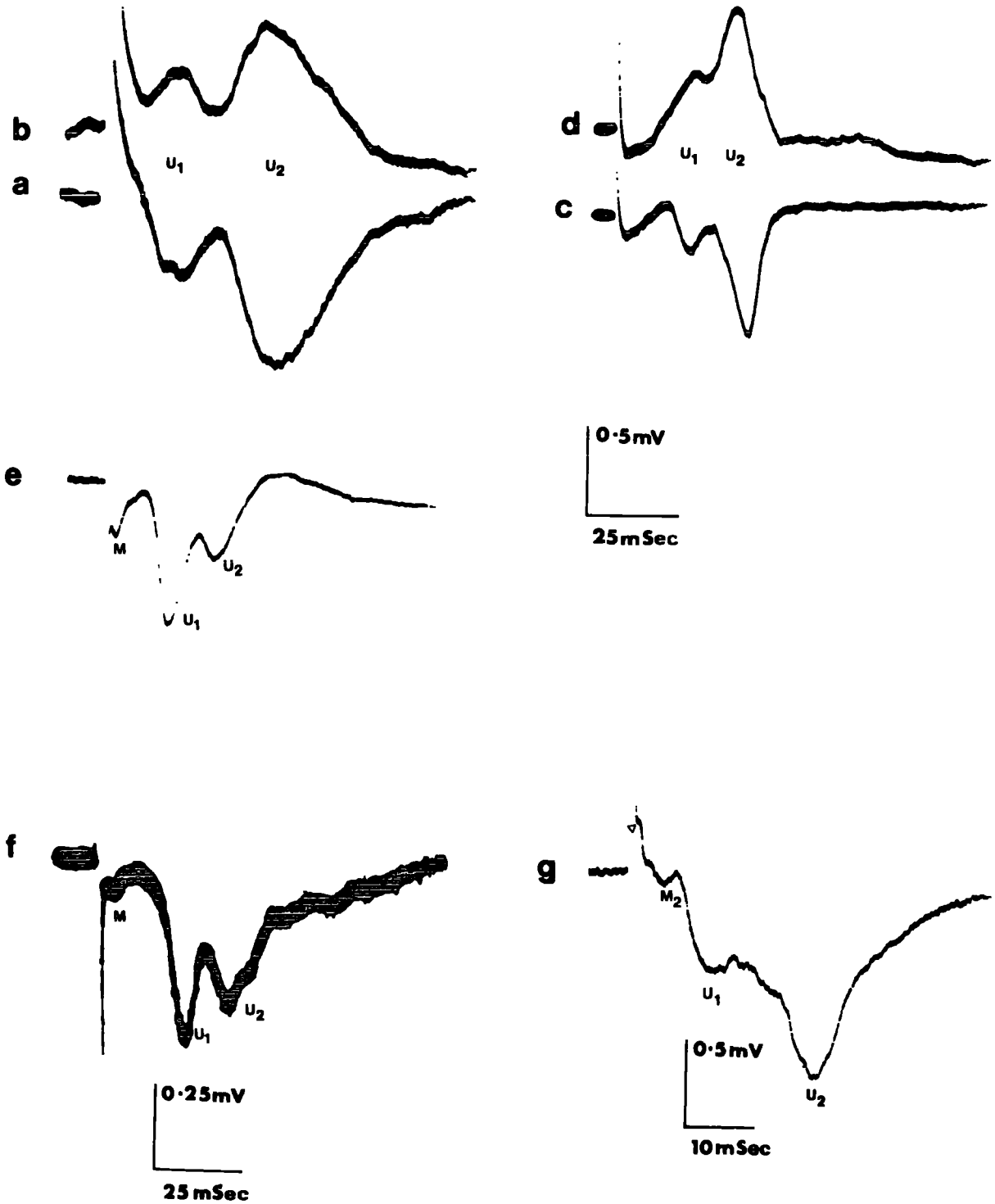
b
a
U1
U2
d
c
U1
U2
0·5mV
25mSec
e
M
U2
U1
f
M
U2
U1
0·25mV
25 mSec
g
M2
U1
U2
0·5mV
10mSec

of a potential evoked in response to an optic nerve stimulus in a Stage 48 tadpole. Note the two prominent negative deflections. The latencies of 20 and 58 msec indicate that these waves correspond to the u_1 and u_2 postsynaptic waves of the adult (Chapter 5). As the electrode penetrates the tectum, the waves invert from a negative to a positive polarity (fig. 6:3 b). The location of this reversal is uncertain due to the thinness of the tectum. Similar responses can be obtained from all older tadpoles, an example of which is shown for a Stage 52 animal (fig. 6:3 c, d). The responses comprise two negative u_1 and u_2 waves at the surface (fig. 6:3 c) which invert at deeper locations (fig. 6:3 d).

Up to the beginning of metamorphic climax only two waves can be recorded.

At Stage 59, a very short latency negative deflection can be evoked which is usually superimposed on the stimulus artifact (fig. 6:3 e, f). The latency of this wave is similar to an adult 'm' wave (figs. 5:1, 6:3 e, f).

Three waves can be recorded as the animal continues to develop. Two weeks after metamorphosis a small deflection with an extremely short latency inflexion can be recorded on the artifact. This inflexion occurs prior to the m_2, u_1 and u_2 evoked potentials (fig. 6:3 g) and may indicate the

first appearance of an m_1 wave. The m_1 wave is evident one month after metamorphosis.

A stimulus intensity tectal response series from a Stage 63 tadpole is shown in figure 6:4 a for the two 'u' waves and is represented graphically in figure 6:4 b. An electrical stimulus of 8 V produced no response, whereas 10 V elicited a small deflection on the trace base line at a latency equivalent to the u_2 afferent group of fibres. At 16 V the u_2 wave is much more prominent, and the u_1 wave is more evident. Both waves are prominent in response to a stimulus of 24 V. With increasing stimulus voltage the u_2 wave increases in amplitude continuously while the u_1 wave is distorted by an encroaching stimulus artifact (figs. 6:4 a, b).

Figure 6:5 a shows the effect of double stimuli on the u_2 wave from a Stage 63 animal. The results are represented graphically in figure 6:5 b. The graph compares the percentage increase of the evoked wave, with a potential evoked by a single stimulus. An interstimulus interval of 20 msec produces a potentiated response of 25%. As the interval increases the potentiated response increases and becomes maximal (60%) with an interstimulus interval of 50 msecs. Thereafter, the increase in the amplitude wave due to a conditioning stimulus is reduced as the inter-

Fig. 6:4 Stimulus strength - tectal response

The records of stimulus strength - tectal response characteristics are illustrated in (a) and represented graphically in (b). A 10 V stimulus evokes a small response which becomes more evident in response to a 16 V stimulus. The u_1 wave increases in amplitude with increasing stimulus intensity only slowly, whereas the u_2 wave increases in amplitude dramatically. The u_1 wave gradually becomes superimposed on the stimulus artefact, which is denoted by a dot. The u_2 wave is not saturated by a 60 V stimulus.

The figures below the traces indicate stimulus voltage. Note the change in the calibration for stimulus intensities of 30, 40, 50 and 60 V.

6-4

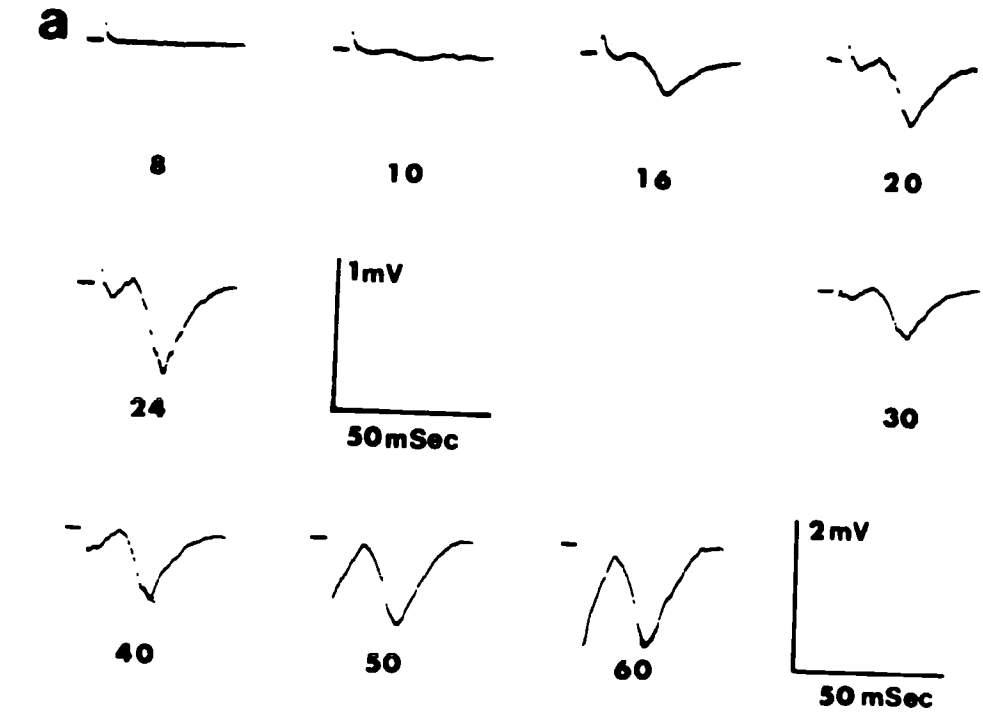
a
8
10
16
20
1mV
24
50mSec
30
40
50
60
2mV
50 mSec

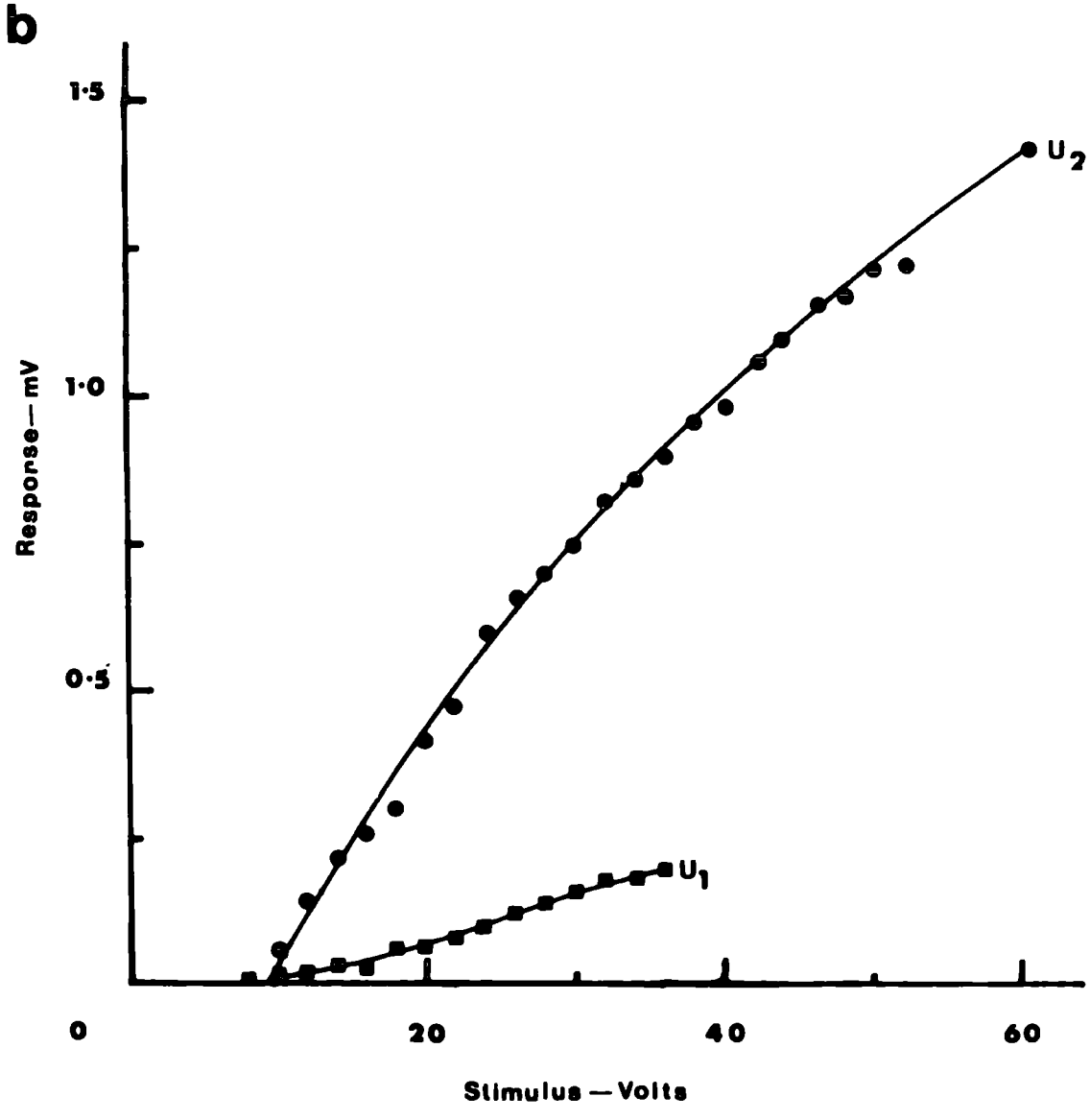
b
1·5
1·0
0·5
Response — mV
U_2
U_1
0
20
40
60
Stimulus — Volts

Fig. 6:5 U_2 wave potentiation at Stage 63

Records of the responses of the effects of double stimuli are shown in (a) and represented graphically in (b). When a stimulus preceeds the test stimulus by 20 mSec the test wave is potentiated by 25%. With increasing intervals the degree of potentiation increases and is maximal (60%) with an interval of 50 mSec. With even further increases in the interval the degree of potentiation decreases sharply at first and then more steadily and is only 5% with an interval of 200 mSec.

6·5

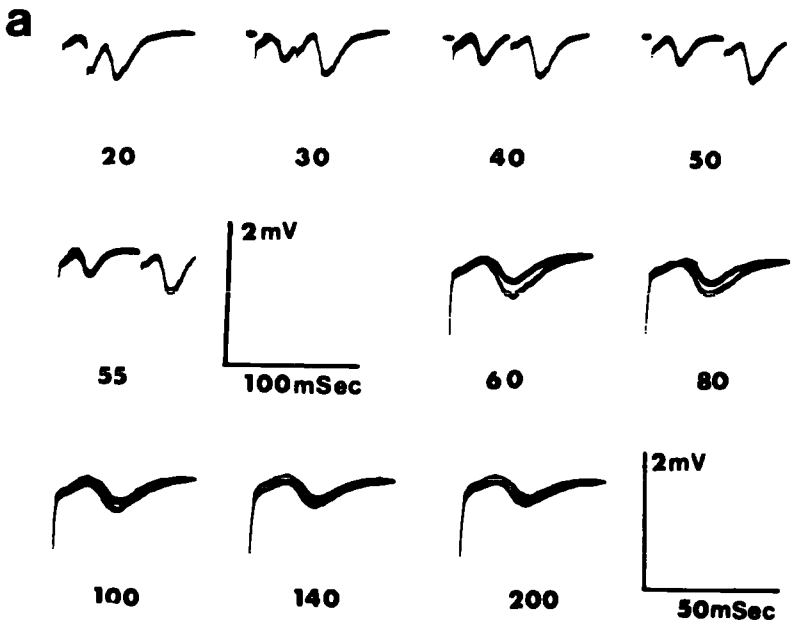
a
20
30
40
50
2mV
55
100mSec
60
80
100
140
200
2mV
50mSec

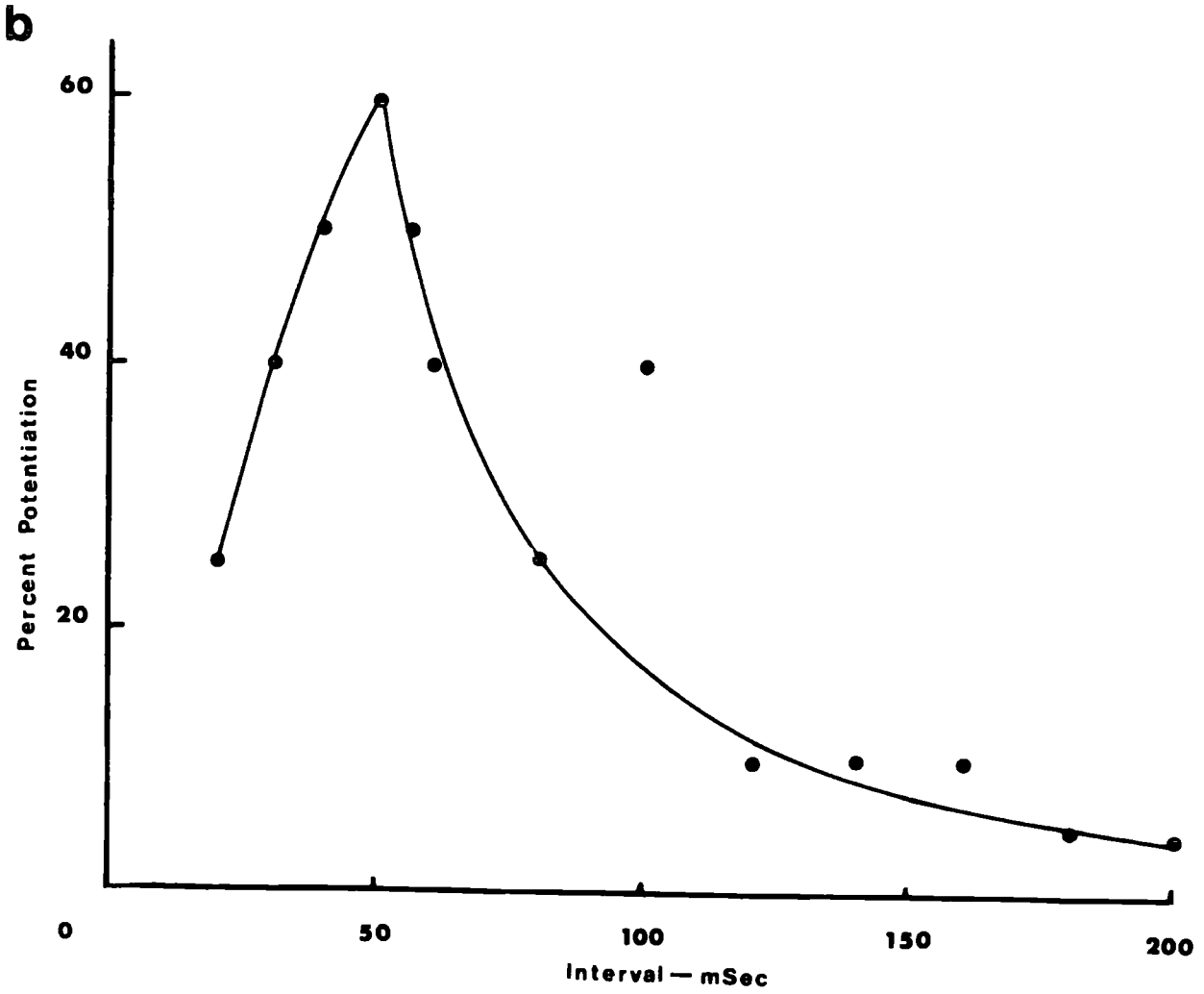
b
60
40
20
0
Percent Potentiation
50
100
150
200
Interval — mSec

stimulus interval increases until an interval of 200 msec, the potentiating effect is minimal. The inter-stimulus interval for which u_2 potentiation is maximum in a Stage 63 animal and the range of intervals for which potentiation occurs is similar to those values obtained in an equivalent experiment in the adult.

Figure 6:6 a shows the potentiated responses recorded from a Stage 57 tadpole, of both the u_1 and u_2 postsynaptic waves with an interstimulus interval of 160 msec.

The effects of a tetanizing stimulus train at Stage 57 can be seen in figure 6:6 b. When stimulu are applied to the nerve at a frequency of 0.25 Hz, all stimuli evoke the same response. At a frequency of 1 Hz the evoked u_2 wave is potentiated. At a frequency of 5 Hz the u_2 wave decreases in amplitude, while at 10 Hz the u_2 wave is not evoked after the initial stimulus.

These two tests of potentiating and tetanizing stimuli, combined with the fact that the polarity of the 'u' waves reverses with depth in the tectum indicate that these waves are derived from postsynaptic elements.

The effects of double and tetanizing stimuli on the 'm' wave in tadpoles could not be tested thoroughly. The nature of this wave can therefore only tentatively be assumed to be postsynaptic.

Fig. 6:6 Evidence for postsynaptic nature of the evoked wave

(a) The response to double stimuli is shown in this figure. The dots above the trace indicate the time of stimulation. The second u_2 wave is clearly potentiated by the conditioning stimulus. The interval between stimuli is 160 mSec. Filled circles indicate the position of the stimuli.

(b) The effects of mild tetanizing stimulus trains on the u_2 wave are shown. A pulse train at a frequency of 0.25 Hz shows the constancy of the response. The record of the response to a stimulus pulse train a 1 Hz shows a small degree of potentiation. The response to a stimulus train at 5 Hz decreases in amplitude after the initial normal response. The response fails after the initial normal response to a stimulus train at 10 Hz.

(c) The response recorded in the tectum of a Stage 62 tadpole shows a u_1 wave (U_1) and is preceeded by a brief diphasic potential. Evidence from tetanizing stimulus trains suggests that it is a presynaptic action potential.

(d) In the same Stage 62 tadpole an 'm' wave (M) is followed by a triphasic potential which is indicative of a postsynaptically activated spike.

Calibrations are as indicated for each figure.

6·6

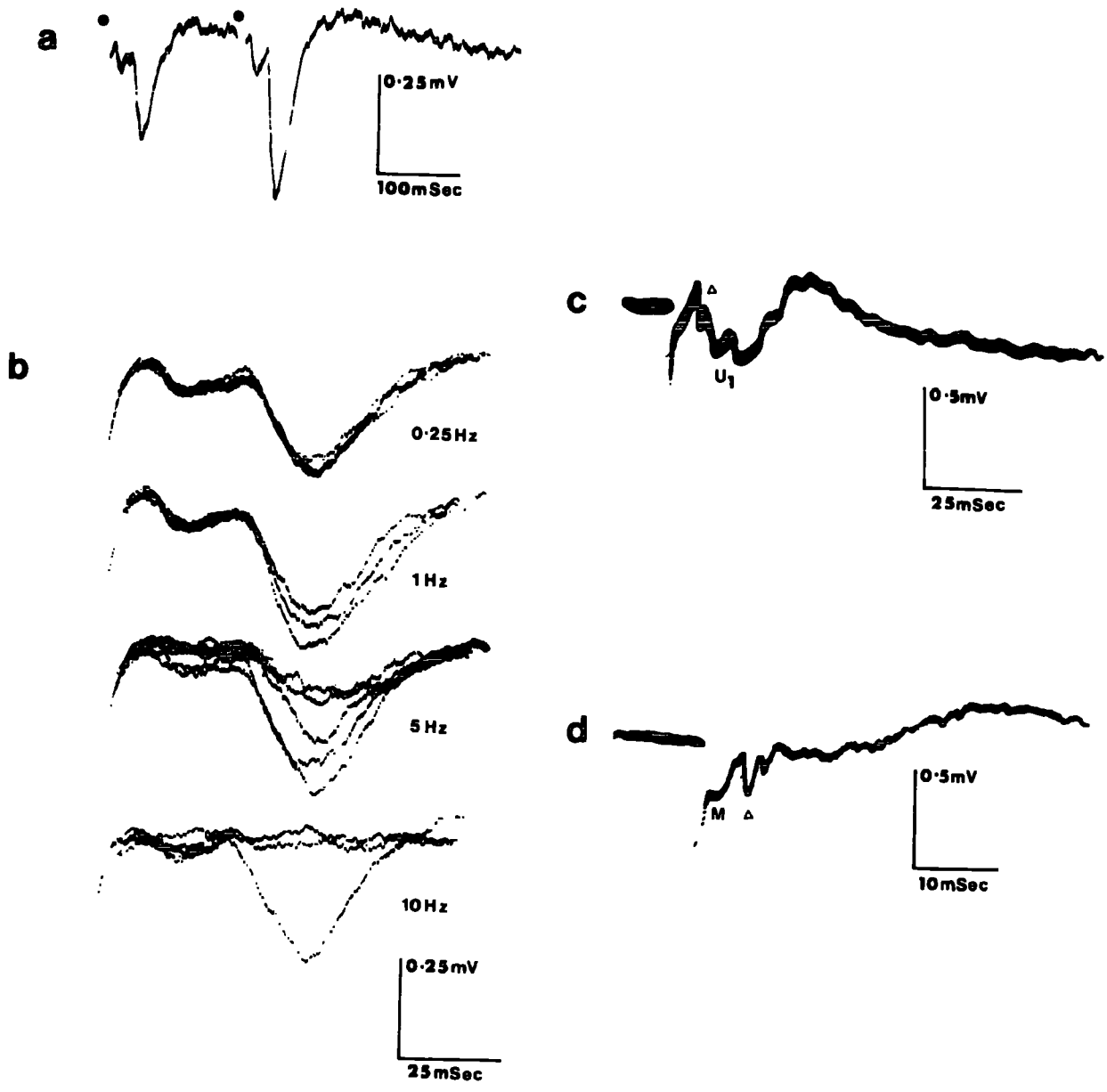
a
0·25mV
100mSec
b
0·25Hz
1Hz
5Hz
10Hz
0·25mV
25mSec
c
Δ
U1
0·5mV
25mSec
d
M
Δ
0·5mV
10mSec

Unitary Potentials

The waves elicited in the tectum may be preceded by a small presynaptic component, a diphasic example of which is illustrated in figure 6:6 c. In the same Stage 62 animal, an 'm' wave was evoked which was followed by a small triphasic spike, which indicates that an action potential passed the electrode tip (fig. 6:6 d) and may indicate the activation of a postsynaptic neuron.

Similar small triphasic spikes have been recorded in association with other potential waves. The responses illustrated in figure 6:7 a were obtained on the same electrode penetration. A small diphasic spike preceeding the u_2 wave was recorded at a depth of 100 μm. At 110 μm depth, small triphasic spikes were present on both 'u' waves, and at a depth of 160 μm a number of these spikes could be recorded on the inverting waves.

Small negative deflections are illustrated in figure 6:7 b at depths of 170 and 180 μm in a Stage 58 tadpole tectum. The shape of these negative deflections indicate that they comprise part of a discharge of action potentials orginating from one neuron. As in the adult tectum, monophasic positive spikes can be recorded in the tectum in response to an electrical stimulus to the nerve. An example is shown (fig. 6:7 c) which was recorded at a depth of 290 μm in the tectum of a Stage 57 tadpole.

Fig. 6:7 Unitary potentials

(a) Unitary potentials (triangles) are evident at the three depths from which recordings were taken in a single electrode penetration into the tectum of a Stage 55 tadpole. At a depth of 100 μm a brief diphasic presynaptic spike preceeds the postsynaptic wave. At 110 μm the same diphasic spike is evident and is followed by a triphasic potential. At a depth of 160 μm three small triphasic spikes are present on the inverted u_2 wave.

(b) Records at the indicated depth of 170 and 180 μm in a Stage 58 tadpole tectum. A brief diphasic spike preceeds the u_2 wave. During the u_2 wave two or three negative deflections are present (triangles). The constancy of shape of these potentials possibly indicate the same origin.

(c) A purely monophasic spike (triangle) is superimposed on an inverted u_2 wave in the tectum of a Stage 57 tadpole.

(d) Purely monophasic multiple discharges recorded at a depth of 250 μm in the tectum of a Stage 58 tadpole. The spikes are superimposed on an inverted u_1 wave. The discharges were usually of two spikes although occasionally more were evoked. Lower calibration time scale refers to lower trace.

Calibrations are as indicated.

6·7

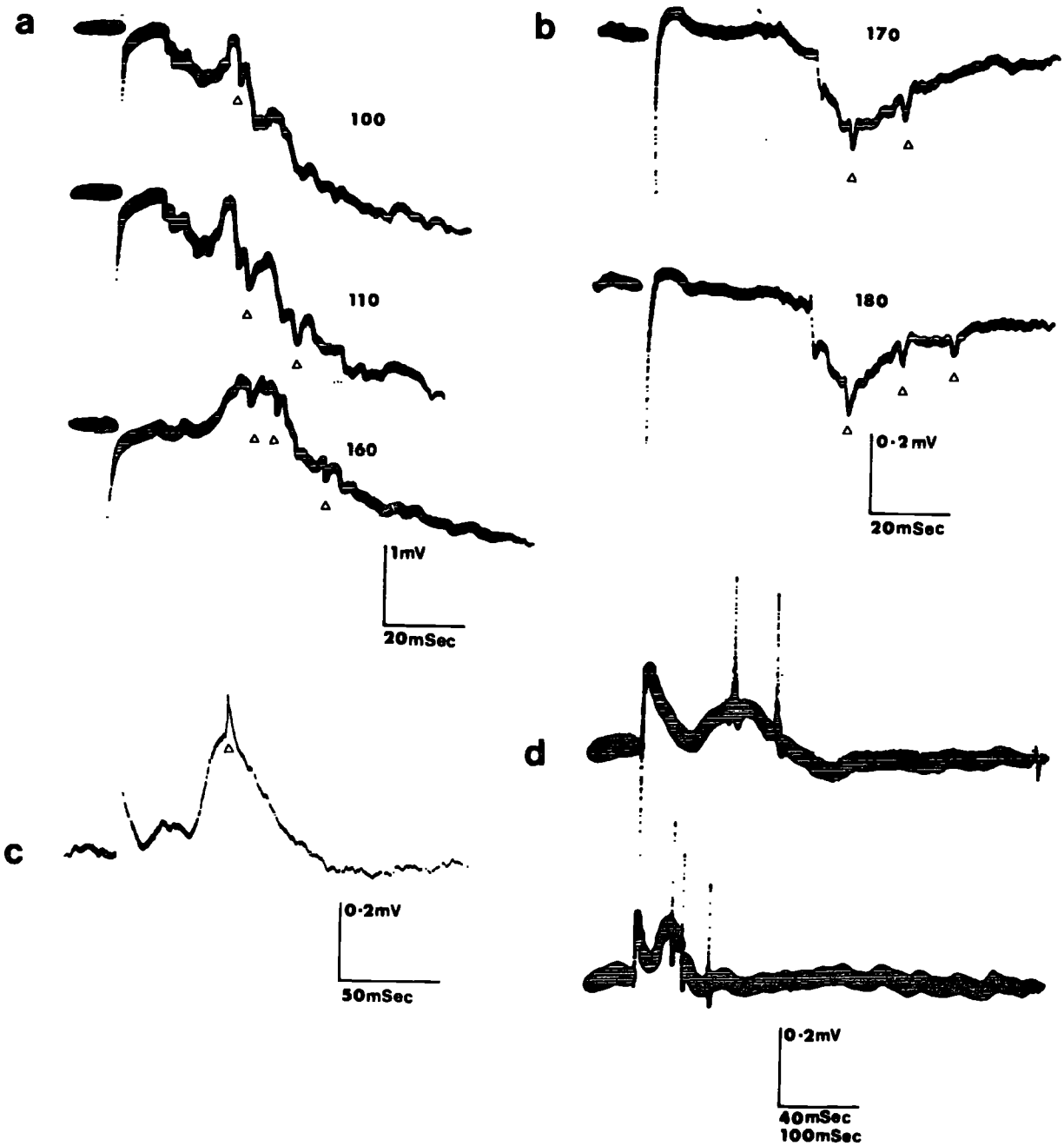
a
100
110
160
1mV
20mSec
b
170
180
0·2mV
20mSec
c
0·2mV
50mSec
d
0·2mV
40mSec
100mSec

Figure 6:7 d shows the responses of a postsynaptic neuron recorded at a depth of 250 μm in the tectum of a Stage 58 tadpole. The spikes are superimposed on an inverted u_1 wave and are evoked every time by a stimulus to the nerve which elicits a burst of action potentials. The earliest stage at which similar action potentials could be recorded was Stage 48, then only at the antero-lateral pole of the tectum. The earliest stage at which postsynaptic spontaneous activity could be recorded was Stage 58.

Field Potential Analysis

Tectal dendritic arborizations, while clearly well developed at Stage 48, are not radially oriented (fig. 6:2). This point, in conjunction with other problems such as the variable thickness and the softness and stickiness of the tectal plate, makes the use of current source density analysis inapplicable in determining the locations of the optic afferent synapses and postsynaptic neurons in the tadpole tectum. When the method was attempted, variable results were obtained and no detailed results are reported.

The general features of electrode penetration in tadpole tecta are described. The potentials evoked by unmyelinated fibres, which are comparable to the u_1 and u_2 waves of the adult, can be recorded as negative potentials through most of layer 9 of the tectum.

The 'm' wave which is elicited in Stage 59 tadpoles is located deeper in the tectum than the 'u' waves. In a Stage 62 tadpole, dye was deposited at two sites which correspond to the site of maximum negatives of the 'm' wave and the u_1 wave (fig. 6:8). The u_1 dye spot is located just superficial to the main band of cell bodies of layer 8 cells, and the m dye spot is located slightly deeper within the layer of somata. In the adult, these two locations correspond to the maximum negatives of the m_1 and m_2 waves. In the tadpole tectum a maximally evoked u_2 wave could be recorded over a range of depths, and this fact possibly indicates that synapses are distributed throughout layer 9 of the tectum, since the potential wave decreased and inverted sharply.

The adult pattern of current sources and sinks appeared at about one month after metamorphosis.

Fig. 6:8 Deposited dye spots

Two dye spots were recovered in the same section of a Stage 62 animal. The penetration was made at the anterior part of the tectum. Layers 7, 8 and 9 are indicated. The two dye spots correspond to the sites of maximum negativity of the u_1 and 'm' waves. The location of the u_1 dye spot is located slightly superficial to the main band of cell bodies of layer 8. The M dye spot is located slightly deeper within layer 8.

6-8

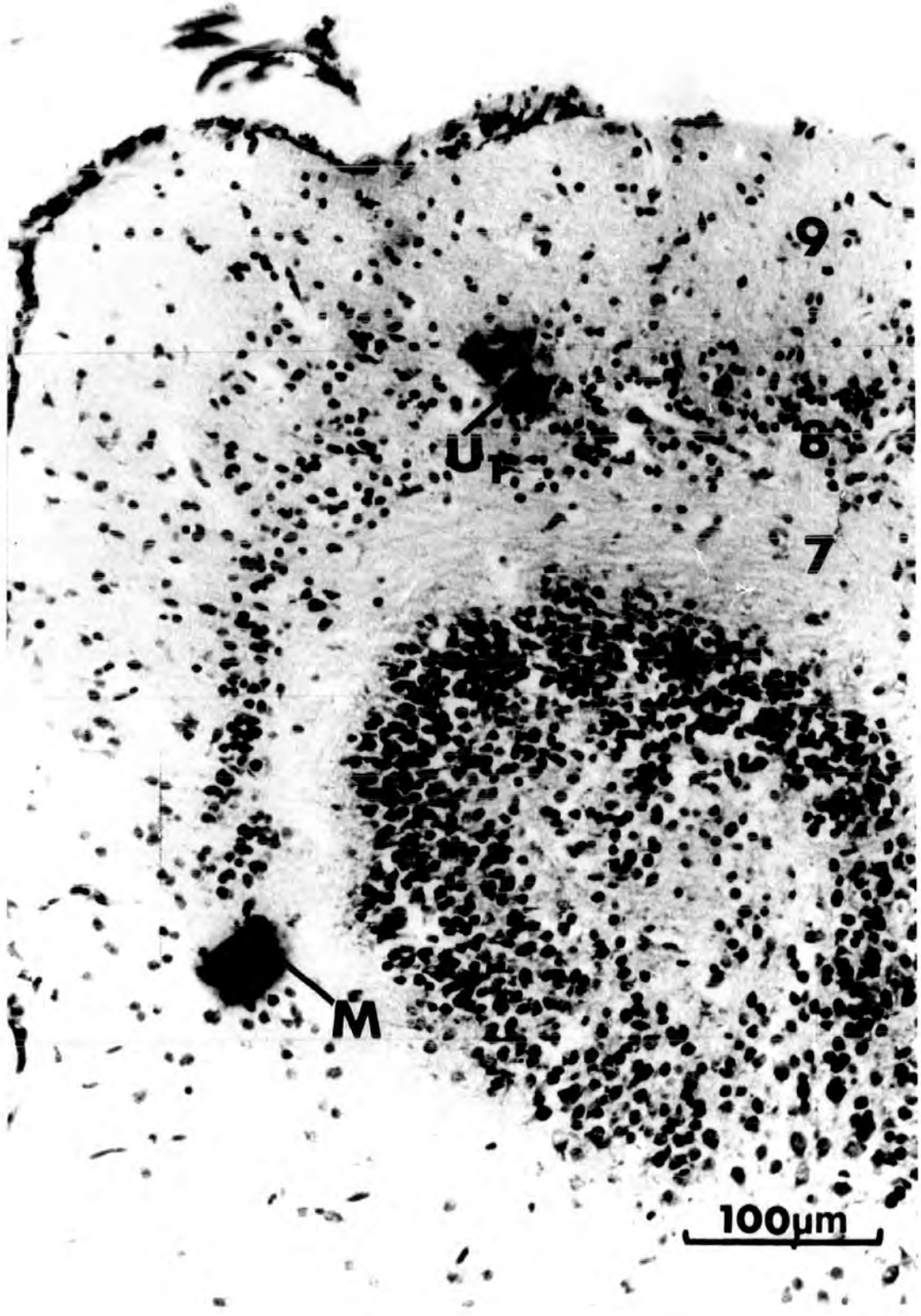

DISCUSSION

The waves evoked in the tadpole optic tectum are similar to those of the adult, and physiological tests show they fulfil the criteria for postsynaptic potentials. However, these tests only apply to the 'u' waves since the tests could not be carried out with confidence for the 'm' wave evoked at metamorphosis.

The 'u' waves are often preceeded by a presynaptic component (fig. 6:6 c). They may be potentiated (figs. 6:5 a and 6:6 a), the waves invert as the electrode penetrates the tectum (fig. 6:3 b, d) and the postsynaptic component fails with a tetanic train of stimuli (fig. 6:6 b). The clearest evidence for postsynaptic activation is that action potentials can be evoked from the postsynaptic neurons (fig. 6:7 d).

The results show that excitable synapses are formed early in development at Stage 46. This point is of interest in the light of the finding that, at this time, the explosive increase in the numbers of synapses in the central region of the retina begins to decline (Fisher, 1976). It is known that ganglion cell axons transmit visual information to the optic tectum at this early stage (Chapter 4; Chung et al, 1975). Identification

of the tadpole 'u' waves indicates that the predominant input to the tectum in tadpoles is via unmyelinated fibres, which is not surprising since only 500 myelinated fibres are present in the optic nerve at Stage 58.

A. MORPHOLOGY

At Stage 46, many unmyelinated fibres are present below the pia and the occasional synapse is observed (fig. 6:1). This correlates with the physiological results which suggest that synapses are present at this time. It is, however, difficult to state unequivocally that presynaptic fibres observed under the electron microscope have a retinal origin, although they are located in the region of the tectum which first receives optic afferent information. Scott (1974) attempted to locate the ganglion cell terminals in the tectum of tadpoles, using degeneration methods. He found large amounts of spontaneous degeneration, but produced results which demonstrated the presence of ganglion cell axon terminals at Stage 47.

The synapses present at this time are only axodendritic as is the case in the developing cat cerebral cortex (Pappas and Purpura, 1961; Voeller et al, 1963). Rager (1976 b) has found similar results in the embryonic chick optic tectum.

It is known that the receptors in the central retina are functional at Stage 38 (Witkovsky et al, 1976), that functional ribbon synapses in the outer plexiform layer are present at Stage 40 (Witkovsky et al, 1976), and that extensive lateral connexions within the outer plexiform layer form by Stage 46 (Fisher, 1976; Tucker and Hollyfield, 1977). At this stage, ganglion cell responses can be recorded at the site of their terminals in the tectum. Synapses have been observed electron microscopically at this location (fig. 6:1) and postsynaptic potentials can be evoked by electrical stimuli applied to the nerve. However, postsynaptic spikes, which are possibly indicative of efferent output, could not be activated at stages earlier than Stage 48. All these points indicate that the Xenopus tadpole visual system develops sequentially from the receptors through to the tectal efferents.

In contrast, the chick retina and tectum develop independently up to 12 to 14 days of incubation (Kelly and Cowan, 1972). Ganglion cell generation is almost complete by the twelfth day of incubation (Kahn, 1973). Synapses form in the inner as well as the outer plexiform layer before the outer segments of the photoreceptors develop (Rager, 1976 a). At the same time, the area of tectum which will receive the first afferent fibres is highly differentiated and approximates that of the adult (Rager, 1976 b). Because of the late maturation of receptor outer segments, visual stimuli become effective

only when synaptic contacts have been made over the entire tectal surface and ganglion cell axons have invaded the deeper layers. The individual elements in the chain of retino-tectal connexions are also functional before receptor activity can be elicited (Rager, 1976 a, b).

In Xenopus the retinal components begin to function very soon after differentiation, and the Golgi method shows cells in the tectum have well developed dendritic arborizations, which by Stage 48 can integrate afferent information (fig. 6:6 b).

B. PHYSIOLOGY

At Stage 46, synapses on to tectal dendrites could be detected with the electron microscope and postsynaptic potentials could be recorded as part of the evoked potentials at the tectal surface. Physiological tests indicate that the necessary conditions for synaptic transmission are established. However, it is not until Stage 48 that single cells driven by optic nerve input can be recorded. At Stage 46, synapses are small but well formed, and are located on the terminal sprigs of tectal cell dendrites. These are usually of a small diameter and therefore would be expected to have only a small length constant. It is possible that action potential electrogenesis is not developed, however

postsynaptic events due to tectal cell dendrite depolarization may still be recorded. It was only prior to metamorphosis that spontaneously active neurons could be recorded.

The failure to evoke a postsynaptic wave in the tectum in response to repetitive stimuli is not necessarily indicative of synaptic failure. It is known that the optic nerve contains mainly unmyelinated axons which are separated by glial septae (Chapter 1). It is possible that, if all the fibres in a bundle are activated simultaneously by electrical stimulation, potassium ions released from the axon may accumulate in the extracellular space (Orkand et al, 1966). This may result in a long lasting diminution in the membrane potential. The extracellular potassium may not be removed rapidly enough by the glial processes present. The second possibility is that the effects of repetitive tetanizing stimuli are to decrease the postsynaptic response (Wedensky inhibition). The evidence so far suggests that tetanizing stimuli produce a breakdown of signal transmission at the synapse.

Chung, Keating and Bliss (1974) carried out experiments on similar evoked tectal waves in Xenopus tadpoles and came to similar conclusions on the nature and the properties of the evoked response. They have interpreted their results of evoked potentials in the Xenopus tadpole tectum in terms of the current theories of neuronal specificity and shifting synapses.

Depth recordings indicate that the ganglion cell axons form synapses throughout layer 9, although no stratification of synapses can be seen prior to metamorphosis. However, at this time the synapses of the u_2 postsynaptic potential are distributed throughout the whole of tectal layer 9, with the u_1 synapses deeper than most of the u_2, and the myelinated afferents synapse in the region of layer 8. These results are in slight contradiction to those of the adult, where the u_1 synapses are located slightly nearer to the pia than the u_2 synapses. The result in a tadpole may be accounted for by the fact that many of the tadpole u_1 fibres may be destined for myelination.

GENERAL DISCUSSION

GENERAL DISCUSSION

The purpose of this study was to investigate the development of the primary visual system of Xenopus laevis, using both morphological and physiological methods. However, an understanding of the adult retinotectal visual system is essential prior to an investigation of development.

A. COMPARISONS OF THE PHYSIOLOGICAL AND MORPHOLOGICAL FEATURES OF THE ADULT RETINOTECTAL VISUAL SYSTEM

Electron microscopical investigation of the structure of the adult optic nerve reveals that both unmyelinated and myelinated axons are present, although the majority are unmyelinated. The axonal diameters of these two groups of fibres show unimodal, skewed distributions and there was no evidence for the presence of any sub-populations. However, electrophysiological recordings of the evoked potentials in the optic nerve in response to electrical stimulation show there are four conduction velocity groups. It is difficult to correlate these four evoked waves with the presence of two morphological fibre groups.

Correlation between the evoked potentials and fibre classes within the nerve

The conduction velocity groups recorded from the optic nerve are in good agreement with the conduction velocity values calculated from the latencies of the responses recorded in the tectum. Since the path, along which the action potentials travel from the retina to the tectum cannot be measured accurately the latency values may be subject to error. The conduction velocity values of the fibres evoking the m_2, u_1 and u_2 waves reported here are 1.1 - 1.3, 0.6 and 0.2 m/sec^{-1} respectively. Comparable values obtained from the nerve alone are 1.2, 0.7 and 0.2 m/sec^{-1} respectively (Chapter 3). As discussed in chapter 3, these values are different from those obtained in Rana (Chung, Bliss and Keating, 1974). Although no conduction velocity could be determined for the fibres which elicit the m_1 wave, this wave always appears at a shorter latency than the m_2 wave and consequently the fibres evoking this wave must have a faster conduction velocity.

The stimulus strength-tectal response characteristics (fig. 5:4) show similar trends to the stimulus strength-optic nerve CAP responses reported in Chapter 3. The relative thresholds for evoking m_1 and m_2, u_1

and u_2 waves are the same for both the isolated optic nerves and in recordings of tectal waves. This occurs in exactly the same manner in the nerve. Since the events reported in Chapter 5 are postsynaptic no direct comparison with the CAP results of Chapter 3 can be made in terms of absolute thresholds. However, the trends exhibited are the same with the m_1, m_2, u_1 and u_2 waves appearing sequentially with increasing stimulus voltage. Because these are postsynaptic recordings, they do not give a direct measure of fibre excitability, since the interposed synapses may distort the values, depending on their efficacy and number.

Correspondence of the location of current sinks and ganglion cell terminals

The second spatial derivatives of the m_2, u_1 and u_2 waves localize the postsynaptic neurons as cells whose somata lie in layer 8 of the tectum. The location of the current sinks of these three waves, determined from depth profiles and subsequent deposition of dye spots at the sites of the current sinks, corresponds to the location of ganglion cell axon terminals, determined by Prussian blue marking, following single unit microelectrode recording. It is possible, therefore, to conclude that the ganglion cell axon terminals synapse on to layer 8 tectal cells. These cells, however, may not be the only postsynaptic elements present, since

most neurons in the amphibian tectum have dendrites which ascend into layer 9 (Székely et al, 1973; Székely and Lázár, 1976), whether their somata are situated in layer 8 or in the periventricular layers of 2, 4 or 6. Indeed evidence presented here may indicate that monosynaptic activation of deeply lying neurons occurs (figs. 5:18) Also evidence from current source density analysis indicate that a current source in response to optic afferent activation can be located deeper in the tectum, since small deflections occur on the depth profiles in regions equivalent to the periventricular layers.

The u_1 fibre terminals synapse most superficially in the tectum, in the same region where optic afferent fibres can be recorded. These afferents are the terminals of Class I (Maturana et al, 1960; Grüsser and Grüsser-Cornehls, 1976) ganglion cells (Chapter 4). These terminals often overlap in distribution with those of class II ganglion cells but dye marking indicates that class I terminals are usually more superficial than class II. The data presented here indicate that the maximum current sink of the u_2 postsynaptic wave is located slightly deeper in the tectum than that for the u_1 sink. It is therefore possible to associate tentatively the class I terminals with the u_1 postsynaptic response and the class II terminals with the u_2 postsynaptic response.

Deeper in the tectum, terminals of class III ganglion cells could be recorded. The distribution of these terminals rarely overlaps with that of other actively responsive axon terminals. The location of dye spots deposited at the m_2 sink corresponds closely to that of dye spots marking the sites of class III units. These sites are found superficial to the somata of layer 8 cells (figs. 4:11 c, 5:13 a). The location of the dye spots at the site of maximum negativity of the m_1 wave is below layer 8, as are the Prussian blue marked sites of class IV terminals (figs. 4:11 d, 5:13 b). On the basis of this evidence one can conclude that the four retinal ganglion cell types send axonal projections to four laminae in the optic tectum, the locations of which are identical to the sites of maximum inward current for postsynaptic neurons recorded in response to optic nerve stimulation. The four retinal ganglion cell classes may be regarded, therefore, as giving rise to the four postsynaptic waves recorded in the tectum of Xenopus. Similar results have been obtained by Chung, Bliss and Keating (1974) in Rana pipiens

These results would suggest that in Bufo and Hyla, which possess only three classes of ganglion cell responses (Ewert and Hock, 1972; Grüsser and Grüsser-Cornehls, 1976), only three conduction velocity groups in the nerve and three postsynaptic field potentials in the tectum would be evoked.

The nature of the optic input

The present data indicates that the optic afferent input is excitatory and that postsynaptic neurons are depolarized by this afferent activity. This conclusion is confirmed by the location of current sinks which correspond to the regions of ganglion cell terminals in the tectum. Inhibitory synapses would have produced hyperpolarizations and hence current sources at the site of transmembrane current movement in the superficial layers. The conclusion that the synapses are excitatory is further strengthened by the presence of unitary potentials which are superimposed on the postsynaptic waves. These potentials are recorded mainly when the electrode is in the vicinity of layer 8.

Ewert and von Wietersheim (1974 b, c) have shown in the toad Bufo bufo that there are two classes of neurons in the stratum griseum et album centrale (layers 7 and 8) which are excited by visual stimuli. This finding that tectal neurons of layer 8 are excited by optic afferents is in good agreement with the results reported here.

Correlation with Anatomical Data

Most studies on the structure and innervation of the optic tectum have been carried out on Ranid anurans

(reviewed by Scalia, 1976; and Székely and Lázár, 1976). Only one study has been published on the morphology of the Xenopus optic tectum and this was a comparison with the developing tectum of the tadpole (Lázár, 1973).

From the results presented here and from morphological studies (Payne, in preparation) the optic tectum of Xenopus is similar to other anurans in both its constituent elements and its optic afferent innervation. The layering of optic afferent fibres and neurons within the tectum is not as distinct as in Rana sp. However, the general data on the frog optic tectum can also be applied to Xenopus, although it is known that optic afferent fibres form synapses on to the ends and the shafts of dendrites and on to the somata of layer 8 cells in Xenopus (Chapter 5).

Early morphological studies (Ramon, 1890; Wlassak, 1893; Ramon y Cajal, 1911) have shown three layers of optic afferent terminals in layer 9 of the tectum. Results obtained using degeneration methods (Knapp et al, 1965), autoradiography (Scalia, 1973) and horseradish peroxidase marking (Scalia and Colman, 1974) show three or four bands of terminals (reviewed by Scalia, 1976 and by Székely and Lázár, 1976). The depths of these terminals correspond well with the results presented here for Rana. No comparable studies have been carried out on Xenopus. Since optic terminals may be found at the sites of the maximum current sinks and the electrophysiological results obtained from Xenopus agree well with

those obtained from Rana, at least in their qualitative location, it may be safe to assume that four layers of terminals exist in Xenopus, although their stratification is less distinct.

The most superficial terminals are located some 50 μm below the tectal surface in Rana (Székely, 1973) with a second sheet located adjacent to the first. In Xenopus, optic nerve terminals can be found immediately below the pia. The majority of axons in the most superficial part of tectal layer 9 are unmyelinated Rana, the second spatial derivative current sinks correspond to the layers of unmyelinated fibres, as the u_1 and u_2 postsynaptic current sinks in Xenopus correspond to the upper region of unmyelinated fibres.

The m_2 current sink in both Rana and Xenopus is located in a region of myelinated fibres which have a retinal origin. Again, the location of the m_2 sink in Rana corresponds well with the results of anterograde tracing of myelinated fibres. The location of the m_2 current sink in Xenopus also corresponds to a region of myelinated fibres and the class III retinal ganglion cell terminals. These fibres are probably of retinal origin. The fibres which give rise to the m_1 wave in Rana occupy a distinct layer between layers 7 and 8 of the tectum and ganglion cell axons have been shown to

terminate in this region (Scalia et al, 1968; Székely, 1973; Lázár and Székely, 1969). However, a distinct layer at this location is not evident in Xenopus, and it is not so easy to correlate this situation with that found in Rana.

Lázár and Székely (1969) and Székely (1973) found the largest diameter fibres of the retinal input terminate just below the cells of layer 8 in the tectum. This corresponds well with the location of the maximum negativity of the depth profile of the m_1 wave.

The obvious inference from the data for the m_1 wave is that m_1 afferent fibres are distributed as in Rana and the postsynaptic neurons may well lie in layer 8, with synapses formed with the basal dendrites and the somata of these cells.

The results of current source density analysis suggest that the m_2 fibre group terminals synapse principally on to the shafts of the apical dendrites of layer 8 cells or on to the cell bodies of these neurons. In conjunction with this, retinal ganglion cell terminal synapses on to the somata of layer 8 cells have been observed. Comparable anatomical work to that of Knapp et al (1965) and Scalia (1973) would be useful confirmation of the location of optic afferent synapses reported here.

The anatomical observations of myelinated fibres in Xenopus (Payne, in preparation) and in Rana (Scalia et al, 1968; Potter, 1972; Székely, 1976) show that these fibres may be located in regions of the tectum other than that which corresponds to the m_1 and m_2 sinks. In Rana, Potter (1972) recognised the problem of reconciling this finding with the electrophysiological data of Lettvin et al (1959) and Maturana et al (1960), who reported that the two superficial layers of optic nerve terminals were derived from fibres with conduction velocities which indicated that they were unmyelinated. The results reported here and those of Chung, Bliss and Keating (1974) are in substantial agreement with those of Lettvin et al (1959) and Maturana et al (1960), although Chung, Bliss and Keating obtained results which indicated myelinated fibre input in the superficial layers of the tectum. In Xenopus, with its compressed receptive region of retinal afferents, it is difficult to discern superficial myelinated activity from the deeper myelinated activity. However, the result in figures 5:19 e and 5:19 f indicates that superficial myelinated fibres can lead to spike activity in superficially located neurons, although most fibres in this region are unmyelinated and produced activity which has a much longer latency. An m_2 associated unitary potential (fig. 5:19 e, f), which was located more superficially in the tectum than the m_2 sink, was found.

This result indicates that not only are some superficial fibres myelinated (based on latency measurements) but that they produce action potentials in the cells with which they synapse. The postsynaptic spike was recorded from layer 9 and therefore probably originated from a stellate or amacrine cell (Székely and Lázár, 1976). The question which arises is whether these are fibres from class I or II retinal ganglion cells, as expected from their location, or whether they are fibres of class III ganglion cells, as would be predicted from the latency of the response.

Székely and Lázár (1976) discuss the inconsistency of the data obtained by anterograde tracing methods on the location of optic afferents in the tectum and the physiological data on the location of optic afferent fibres in the tectum. They conclude that it is conceivable that all terminal recordings are derived from myelinated fibres. This seems to be unlikely since the data reported in Chapter 4 and the data reported by Gaze et al (1974) and Chung et al (1975) show that optic afferent fibres could be recorded in the tectum of very young tadpoles when it is known that all of the fibres in the optic nerve of Stage 46 animals are unmyelinated (Chapters 1 and 2). Since it is known that the recording situations used in the studies reported in this thesis were identical for adult and tadpole Xenopus, the suggestion of Székely and Lázár (1976) is untenable.

Implications

The work of Lettvin et al (1959) and Maturana et al (1960) suggests that behaviourally significant features of the image impinging on the frog's retina are abstracted, encoded and transmitted to four tectal depths.

Evidence from Golgi impregnated neurons in both Rana (Ramon, 1890; Lázár and Székely, 1967) and Xenopus indicate that all layer 8 neurons extend their dendrites into layer 9. The vast majority of these neurons are small, pear-shaped cells which have essentially radially oriented dendrites, although a number of large ganglionic cells similar to those of Rana (Lázár and Székely, 1967) are present whose dendrites inscribe a conical volume.

On the evidence of a common current source for the m_2 and both 'u' waves, one may conclude that layer 8 cells receive not only myelinated (m_2) but also unmyelinated (u_1 and u_2) input. The m_1 input cannot be ascribed conclusively to these cells.

Not only do optic afferents arrive in the tectum at different times because of their axon calibre and hence conduction velocity, but they also synapse at different depths within the tectum.

The evidence, that layer 8 cells are postsynaptic to m_2, u_1 and u_2 fibres may suggest that convergence of retinal input occurs at these cells. While there is no

direct evidence for convergence of different classes of retinal input to these cells in either Xenopus or Rana pipiens (Chung, Bliss and Keating, 1974) this possibility cannot be ruled out.

A possible consequence of convergence is that considerable economy might be achieved in terms of the numbers of neurons in the tectum which process visual information, since one postsynaptic cell may respond to a class of visual inputs without losing the ability to process information arriving along other optic afferent channels. For example, the location of m_2 fibre input on the bases of layer 8 apical dendrites will be more effective in evoking a rapid response. Since the input fibres are myelinated, the conduction velocity is greater than that of unmyelinated fibres. The synapses are located nearer to the cell body and the site of action potential initiation. In contrast, the unmyelinated fibre activity, which is conducted at a lower velocity, activates layer 8 cells at the distal ends of the dendrites.

Current source density analysis only produces results on the activation of a population of neurons and not on the source/sink distribution of single units. If convergence does occur, it cannot be determined whether all four retinal ganglion cell classes synapse on to single layer 8 cells. An alternative is that different retinal ganglion cell terminals synapse on sub-populations of

neurons which combine different inputs. The method of current source density analysis does not permit a distinction between these two alternatives. If combinatorial convergence does occur in the amphibian tectum, it is an alternative method of feature extraction to that of sequential convergence employed in the visual cortex (Kuffler and Nicholls, 1976).

In the absence of temporal segregation, cells with radially oriented dendrites would be restricted to one degree of freedom, which would be determined by the summation of the various inputs. Temporal segregation permits an increase in the amount of information processed. The spatiotemporal distribution of afferent input to the tectum also permits interaction with other afferent visual information which may be transmitted along a different path (e.g. via the thalamic/pretectal region) to the tectum since it is known, at least in frogs and Bufonid toads, that thalamic regions project to the tectum (Ewert, 1968, 1970; Ewert and von Wietersheim, 1974 c; Ewert et al, 1974; Trachtenberg and Ingle, 1974; Wilczynski and Northcutt, 1977).

Since no information is available for the current sources of the m_1 wave in Xenopus, it is difficult to assess the role of these afferent fibres in the scheme, although there is evidence that they too synapse on to layer 8 cells.

B. THE DEVELOPMENT OF THE RETINOTECTAL VISUAL SYSTEM

The main emphasis of this work has been on the changes in structure and function of the optic nerve during development and on the development of the innervation of the optic tectum by the ganglion cell axons that leads to the pattern found in the adult.

During development glial cells in the optic nerve differentiate from ependymoglial cells (Turner and Singer, 1974) which have also been termed astroblasts by Blunt et al (1972) and Skoff et al (1976 a, b). These cells differentiate to give typical astrocytes and oligodendrocytes (Peters et al, 1970) between Stages 46 and 50. This differentiation occurs prior to the start of myelination, a finding which is in agreement with the findings of Vaughn (1969), Hirose and Bass (1973) and Skoff et al (1976 a, b) in the rat optic nerve and by Moore et al (1976) in the cat optic nerve. It is also at this time that increasing numbers of newly developing axons enter the nerve, and it is postulated that the sheet-like processes of the newly differentiated astrocytes act as guides for the growing axons.

The morphological characteristics of the glial cells change at, and after, the time of metamorphosis, such that they all take on a uniform appearance which may be considered

to be a dedifferentiated state. This dedifferentiated state may be associated with (i) a reduction of myelogenesis, although myelination does continue into adult life, and (ii) with the absence of large numbers of growing axons for guidance to the brain by astrocytes. The adult optic nerve is not overtly fasciculated.

Extensive degeneration of myelin occurs at the time of metamorphosis, Generally, the axons appear to be unaffected, since only three myelinated axons were observed to be degenerating from the total number of nerves studied. Unmyelinated axons may degenerate, although this feature is unlikely to be observed readily. The degeneration is presumed to be related to the shortening of the optic nerve when the distance between the eye and the brain decreases. The lamellated structure of the myelin results in the sheaths being thrown into folds at the time of optic nerve shortening.

The effect of degenerating myelin on the conduction properties of ganglion cell axons, as judged by CAP and field potential recordings from the optic nerve and optic tectum respectively could not be resolved. The effects of the demyelination on the responses of single units could not be assessed.

Ganglion cell axons in the optic nerve continuously increase in number during development (Chapter 3; Wilson, 1971). The mean diameter of the axons fails to increase

at metamorphosis and may even decrease, although there is a general trend of increasing axonal diameter with maturity. Myelination of axons is continuous and indicates that the majority of axons in the Xenopus optic nerve receive a sufficient amount of myelin to confer optimum conduction velocity values only at adulthood.

CAP recordings from the optic nerve show that, prior to Stage 50, only one conduction velocity group of fibres is present. At Stage 50, two groups may be evident, and at Stage 54 a fast short latency group can also be recorded. This group is presumed to be myelinated, since it shows similar conduction velocity values to an adult myelinated fibre group. Slightly older tadpoles show multiple waves in CAP recordings, although these potentials are recorded mainly from one group of fibres whose conduction velocities allow them to fractionate into component groups over the length of nerve used. This will occur with conduction velocities which vary by as little as 0.02 $msec^{-1}$ in the lengths of nerves studied. At metamorphosis, when the optic nerve decreases in length, these potential waves are lost.

At the end of metamorphosis, and shortly afterwards, a fourth wave appears, which corresponds to the fastest myelinated group in the adult. The conduction velocity groups recorded from the optic nerve do not significantly alter at metamorphosis when the nerve shortens. Since

visual information is conducted along channels with different conduction velocities, temporal asynchrony between events arriving at the tectum will be less for shorter conduction distances. These differences will be most apparent if centrifugal fibres are involved.

Discrepancies arise between the evoked potentials recorded from the tectum in response to optic nerve stimulation (Chapter 6), and the CAPs recorded from the optic nerves of tadpoles (Chapter 3). Figures 6:3 a and 6:3 b show that two postsynaptic potentials are evoked from the tectum at a Stage 48 tadpole, although only one wave forms the CAP recorded from the optic nerve (fig. 3:2). Two possible explanations are possible for these effects. Firstly, the distance over which the CAP was recorded was not sufficient to permit the conduction velocity groups to fractionate into their components. Secondly, synaptic effects with different time courses are present in the tectum.

Two postsynaptic waves, which are activated by unmyelinated fibre synapses, are recorded throughout tadpole and indeed adult life. Whereas postsynaptic waves activated by myelinated fibre synapses do not appear in the tectum until Stage 59. In contrast, the responses recorded from optic nerves of tadpoles at Stage 56 and 58 show CAPs which have four component conduction velocity groups, an 'm' wave, two 'u' waves, and a small fourth negative

deflection. It is difficult to reconcile the presence of these four waves in the CAP recordings with the two post-synaptic waves recorded in the tectum prior to Stage 59.

A major discrepancy in the results obtained from CAP recordings and the results of the presumed postsynaptic activation of tectal neurons occurs at a latency equivalent to 'm' wave activation. Field potential activity with a short latency 'm' wave component first appeared in the recordings from tadpole optic tectum at Stage 59, which corroborates the results of Chung, Keating and Bliss (1974). However, a CAP could be recorded from the nerve with an 'm' wave latency as early as Stage 54.

A number of reasons may be advanced to explain this discrepancy.

(i) The terminals are too few in number and too sparsely distributed for postsynaptic events to be recorded. The small size of the myelinated fibre population in young tadpole optic nerves (prior to Stage 54) probably precludes their recording (Chapters 1, 2 and 3).

(ii) The fibres which give rise to the 'm' wave in tadpole optic nerves are myelinated for only part of their length. The conduction velocity of an action potential which passes along this

fibre will be decreased considerably by the unmyelinated portion of the axon. The recording of neuronal activity would then show a potential which is not separated into its components.

(iii) The myelinated fibres present in the optic nerve from Stage 50 do not project to and form connexions with the tectum until Stage 59. The evidence against this is the fact that axons usually form connexions with a postsynaptic element before the process of myelinogenesis is initiated (Rager, 1976 a).

(iv) The myelinated fibres do not connect with the tectum until Stage 59, and in younger tadpoles the observed myelinated fibres may project to other regions of the brain. It is known in Rana pipiens that the retina forms connexions with contralateral diencephalic visual nuclei in tadpoles (Currie and Cowan, 1974 a) and that Xenopus tadpoles can produce optokinetic nystagmus when the tectum has been ablated to leave the pretectum and basal optic nucleus (Mark and Feldman, 1972). Lázár (1973 a) has shown that adult frogs can perform optokinetic nystagmus when only the basal optic nucleus remains. If visual behaviour of the tadpole is mediated

by an optic centre other than the optic tectum, this would permit the tectum to develop directly into the adult pattern, and so avoid possible reorganization at metamorphic climax.

(v) Although myelinated fibres are projecting to the tadpole tectum, the synapses are not functional.

Unfortunately, present morphological and physiological techniques are inadequate for determining which one or which combination of the above five possibilities is correct.

The responses of ganglion cells recorded in the optic tectum are qualitatively similar to four of the five original classes reported by Lettvin et al (1959) in the frog. The fifth type has not been reported since the initial studies of Lettvin and his colleagues were carried out.

The ganglion cell responses develop greater complexity from the time when they are first recorded in the tectum (Stage 46) and have "crude" responses to only the "on" and "off" of light. Their appearance in the tectum corresponds to the time when the first synapses appear and when post-synaptic activity can first be recorded. As the tadpole develops, class III and IV type responses can be recorded in early Stage 50 tadpoles. The class II responses appear at Stage 61 and class I at one week after metamorphosis.

During and after tadpole life, the receptive fields increase in complexity. This may be correlated with the results of a study by Fisher (1976) who showed that after an initial rapid increase in the numbers of conventional and serial conventional synapses, the rate of increase declined.

The evoked field potentials in the tadpole tectum indicate that the afferent input is unmyelinated, and myelinated fibres only give rise to postsynaptic activity from Stage 59 onwards (Chapter 6; Chung, Keating and Bliss, 1974). It is only some time after metamorphosis that m_1 activity can be recorded, although it is known that myelinated fibres are present in the tectum at earlier stages (Payne, in preparation) and that their activity can be recorded in the optic nerve.

The evoked potentials indicate that the optic afferent input is excitatory at all stages of development. Synapses are formed at Stage 46, postsynaptic units may be synaptically driven from Stage 48 and spontaneous postsynaptic activity can be recorded from Stage 58 onwards. Development continues after metamorphosis and the adult pattern is established at one month postmetamorphosis.

The mode of innervation of the tectum by retinal afferents

The development of the laminar arrangement of optic afferents in the tectum is a complex process, further complicated by the different modes of growth of the retina and the tectum (Straznicky and Gaze, 1971, 1972; but see also Jacobson, 1976; Straznicky and Tay, 1977). It is known that the class III and IV type units in the tectum of tadpoles arborize in the superficial layer and form excitable synaptic contacts with apical dendrites and cell bodies (see Chapter 5). In tadpoles, very few ganglion cell axons are myelinated and myelin production increases with maturation (Chapter 2; Gaze and Peters, 1961; Wilson, 1971). In the adult, synapses from myelinated fibres are formed between class III terminals and the apical dendrites, between class IV terminals and the somata and the basal dendrites of cells in layer 8. Unmyelinated fibres of class I and II synapse above these two layers also on to the apical dendrites of layer 8 cells. Chung et al (1975) suggest that the sites of synapses in tadpoles differ from those of the adult. They also suggest two possible explanations. The first is that unmyelinated fibres remain unmyelinated and change in function from class III and IV to the class I and II fibres. The second explanation is that synaptic contacts formed during embryonic development are transitory and shift continually during the course of maturation of the retinotectal pathway. Chung et al

(1975) consider the first explanation to be unlikely as this implies reorganization of retinal connexions for which there is as yet no evidence. They find the second alternative more appealing since it is known that the Xenopus optic tectum grows linearly in contrast to the retina which grows concentrically at the ciliary margin (Straznicky and Gaze, 1971). According to Straznicky and Gaze (1972), the only way to account for this incongruence in growth is to postulate shifting synaptic connexions. Further electrophysiological evidence has been produced to show that ganglion cell axons arborize consecutively at a series of tectal positions and form functional synapses (Gaze, Chung and Keating, 1972; Gaze et al, 1974; Chung, Keating and Bliss, 1974). Scott and Lázár (1976), using anatomical methods, have shown that labelled ganglion cell terminals do indeed move relative to labelled tectal cells during development. Longley (1975), has observed similar results using degeneration methods. Chung et al (1975) conclude from their findings concerning the layering of the ganglion cell terminals in the adult optic tectum that the end result of the process is the formation and destruction of many temporary and labile synapses.

More recently, Jacobson (1976) investigated the mode of growth of the retina, by giving tadpoles multiple injections of tritiated thymidine. From

this pulse labelling, he noted that the ventral retina in tadpoles grows at a much faster rate than the dorsal margin. He suggests that Straznicky and Gaze (1971) missed this asymmetrical growth partly by only administering a single pulse of tritiated thymidine but mainly because they chose a horizontal sectioning plane. The observations of Jacobson have been confirmed by Straznicky and Tay (1977). Jacobson suggests that, because the retina and the tectum do not grow incongruently, it is unnecessary to postulate shifting synaptic connexions.

Using data based on mitotic criteria, Currie (1974) suggests that the axial polarity of the tectum is set up at the time of the arrival of the first ganglion cell axons. Chung and Cooke (1975) provide evidence that the axial polarities of the tectum are labelled irrevocably between Stages 37 and 45.

Between Stage 46 and adulthood, the tectum increases in thickness especially layer 9. This is due to the increasing numbers of afferent fibres (Currie, 1974; Currie and Cowan, 1974 b, 1975) and the increasing arborization of the tectal dendrites in this region (Lázár, 1973). Currie (1974) reports that in Rana pipiens tectal cell differentiation begins when the first optic axons innervate the tectum. The first cells to migrate from the ventricular zone are the

larger projection neurons of layers 7 and 8. The pyramidal cells of layers 6 and 4 are then produced, followed by the pyramidal and granular cells of layers 8 and 9. The cells of layers 1 and 2, including most of the ependymoglial cells, are the last to be produced in any given region of the tectum.

The pattern of cell generation is not a simple "inside-out" sequence as in the mouse cerebral cortex (Angevine and Sidman, 1961; Hinds and Angevine, 1965) or "outside-in" as in the cerebellum (Miale and Sidman, 1961; Fujita, 1967) or in the retina (Sidman, 1961). The closest resemblance is the mouse olfactory bulb (Hinds, 1969), where a small proportion of large mitral cells is produced before the larger population of granule and tufted cells. Those which are deep, in the bulb arise before those which migrate out past the mitral cells. This pattern is similar to the development of the anuran tectum, if the mitral cells may be regarded as equivalent to the large ganglionic or candelabra cells of layers 7 and 6. Also occurring in the tectum is a secondary "inside-out" gradient of cells, with those deep in layer 6 appearing before those in the most superficial layers and those in layer 8 appearing before the neurons in layer 9.

The pattern of afferent innervation and synapse formation, where the afferent fibres arrive at their future termination area either prior to or during

cell migration, is found in the rhesus monkey visual cortex (Rakic, 1977), the contralateral projection of the rat commisural fibres (Wise and Jones, 1976), rat optic tectum (Lund and Bunt, 1976) and the human cerebellum (Rakic and Sidman, 1970; Zečević and Rakic, 1976).

The ingrowth of optic afferents to the visual cortex in the rhesus monkey occurs before embryonic day 78, but axonal endings initially do not invade the cortical plate. Instead axons accumulate in the intermediate zone below the cortical plate. At this foetal age, the majority of neurons of layer IV, which eventually receive input from the geniculocortical fibres, are either as yet ungenerated, or are in the process of migration. Rakic (1977) suggests that the geniculocortical axons remain below the cortex and "wait" there in a densely packed fibre layer until the conditions become established for their entry into the cortical plate. Therefore geniculocortical fibres may contact migratory neurons, which pass through the intermediate zone before they reach the appropriate level in the cortex. This has also been observed by Kostovic and Molliver (1974) in the human telencephalon.

Similar observations have been made with regard to the commissural fibres in the neonatal rat. After entering the contralateral hemisphere, they remain in the white matter for several days before invading the

cortex (Wise and Jones, 1976). Another relevant example is the histogenesis of the human cerebellum, where a transient embryonic layer, the lamina dissecans (Jakob, 1928) develops between the Purkinje cell layer and the granular layer. This transient cerebellar layer in the human foetus contains various cerebellar afferents, including mossy fibre terminals and a small number of immature synapses (Rakic and Sidman, 1970; Zécévic and Rakic, 1976). This lamina may represent a "waiting compartment" of cerebellar afferents which become depleted as young granule cells "pick up" their synapses while migrating through this layer (Rakic, 1977).

During development of the optic tectum in the rat (Lund and Bunt, 1976), synapses are initially formed at the surface of the superior colliculus. Whereas in the adult rat, the synapses are situated in the stratum opticum, deep to the neurons in the stratum griseum superficiale. Either the synapses descend from the surface or neuronal somata migrate through the synaptic zone to the surface and displace the synapses ventrally in a manner similar to the penetration of the lamina dissecans by cerebellular granule cells. Lund and Bunt (1976) also show that, as the neurons differentiate, synapses are formed with the optic afferent fibres.

Since Jacobson (1976) has questioned and Straznicky and Tay (1977) have confirmed that the Xenopus retina grows asymmetrically this point, coupled with the above evidence from mammalian species and Currie's (1974) excellent elucidation of the time of origin and migration of the cells in the tectum of Rana pipiens, leads one to postulate a hypothetical, but very possible, mode of innervation of ganglion cell afferents to the optic tectum and the formation of the adult pattern of synaptic connexions in Xenopus.

I suggest that the first ganglion cell axons to invade the tectum have responses which are primordial to either class III or IV. These fibres arrange themselves in the marginal zone (Boulder Committee, 1970) of the tectum, and the cells of the future layer 8 migrate into this marginal zone of fibres and form synapses. All or most of the fibres make synaptic connexions either with the soma or newly emerging basal or apical processes which are known to have terminal growth cones (Payne, in preparation). The afferents may also make contact with the apical dendrites of the cells of layer 6. Even at Stage 49, the neurons of layers 6 and 8 have differentiated with prominent dendritic trees (Chapter 6), although these are not radially oriented. These fibres arrange themselves in the region of the somata of layer 8 cells,

and as more fibres enter the tectum synaptic formation is forced more dorsally by the absence of possible synaptic sites. The increasing length of the dendrite production of new postsynaptic sites is possible because of the increasing length of the dendrite due to the growth cone. A precedent for this may be found in the cerebellum where a developmental gradient is present, with the most recently formed parallel fibres located most dorsally (Rakic, 1971).

When the future class I and II retinal ganglion cell fibres invade the tectum at or shortly after metamorphosis, all or most of the synaptic sites on tectal cell apical dendrites are occupied by the future myelinated fibres of the class III and IV ganglion cells. Hence class I and II fibres must synapse more dorsally on to tectal cells following the growth of the apical dendrites. Evidence for or against this hypothesis could be obtained by labelling ganglion cell axons with tritiated proline at a particular stage of development, e.g. prior to metamorphic climax, Stage 57. Throughout this period of development the tectal cells are differentiating more and more, especially the intrinsic tectal cells. Afferents from other regions of the brain are arriving in the superficial zone (Trachtenberg and Ingle, 1974; Wilczynski and Northcutt, 1977). Since

transported radioactive proline is known to remain in axon terminals of mice for at least four weeks (Grafstein et al, 1972), the accurate location of the terminal synapses in the optic tectum could be determined over a long period of development, using electron microscopic autoradiography.

SUMMARY

Light and electron microscopical methods were used to study the morphology of the tadpole and adult Xenopus optic nerve and optic tectum. Retinal ganglion cell terminal responses to visual stimuli were characterized, the conduction velocities of their axons measured and the location of their synapses and postsynaptic neurons in the contralateral tectum were determined. These physiological features were studied in the adult and where possible throughout development.

1. The optic nerve of the adult comprises myelinated fibres, unmyelinated fibres and ependymoglial cells. Physiological recording has demonstrated four conduction velocity groups with velocities of 3, 1.2, 0.7 and 0.2 m/sec^{-1}. The two groups with the fastest conduction velocities were attributed to the myelinated fibres, whereas the two groups with the slowest conduction velocities were attributed to the unmyelinated fibres. These velocity groups could not be readily correlated with the two fibre diameter distributions in the optic nerve.

2. Four ganglion cell response classes were recorded from ganglion cell axon terminals in the tectum. The terminals of these four classes were located at different depths in the optic tectum. These response classes were found to be similar to classes I-IV recorded by Maturana et al (1960).

3. Four postsynaptic waves were recorded in the tectum in response to contralateral optic nerve electrical stimulation. These waves were termed m_1, m_2, u_1 and u_2. The current sinks of these waves, determined by current source density (CSD) analysis, were located in layer 9 of the tectum, with the u_1 sink located most superficially at 70 μm tectal depth, the u_2 sink at 90 μm tectal depth, and the m_2 sink at 150 μm tectal depth. It was not possible to carry out CSD analysis on the m_1 wave, but the location of the m_1 wave maximum negativity was found to be deeper than the cells of layer 8.

4. It was determined, by CSD analysis, that the cells of layer 8 were the postsynaptic neurons which generate the m_2, u_1 and u_2 tectal waves in response to excitatory transmission from the contralateral optic afferent fibres.

5. A good correlation exists between the four conduction velocity groups of optic nerve axons and the conduction velocities of the afferents which evoke the four tectal waves.

6. It was also found that the locations of the terminals of the four ganglion cell classes correlated with the locations of the three postsynaptic current sinks and the maximum negativity of the fourth postsynaptic m_1 wave.

7. Before tadpole Stage 49 only unmyelinated fibres were observed in the optic nerve. At Stage 49 myelination of axons was evident, and in later stages of development increasing numbers of myelinated fibres were counted. Myelination of axons continues in adult life.

8. Two types of glial cells (astrocytes and oligodendrocytes) were observed in the tadpole optic nerve, these glial cells dedifferentiate at metamorphosis to the ependymoglial cell of the adult. Extensive natural demyelination was observed at the time of metamorphosis probably correlated with optic nerve shortening at this time.

9. Physiological studies on the optic nerve show one conduction velocity group (0.2 m/sec^{-1}) prior to Stage 54. It was concluded that the fibres with this conduction velocity were unmyelinated. This conduction velocity group was present throughout tadpole development and adult life. At Stage 54 a fast conducting group (1.2 m/sec^{-1}) appears which was thought to be indicative of myelinated fibres. This group is also present throughout tadpole life (post-stage 54). Two more conduction velocity groups were recorded in metamorphic animals and juvenile toads (0.6 and 2.6 m/sec^{-1}).

10. Electrical activity in retinal ganglion cell terminals was recorded from tadpole Stage 46 onwards. These responses were "immature". Class III and IV type responses could be recorded from Stage 50 onwards, Class II responses from Stage 61 onwards, and Class I from one week after metamorphosis. The receptive fields of these classes became more complex with time and more resistant to habituation. The first detectable units were recorded at the surface of the tectum at Stage 46 and in later stages at deeper levels in layer 9.

11. The appearance of evoked responses in the tectum at Stage 46 coincides with the stage at which the first synapses were observed morphologically.

12. During development the initial input to the tectum was by unmyelinated fibres, the activity of which was found to be responsible for the initiation of postsynaptic events characteristic of 'u' waves. An 'm' postsynaptic wave was first recorded in the tectum at Stage 59. M_1 postsynaptic activity was only recorded after metamorphosis was completed.

13. The discrepancy between the appearance, during development, of myelinated fibre activity in the optic nerve and the myelinated fibre evoked postsynaptic wave in the tectum was discussed.

14. The sequence of the timing, the distribution and the extent of innervation of the tectum by optic nerve afferents was discussed in relationship to the development of the visual system in Xenopus and in relationship to the evidence concerning visual pathway development in higher vertebrates.

BIBLIOGRAPHY

BIBLIOGRAPHY

The abbreviations in this bibliography are those quoted by the Biosciences Information Service of Biological Abstracts.

Adrian, E. D. and G. Moruzzi. (1939) Impulses in the pyramidal tract. J. Physiol. (Lond.) 97: 153-199.

Alley, K. E. (1974) Morphogenesis of the trigeminal mesencephalic nucleus in the hamster: Cytogenesis and neuron death. J. Embryol. Exp. Morphol. 31: 99-121.

Anderson, D. R. and W. F. Hoyt. (1969) Ultrastructure of intraorbital portion of human and monkey optic nerve. Arch. Ophthalmol. 82: 506-530.

Anderson, D. R., W. F. Hoyt and M. J. Hogan. (1968) The fine structure of the astroglia in the human optic nerve and optic nerve head. Trans. Am. Ophthalmol. Soc. 65: 275-305.

Andrew, A. M. (1955) Action potentials from the frog colliculus. J. Physiol. (Lond.) 130: 25P.

Angevine, J. B. and R. L. Sidman. (1961) Autoradiographic study of cell migration during histogenesis of cerebral cortex in the mouse. Nature (Lond.) 192: 766-768.

Attardi, D. G. and R. W. Sperry. (1963) Preferential selection of central pathways by regenerating optic fibres. Exp. Neurol. 7: 46-64.

Barden, C. R. (1903) The growth and histogenesis of the cerebrospinal nerves in mammals. Am. J. Anat. 2: 231-257.

Barlow, H. B. (1953) Action potentials from the frog's retina. J. Physiol. (Lond.) 119: 58-68.

Barlow, H. B. (1975) Visual experience and cortical development. Nature (Lond.) 258: 199-204.

Beal, J. A. and M. H. Cooper. (1976) Myelinated nerve cell bodies in the dorsal horn of the monkey (Saimiri sciureus). Am. J. Anat. 147: 33-49.

Beazley, L., M. J. Keating and R. M. Gaze. (1972) The appearance, during development, of responses in the optic tectum following visual stimulation of the ipsilateral eye in Xenopus laevis. Vision Res. 12: 407-410.

Berman, N. and R. K. Hunt. (1975) Visual projections in the optic tecta in Xenopus after partial extirpation of the embryonic eye. J. Comp. Neurol. 162: 23-42.

Berthold, C.-H. and T. Carlstedt. (1977 a) Observations on the morphology at the transition between the peripheral and central nervous system in the cat. II. General organization of the transitional S_1 dorsal rootlets. Acta. Physiol. Scand. Suppl. 446: 23-42.

Berthold, C.-H. and T. Carlstedt (1977 b) Observations on the morphology at the transition between the peripheral and central nervous system in the cat. III. Myelinated fibres in S_1 dorsal rootlets. Acta. Physiol. Scand. Suppl. 446: 43-60.

Berthold, C.-H. and S. Skoglund. (1968 a) Postnatal development of feline paranodal myelin-sheath segments. I. Light microscopy. Acta. Soc. Med. Upsal. 73: 113-126.

Berthold, C.-H. and S. Skoglund. (1968 b) Postnatal development of feline paranodal myelin sheath segments. II. Light microscopy. Acta. Soc. Med. Upsal. 73: 127-144.

Billett, F. S. and A. E. Wild. (1975) Practical studies of animal development. London: Chapman and Hall.

Bishop, G. H., M. H. Clare and W. M. Landau. (1969) Further analysis of fibre groups in the optic tract of the cat. Exp. Neurol. 24: 386-399.

Blakemore, C. (1974) Development of functional connections in the mammalian visual system. Br. Med. Bull. 30: 152-156.

Blakemore, C. (1977) Genetic instructions and developmental plasticity in the kitten's visual cortex. Phil. Trans. R. Soc. Lond. B. 278: 425-434.

Blinzinger, K. and H. Hager. (1964) In: Progress in Brain Research. W. Bargmann and J. P. Schadé (Eds.) Vol. 6. pp. 99-112.

Blunt, M. J., F. Baldwin and C. P. Wendell-Smith (1972) Gliogenesis and myelination in kitten optic nerve. Z. Zellforsch Mikrosk. Anat. 124: 293-310.

Bodian, D. (1966) Spontaneous degeneration in the spinal cord of monkey foetuses. Bull. Johns Hopkins Hosp. 119: 212-234.

Boulder Committee. (1970) Embryonic vertebrate central nervous system: revised terminology. Anat. Rec. 166: 257-262.

Brown, W. T. (1973) The Caudal Thalamus of the frog: a microelectrode study. Ph.D. Thesis, John Hopkins University, Baltimore.

Brown, W. T. and D. Ingle. (1973) Receptive field changes produced in frog thalamic units by lesions of the optic tectum. Brain Res. 59: 405-409.

Bunge, R. P. (1968) Glial cells and the central myelin sheath. Physiol. Rev. 48: 197-251.

Bunge, R. P., M. B. Bunge and E. Peterson. (1965) An electron microscope study of cultured rat spinal cord. J. Cell Biol. 24: 163-191.

Caldwell, J. H. and N. Berman. (1977) The Central Projections in the retina in Necturus maculosus. J. comp. neurol. 171: 455-464.

Caley, D. W., C. Johnson and R. A. Liebelt. (1972) The postnatal development of the retina in the normal and rodless CBA mouse: A light and electron microscopic study. Am. J. Anat. 133: 179-211.

Cantino, D. and L. S. Daneo. (1973) Synaptic junctions in the developing chick optic tectum. Experientia 29: 85-87.

Carlstedt, T. (1977 a) Observations on the morphology at the transition between the peripheral and central nervous system in the cat. I. A preparative procedure useful for electron microscopy of the lumbosacral dorsal rootlets. Acta. Physiol. Scand. Suppl. 446: 5-21.

Carlstedt, T. (1977 b) Observations on the morphology at the transition between the peripheral and central nervous system in the cat. IV. Unmyelinated fibres in S_1 rootlets. Acta. Physiol. Scand. Suppl. 446: 61-71.

Chung, S. H., T. V. P. Bliss and M. J. Keating. (1974) The synaptic organization of optic afferents in the amphibian tectum. Proc. R. Soc. Lond. B. 187: 421-447.

Chung, S. H. and J. Cooke. (1975) Polarity of structure and of ordered nerve connections in the developing amphibian brain. Nature (Lond.) 258: 126-132.

Chung, S. H., M. J. Keating and T. V. P. Bliss. (1974) Functional synaptic relations during the development of the retino-tectal projection in amphibians. Proc. R. Soc. Lond. B. 187: 449-459.

Chung, S. H., R. V. Stirling and R. M. Gaze. (1975) The structural and functional development of the retina in larval Xenopus. J. Embryol. Exp. Morphol. 33: 915-940.

Clarke, P. G. H. and W. M. Cowan. (1976) The development of the isthmo-optic tract in the chick, with special reference to the occurrence and correction of developmental errors in the location and connections of isthmo-optic neurons. J. Comp. Neurol. 167: 143-164.

Clarke, P. G. H., L. A. Rogers and W. M. Cowan. (1976) The time of origin and the pattern of survival of neurons in the isthmo-optic nucleus of the chick. J. Comp. Neurol. 167: 125-142.

Cohen, A. I. (1967) Ultrastructural aspects of human optic nerve. Invest. Ophthal. 6: 294-308.

Colonnier, M. (1964) The tangential organization of the visual cortex. J. Anat. 98: 327-344.

Cook, R. D., B. Ghetti and H. M. Wisniewski. (1974) The pattern of Wallerian degeneration in the optic nerve of newborn kittens: an ultrastructural study. Brain Res. 75: 261-276.

Cook, R. D. and H. M. Wisniewski. (1973) The role of oligodendroglia and astroglia in Wallerian degeneration of the optic nerve. Brain Res. 61: 191-206.

Cowan, W. M. (1970) Centrifugal fibres to the avian retina. Br. Med. Bull. 26: 112-118.

Cowan, W. M., D. I. Gottlieb, A. E. Hendrickson, J. L. Price and T. A. Woolsey. (1972) The autoradiographic demonstration of axonal connections in the C.N.S. Brain Res. 96: 1-23.

Cowan, W. M. and E. Wenger. (1967) Cell loss in the trochlear nucleus of the chick during normal development and after radical extirpation of the optic vesicle. J. Exp. Zool. 164: 267-280.

Cragg, B. G. (1975) The development of synapses in the visual system of the cat. J. Comp. Neurol. 160: 147-166.

Cragg, B. G., D. H. L. Evans and L. H. Hamlyn. (1954) The optic tectum of Gallus domesticus. A correlation of the electrical responses with the histological structure. J. Anat. 88: 293-305.

Cross, B. A. and I. A. Silver. (1963) Unit activity in the hypothalamus and the sympathetic response to hypoxia and hypercapnia. Exp. Neurol. 7: 375-393.

Crossland, W. J., W. M. Cowan and J. P. Kelly. (1973) Observations on the transport of radioactively labelled proteins in the visual system of the chick. Brain Res. 56: 77-105.

Crossland, W. J., W. M. Cowan, L. A. Rogers, and J. P. Kelly. (1974) The specification of the retinotectal projection in the chick. J. Comp. Neurol. 155: 127-164.

Cullen, M. J. and H. de F. Webster. (1976) The effects of low temperature on optic nerves of Xenopus tadpoles during myelin formation. Anat. Rec. 184: 385-386.

Currie, J. R. (1974) Some observations on the development of the visual system in the frog Rana pipiens. Ph.D. Thesis, Washington University, St. Louis, MO.

Currie, J. and W. M. Cowan. (1974 a) Evidence for the late development of the uncrossed retinothalamic projections in the frog Rana pipiens. Brain Res. 71: 133-139.

Currie, J. and W. M. Cowan. (1974 b). Some observations on the early development of the optic tectum in the frog (Rana pipiens) with special reference to the effects of early eye removal on mitotic activity in the larval tectum. J. Comp. Neurol. 156: 123-142.

Currie, J. and W. M. Cowan. (1975) The development of the retinotectal projection in Rana pipiens. Dev. Biol. 46: 103-119.

Das, G. D., G. L. Lammeit and J. P. McAllister. (1974) Contact guidance and migratory cells in the developing cerebellum. Brain Res. 69: 13-29.

Davison, A. N. and J. Dobbing. (1966) Myelination as a vunerable period in brain development. Br. Med. Bull. 22: 40-44.

Daw, N. W. (1968) Colour-coded ganglion cells in the goldfish retina: extension of the receptive fields by means of new stimuli. J. Physiol. (Lond.) 197: 567-592.

DeLong, G. R. and A. J. Coulombre. (1965) Development of the retinotectal topographic projection in the chick embryo. Exp. Neurol. 13: 351-363.

Dixon, J. S. and J. R. Cronly-Dillon. (1972) The fine structure of the developing retina in Xenopus laevis. J. Embryol. Exp. Morphol. 28: 659-666.

Donovan, A. (1966) The postnatal development of the cat retina. Exp. Eye Res. 5: 249-254.

Dubin, M. W. (1970) The inner plexiform layer of the vertebrate retina: A quantitative and comparative electron microscopic analysis. J. Comp. Neurol. 140: 479-506.

Easter, S. S. Jr., P. R. Johns and L. R. Baumann. (1977) Growth of the adult goldfish eye. I. optics. Vision Res. 17: 469-477.

Eccles, J. C., R. Llinás and K. Sasaki. (1966) Parallel fibre stimulation and responses induced thereby in Purkinje cells of the cerebellum. Exp. Brain Res. 1: 17-39.

Ewert, J.-P. (1968) Der Einfluss von Zwischenhirndefekten auf der Visuomotorik in Beutefang und Fluchtverhalten der Erdkröte (Bufo bufo L.) Z. vergl. Physiol. 61: 41-70.

Ewert, J.-P. (1970) Neural mechanisms of prey-catching and avoidance behaviour in the toad (Bufo bufo L.) Brain Behav. Evol. 3: 36-57.

Ewert, J.-P. (1971) Single unit response of the toad's (Bufo americanus) Caudal Thalamus to visual objects. Z. Vergl. Physiol. 74: 81-102.

Ewert, J.-P. (1977) In: Comparative neurology of the optic tectum. S. O. E. Ebbeson and H. Vanegas (Eds.) New York, Plenum Press. (In press)

Ewert, J.-P. and H.-W. Borchers. (1971) Reaktions-charakteristik von neuronen aus dem tectum opticum und subtectum der Erdkröte Bufo bufo (L.). Z. Vergl. Physiol. 71: 165-189.

Ewert, J.-P. and H.-W. Borchers. (1974) Inhibition of toad (Bufo bufo L.) retina on-off and off- ganglion cells via active eye closing. Vision Res. 14: 1275-1276.

Ewert, J.-P. and H. Burghagen. (1977) Manuscript submitted to Brain, Behaviour and Evolution.

Ewert, J.-P. and F. J. Hock. (1972) Movement sensitive neurons in the toad's retina. Exp. Brain Res. 16: 41-59.

Ewert, J.-P., F. J. Hock and A. von Wietersheim. (1974) Thalamus, pretectum, tectum: Retinal topography and physiological interactions in the toad Bufo bufo (L.) J. Comp. Physiol. 92: 343-356.

Ewert, J.-P. and A. von Wietersheim. (1974 a) Types of ganglion cells in the retinotectal projection of the toad Bufo bufo (L.). Acta. Anat. 88: 56-66.

Ewert, J.-P. and A. von Wietersheim. (1974 b) Musterauswertung durch tectale und thalamus/praetectale Nervennetze im visuellen System der Kröte Bufo bufo (L.). J. Comp. Physiol. 92: 131-148.

Ewert, J.-P. and A. von Wietersheim. (1974 c) Der Einfluss von Thalamus/Praetectum-Defekten auf die Antwort von Tectum-Neuronen geganuber visuellen Mustern bei der Kröte Bufo bufo (L.). J. Comp. Physiol. 92: 149-160.

Feldman, J. D. and R. M. Gaze. (1975) The development of the retinotectal projection in Xenopus with one compound eye. J. Embryol. Exp. Morphol. 33: 775-787.

Feldman, J. D., R. M. Gaze and M. J. Keating. (1971) Delayed innervation of the optic tectum during development in Xenopus laevis. Brain Res. 14: 16-23.

Fink, P. P. and L. Heimer. (1967) Two methods for selective silver impregnation of degenerating axons and their synaptic endings in the central nervous system. Brain Res. 4: 369-374.

Fisher, L. J. (1972) Changes during maturation and metamorphosis in the synaptic organization of the tadpole retina inner plexiform layer. Nature 235: 391-393.

Fisher, L. J. (1976) Synaptic arrays of the inner plexiform layer in the developing retina of Xenopus. Dev. Biol. 50: 402-412.

Fisher, S. and M. Jacobson. (1970) Ultrastructural changes during early development of retinal ganglion cells in Xenopus. Z. Zellforsch. Mikrosk. Anat. 104: 165-177.

Fite, K. V. (1969) Single unit analysis of binocular neurons in the frog optic tectum. Exp. Neurol. 24: 475-486.

Fite, K. V., G. C. Russell and D. Vicario. (1977) Visual neurons in frog anterior thalamus. Brain Res. 127: 283-290.

Fraher, J. P. (1972) A quantitative study of anterior root fibres during early myelination. J. Anat. 112: 99-124.

Freeman, J. A. (1969) The cerebellum as a timing device: an experimental study in the frog. In: Neurobiology of Cerebellar Evolution and Development. R. Llinás (Ed.). Chicago. American Medical Association pp. 397-420.

Freeman, J. A. (1977) Possible regulatory function of acetylcholine receptor in maintenance of retinotectal synapses. Nature 269: 218-222.

Freeman, J. A. and C. Nicholson. (1975) Experimental optimization of current source-density technique for anuran cerebellum. J. Neurophysiol. 38: 369-382.

Freeman, J. A. and J. Stone. (1969) A technique for current density analysis of field potentials and its application to the frog cerebellum. In: Neurobiology of Cerebellar Evolution and Development. (Ed.) Llinás R. Amer. Med. Ass. Chicago, Ill., 421-430.

Friede, R. L. and T. Samorajski. (1967) Relation between the number of myelin lamellae and axon circumference in fibres of vagus and sciatic nerves of mice. J. Comp. Neurol. 130: 223-232.

Fujita, S. (1967) Quantitative analysis of cell proliferation and differentiation in the cortex of the postnatal mouse cerebellum. J. Cell Biol. 32: 277-287.

Gaillard, F. and G. Galand. (1977). New ipsilateral visual units in the frog optic tectum. Brain Res. 136: 351-354.

Gasser, H. S. and J. Erlanger. (1927) The role played by the sizes of the constituent fibres of a nerve trunk in determining the form of its action potential wave. Am. J. Physiol. 80: 522-547.

Gaupp, E. (1899) A. Ecker's und R. Wiedersheim's Anatomie des frosches. 2 Abt. Braunschweig: F. Vieweg.

Gaze, R. M. (1959) Regeneration of the optic nerve in Xenopus laevis. Q. J. Exp. Physiol. 44: 290-308.

Gaze, R. M. (1970) Formation of Nerve Connections. New York: Academic Press.

Gaze, R. M., S. H. Chung and M. J. Keating. (1972) Development of the retinotectal projection in Xenopus. Nature 236: 133-35.

Gaze, R. M. and M. Jacobson. (1963) A study of the retinotectal projection during regeneration of the optic nerve in the frog. Proc. R. Soc. Lond. B. 157: 420-448.

Gaze, R. M. and M. J. Keating. (1969) The depth distribution of visual units in the tectum of the frog following regeneration of the optic nerve. J. Physiol. 200: 128P.

Gaze, R. M., M. J. Keating and S. H. Chung. (1974) The evolution of the retinotectal map during development in Xenopus. Proc. R. Soc. Lond. B. 185: 301-330.

Gaze, R. M. and A. Peters. (1961) The development, structure and composition of the optic nerve of Xenopus laevis (Daudin). Q. J. Exp. Physiol. 46: 299-309.

George, S. (1970) Studies on optic nerve terminal arborization in the frog's tectum. Ph.D. Thesis, John Hopkin's University, Baltimore, Maryland.

Geren, B. B. (1954) The formation from the Schwann cell surface of myelin in the peripheral nerves of chick embryos. Exp. Cell Res. 7: 558-562.

Gesteland, R. C., B. Howland, J. Y. Lettvin and W. H. Pitts. (1959) Comments on microelectrodes. Proc. Inst. Radio Engineers 47: 1856-1862.

Glendenning, R. L. and T. T. Norton. (1973) Receptive field properties of lateral geniculate neurons in kittens. Soc. Neurosci. 3: 298.

Glücksman, A. (1951) Cell deaths in normal vertebrate ontogeny. Biol. Rev. (Camb.) 26: 58-86.

Grafstein, B., M. Murray and N. A. Ingoglia. (1972) Protein synthesis and axonal transport in retinal ganglion cells of mice lacking visual receptors. Brain Res. 44: 37-38.

Graham, R. C. and M. J. Karnovsky. (1966) The early stages of absorption of injected horseradish peroxidase in the proximal tubules of mouse kidney. Ultrastructural cytochemistry by a new technique. J. Histochem. Cytochem. 14: 271-302.

Gruberg, E. R. (1973) Optic fibre projections of the tiger Salamander Ambystoma tigrinum. J. Hirnforsch. 14: 399-411.

Grüsser, O.-J. and U. Grüsser-Cornehls. (1976) Neurophysiology of the anuran visual system. In: Frog Neurobiology - A Handbook. R. Llinás and W. Precht (Eds.). Heidelberg, Springer-Verlag. pp. 297-385.

Gütner, I. I. (1936) Uber die Entwicklung der peripheren markhaltigen Nervenfasern. Z. Zellforsch. Mikrosk. Anat. 25: 259-282.

Haberly, L. B. (1973) Unitary analysis of opossum prepyriform cortex. J. Neurophysiol. 36: 762-774.

Haberly, L. B. and G. M. Shepherd. (1973) Current-density analysis of summed evoked potentials in opossum prepyriform cortex. J. Neurophysiol. 36: 789-802.

Halpern, H., R. T. Wang and D. R. Colman. (1976) Centrifugal fibres to the eye in a non-avian vertebrate: source revealed by horseradish peroxidase studies. Science 194: 1185-1187.

Hamasaki, D. I. and J. T. Flynn. (1977) Physiological properties of retinal ganglion cells of three-week old kittens. Vis. Res. 17: 275-284.

Hartline, H. K. (1938) The response of single optic nerve fibres of the vertebrate eye to illumination of the retina. Amer. J. Physiol. 121: 400-415.

Hartline, H. K. (1940 a) The receptive fields of the optic nerve fibres. Amer. J. Physiol. 130: 690-699.

Hartline, H. K. (1940 b) The effects of spatial summation in the retina on the excitation of the fibres of the optic nerve. Amer. J. Physiol. 130: 700-711.

Hayes, B. P. (1976) The distribution of intercellular gap junctions in the developing retina and pigments epithelium of Xenopus laevis. Anat. Embryol. 150: 99-111.

Hellon, R. F. (1971) The marking of electrode tip positions in nervous tissue. J. Physiol. 214: 12P.

Heric, T. (1964) An electrophysiological study of the optic tectum of a reptile. Ph.D. dissertation, UCLA.

Heric, T. M. and L. Kruger. (1966) The electrical response evoked in the reptilian optic tectum by afferent stimulation. Brain Res. 2: 187-199.

Herrick, C. J. (1925) The amphibian forebrain. III. The optic tracts and centres of Amblystoma and the frog. J. Comp. Neurol. 36: 433-489.

Hildebrand, C. (1971 a) Ultrastructural and light-microscopic studies of the nodal region in large myelinated fibres of the adult feline spinal cord white matter. Acta. Physiol. Scand. Suppl. 364: 43-80.

Hildebrand, C. (1971 b) Ultrastructural and light-microscopic studies of the developing feline spinal cord white matter. I. The nodes of Ranvier. Acta. Physiol. Scand. Suppl. 364: 81-108.

Hildebrand, C. (1971 c) Ultrastructural and light-microscopic studies of the developing feline spinal cord white matter. II. Cell death and myelin sheath disintegration in the early postnatal period. Acta. Physiol. Scand. Suppl. 364: 109-144.

Hildebrand, C. and S. Skoglund. (1971) Calibre spectra of some fibre tracts in the feline central nervous system during postnatal development. Acta. Physiol. Scand. Suppl. 364: 5-42.

Himstedt, W., U. Freidank and E. Singer. (1976) The change of a releasing mechanism underlying prey-catching behaviour during development of Salamandra salamandra (L.). Z. Tierpsychol. 41: 235-243.

Hinds, J. W. (1969) Autoradiographic study of histogenesis in the mouse olfactory bulb. II. Cell proliferation and migration. J. Comp. Neurol. 134: 305-321.

Hinds, J. W. and J. B. Angevine. (1965) Autoradiographic study of histogenesis in the area pyriformis and claustrum in the mouse. Anat. Rec. 151: 456-457.

Hirano, A. (1972) In: Structure and function of nervous tissue. Ed. G. H. Bourne. Vol. V. New York: Academic Press.

Hirose, G. and N. H. Bass. (1973) Maturation of oligodendroglia and myelinogenesis in rat optic nerve: A quantitative histochemical study. J. Comp. Neurol. 152: 201-209.

Hirsch, H. V. and M. Jacobson. (1973) Development and maintenance of connectivity in the visual system of the frog. II. The effects of eye removal. Brain Res. 49: 67-74.

Holden, A. L. (1968 a) The field potential profile during activation of the avian optic tectum. J. Physiol. 194: 75-90.

Holden, A. L. (1968 b) Types of unitary field response and correlation with the field potential profile during activation of the avian optic tectum. J. Physiol. 194: 91-104.

Hollyfield, J. G. (1968) Differential addition of cells to the retina in Rana pipiens tadpoles. Dev. Biol. 18: 163-179.

Hollyfield, J. G. (1971) Differential growth of the neural retina in Xenopus laevis larvae. Dev. Biol. 24: 264-286.

Hollyfield, J. G. (1972) Histogenesis of the retina in the killifish Fundulus heteroclitus. J. Comp. Neurol. 144: 373-380.

Hölmberg, K. A. J. (1972) Fine structure of the optic tract in the Atlantic hagfish Mxyxine glutinosa. Acta Zool. (Stockh.) 53: 165-171.

Hubbard, J. I., R. Llinás and D. M. J. Quastel. (1969) Electrophysiological analysis of synaptic transmission. Arnold: London.

Hubel, D. H. and T. N. Wiesel. (1963) Receptive fields of cells in striate cortex of very young, visually inexperienced kittens. J. Neurophysiol. 26: 994-1002.

Hubel, D. H. and T. N. Wiesel. (1970) Period of susceptibility to the physiological effects of unilateral eye closures in kittens. J. Physiol. (Lond.) 206: 419-436.

Hubel, D. H., T. N. Wiesel and S. Le Vay. (1977) Plasticity of ocular dominance columns in monkey striate cortex. Phil. Trans. R. Soc. (Lond.) B. 278: 377-409.

Hughes, A. (1961) Cell degeneration in the larval ventral horn of Xenopus laevis (Daudin). J. Embryol. Exp. Morphol. 9: 269-284.

Hughes, A. and H. Wässle. (1976) The cat optic nerve: Fibre total count and diameter spectrum. J. Comp. Neurol. 169: 171-184.

Hughes, W. F. and A. La Velle. (1975) The effects of early tectal lesions on development in the retinal ganglion cell layer of chick embryos. J. Comp. Neurol. 163: 265-284.

Hunt, R. K. (1975 a) Position-dependent differentiation of neurons. In: Development Biology: Pattern Formation, Gene regulation. D. McMahon and C. F. Fox (Eds.). California, W. A. Benjamin Inc. Vol. 2. pp. 227-256.

Hunt, R. K. (1975 b) The cell cycle, cell lineage, and neuronal specificity. In: The Cell Cycle and Cell Differentiation. (Eds.) Holtzer, H. and J. Reinert. New York: Springer-Verlag.

Hunt, R. K. and N. Berman. (1975) Patterning of neuronal locus specificities in retinal ganglion cells after partial extirpation of the embryonic eye. J. Comp. Neurol. 162: 43-70.

Hunt, R. K. and M. Jacobson. (1972 a) Development and stability of positional information in Xenopus retinal ganglion cells. Proc. Nat. Acad. Sci. U.S.A. 69: 780-783.

Hunt, R. K. and M. Jacobson. (1972 b) Specification of positional information in retinal ganglion cells of Xenopus: Stability of the specified state. Proc. Nat. Acad. Sci. U.S.A. 66: 2860-2864.

Hunt, R. K. and M. Jacobson. (1973 a) Specification of positional information in retinal ganglion cells of Xenopus: Assays for analysis of the unspecified state. Proc. Nat. Acad. Sci. U.S.A. 70: 507-511.

Hunt, R. K. and M. Jacobson. (1973 b) Neuronal locus specificity: Altered pattern of spatial deployment in fused fragments of embryonic Xenopus eyes. Science 180: 509-511.

Hunt, R. K. and M. Jacobson. (1974 a) Neuronal specificity revisited. Curr. Top. Dev. Biol. 8: 203-259.

Hunt, R. K. and M. Jacobson. (1974 b) Development of neuronal locus specificity in Xenopus retinal ganglion cells after surgical eye transection or after fusion of whole eyes. Dev. Biol. 40: 1-15.

Jacobson, M. (1967) Retinal ganglion cells: specification of central connections in larval Xenopus laevis. Science 155: 1106-1108.

Jacobson, M. (1968 a) Development of neuronal specificity in retinal ganglion cells of Xenopus. Dev. Biol. 17: 202-218.

Jacobson, M. (1968 b) Cessation of DNA synthesis in retinal ganglion cells correlated with the time of specification of their central connections. Dev. Biol. 17: 219-232.

Jacobson, M. (1970) Developmental Neurobiology. New York: Holt, Rinehart and Winston.

Jacobson, M. (1971) Absence of adaptive modification in developing retinotectal connections in frogs after visual deprivation or disparate stimulation of the eyes. Proc. Natl. Acad. Sci. U.S.A. 68: 528-532.

Jacobson, M. (1976) Histogenesis of retina in the clawed frog with implications for the pattern of development of retinotectal connections. Brain Res. 103: 541-545.

Jacobson, M. and H. V. B. Hirsch. (1973) Development and maintenance of connectivity in the visual system of the frog. I. The effects of eye rotation and visual deprivation. Brain Res. 49: 47-65.

Jakob, A. (1928) Das Kleinhirn. In: Handbuch der Mikroskopischen Anatomie des Menschen. Vol. 4. (Ed.) Von Mollendorff, W. (Pub.) Springer: Berlin.

Kahn, A. J. (1973) Ganglion cell formation in the chick neural retina. Brain Res. 63: 285-290.

Kahn, A. J. (1974) An autoradiographic analysis of the time of appearance of neurons in the developing chick neural retina. Dev. Biol. 38: 30-40.

Katz, B. (1966) Nerve, muscle and synapse. New York: McGraw-Hill.

Keating, M. J. (1974) The role of visual function in the patterning of binocular visual connexions. Br. Med. Bull. 30: 145-151.

Keating, M. J. (1975 a) Plasticity of intertectal connexions in adult Xenopus. J. Physiol. (Lond.) 248: 36-37P.

Keating, M. J. (1975 b) The time course of experience-dependent synaptic switching of visual connections in Xenopus laevis. Proc. R. Soc. (Lond.) B. 189: 603-610.

Keating, M. J. (1977) Evidence for the plasticity of intertectal neuronal connections in adult Xenopus. Phil. Trans. R. Soc. (Lond.) B. 278: 277-294.

Keating, M. J., L. Beazley, J. D. Feldman and R. M. Gaze. (1975) Binocular interaction and intertectal neuronal connections: Dependence upon developmental stage. Proc. R. Soc. Lond. B. 191: 445-466.

Keating, M. J. and R. M. Gaze. (1970 a) Observations on the 'surround' properties of the receptive field of frog retinal ganglion cells. Q. J. Exp. Physiol. 55: 129-142.

Keating, M. J. and R. M. Gaze. (1970 b) The depth distribution of visual units in the contralateral optic tectum following regeneration of the optic nerve of the frog. Brain Res. 21: 197-206.

Keating, M. J. and C. Kennard. (1976) Binocular visual neurones in the frog thalamus. J. Physiol. 258: 69P.

Kelly, J. P. and W. M. Cowan. (1972) Studies on the development of the chick optic tectum. III. Effects of early eye removal. Brain Res. 42: 263-288.

Kemali, M. and E. Sada. (1973) Myelinated cell bodies in the habenular nuclei of the frog. Brain Res. 54: 355-359.

Kennedy, M. C. and K. Rubinson. (1977) Retinal projections in larval, transforming and adult sea lamprey Petromyzon marinus. J. Comp. Neurol. 171: 465-480.

Keurs, H. E. D. J. ter. (1970) An electrophysiological study of the synapses between optic nerve fibres and tectal neurons of Rana temporaria. Thesis, Leiden.

Kicliter, E. and Y. M. Chino. (1976) On-units in the ipsilateral thalamus of Rana pipiens. Vis. Res. 16: 1201-1202.

Kitai, S. T., T. Shimono and D. T. Kennedy. (1969) Inhibition in the cerebellar cortex of the lizard, Lacerta viridis. In: Neurobiology of Cerebellar Evolution and Development. R. Llinás (Ed.). Chicago. American Medical Association. pp. 481-489.

Klee, M. and W. Rall. (1977) Computed potentials of cortically arranged populations of neurons. J. Neurophysiol. 40: 647-666.

Klüver, H. and E. Barrera. (1953) A method for combining staining of cells and fibres in the central nervous system. J. Neuropath. Exp. Neurol. 12: 400-403.

Knapp, H., F. Scalia and W. Riss. (1965) The optic tracts of Rana pipiens. Acta. Neurol. Scand. 41: 325-355.

Kollros, J. J. (1953) The development of the optic lobes in the frog. I. The effects of unilateral enucleation in embryonic stages. J. Exp. Zool. 123: 153-187.

Konishi, J. (1960) Electric response of visual centre to optic nerve stimulation in fish. Jpn. J. Physiol. 10: 28-41.

Kostovic, I. and M. E. Molliver. (1974) A new interpretation of the laminar development of cerebral cortex: Synaptogenesis in different layers of neopaliam in the human fetus. Anat. Rec. 178: 395.

Kruger, L. and D. S. Maxwell. (1969) Wallerian degeneration in the optic nerve of a reptile: an electron microscopic study. Am. J. Anat. 125: 247-270.

Kuffler, S. W. and J. G. Nicholls. (1976) From Neuron to Brain. Sinauer: Sunderland, Mass.

Landau, W. M., M. H. Clare and G. H. Bishop. (1968) Reconstruction of myelinated nerve tract action potentials: An arithmetic method. Exp. Neurol. 22: 480-490.

Larsell, O. (1931) The effect of experimental excision of one eye on the development of the optic lobe and opticus layer in larvae of the tree frog (Hyla regilla). II. The effect on cell size and differentiation of cell processes. J. Exp. Zool. 58: 1-20.

LaVail, J. H. and W. M. Cowan. (1971 a) The development of the chick optic tectum. I. Normal morphology and cytoarchitectonic development. Brain Res. 28: 391-419.

LaVail, J. H. and W. M. Cowan. (1971 b) The development of chick optic tectum. II. Autoradiographic studies. Brain Res. 28: 421-441.

Lázár, G. (1971) The projection of the retinal quadrants on the optic centers in the frog. A terminal degeneration study. Acta. Morph. Acad. Sci. Hung. 19: 325-334.

Lázár, G. (1973) The development of the optic tectum in Xenopus laevis: A Golgi study. J. Anat. 116: 347-355.

Lázár, G. (1973 a) Role of the accessory optic system in the Optokinetic Nystagmus of the frog. Brain, Behav. Evol. 5: 443-460.

Lázár, G. and G. Székely. (1969) Distribution of optic terminals in the different optic centres in the frog. Brain Res. 16: 1-4.

Lettvin, J. Y., H. R. Maturana, W. S. McCulloch and W. H. Pitts. (1959) What the frog's eye tells the frog's brain. Proc. Inst. Radio Engineers 47: 1940-1951

Lettvin, J. Y., H. R. Maturana, W. H. Pitts and W. S. McCulloch. (1961) Two remarks on the visual system of the frog. In: Sensory Communication. W. A. Rosenblith (Ed.). Massachusetts: M.I.T. Press. pp. 757-776.

Llinás, R. and C. Nicholson. (1971) Electrophysiological properties of dendrites and soma in alligator purkinje cells. J. Neurophysiol. 34: 532-551.

Llinás, R. and C. Nicholson. (1974) Analysis of field potentials in the central nervous system. In: Handbook of Electroencephalography and Clinical Neurophysiology Section IV, Part B, Volume 2. A. Remond (Ed.).

Longley, A. (1975) Developing nerve connections in the visual system of the frog. In: Developmental Biology, Pattern Formation, Gene regulation. D. McMahon and C. F. Fox (Eds.). California: W. A. Benjamin Inc. Vol. 2.

Lorente de Nó, R. (1947 a) A study of nerve physiology. Rockefeller Institute 132.

Lorente de Nó, R. (1947 b) Action potential of the motorneurones of the hypoglossus nerve. J. Cell. Comp. Physiol. 29: 207-288.

Lund, R. D. and A. H. Bunt. (1976) Prenatal development in central optic pathways in albino rats. J. Comp. Neurol. 165: 247;264.

Mark, R. F. and S. Feldman. (1972) Binocular interaction in the development of optokinetic reflexes in tadpoles of Xenopus laevis. Invest. Opthal. 11: 402-410.

Matthews, M. A. (1968) An electron microscopic study of the relationship between axon diameter and the initiation of myelin production in the peripheral nervous system. Anat. Rec. 161: 337-352.

Matthews, M. A. and D. Duncan. (1971) A quantitative study of morphological changes accompanying the initiation and progress of myelin production in the dorsal funiculus of the rat spinal cord. J. Comp. Neurol. 142: 1-22.

Maturana, H. R. (1958) Efferent fibres in the optic nerve of the toad Bufo bufo. J. Anat. 92: 21-27.

Maturana, H. R. (1959) Numbers of fibres in the optic nerve and the number of ganglion cells in the retina of Anurans. Nature 183: 1406.

Maturana, H. R. (1960) The fine anatomy of the optic nerve of Anurans - an electron microscope study. J. Biophys. Biochem. Cytol. 7: 107-120.

Maturana, H. R., J. Y. Lettvin, W. S. McCulloch and W. H. Pitts. (1959) Evidence that cut optic nerve fibres in a frog regenerate to their proper places in the tectum, Science 130: 1709-1710.

Maturana, H. R., J. Y. Lettvin, W. S. McCulloch and W. H. Pitts. (1960) Anatomy and physiology of vision in the frog (Rana pipiens). J. Gen. Physiol. 43 (2nd suppl.): 129-176.

Mercer, E. N. and M. S. C. Birbeck. (1966) 'Electron Microscopy. A Handbook for Biologists.' 2nd Edition. Oxford: Blackwell Scientific Publications.

Meyer-Koenig, D., W. M. Treff and W. Schlote. (1972) Stereological study on the submicroscopic structure of the rat optic nerve. Z. Zellforsch. Mikrosk. Anat. 133: 249-265.

Miale, I. L. and R. L. Sidman. (1961) An autoradiographic analysis of histogenesis in the mouse cerebellum. Exp. Neurol. 4: 277-296.

Moore, C. L., R. Kalil and W. Richards. (1976) Development of myelination in optic tract of the cat. J. Comp. Neurol. 165: 125-136.

Mori, S. (1973) Analysis of field response in the optic tectum of the pigeon. Brain Res. 54: 193-206.

Morris, V. B., C. C. Wylie and V. J. Miles. (1976) The growth of the chick retina after hatching. Anat. Rec. 184: 111-114.

Motokawa, K., T. Oikawa and T. Ogawa. (1958) Midbrain response to electrical stimulation of the optic nerve. Tohoku J. Exp. Med. 69: 79-88.

Muntz, W. R. A. (1962) Microelectrode recordings from the diencephalon of the frog (R. pipiens) and a blue-sensitive system. J. Neurophysiol. 25: 699-711.

Neary, T. J. (1976) An autoradiographic study of the retinal projections in some members of "archaic" and "advanced" anuran families. Anat. Rec. 146-487.

Nicholson, C. (1973) Theoretical analysis of field potentials in anisotropic ensembles of neuronal elements. I.E.E.E. Trans. Bio-Med. Engng. 20: 278-288.

Nicholson, C. and J. A. Freeman. (1975) Theory of current source density analysis and determination of conductivity tensor for anuran cerebellum. J. Neurophysiol. 38: 356-368.

Nicholson, C. and R. Llinás. (1971) Field potentials in the alligator cerebellum and theory of their relationship to Purkinje cell dendritic spikes. J. Neurophysiol. 34: 509-531.

Nieuwkoop, P. D. and J. Faber. (1956) Normal table of Xenopus laevis (Daudin). Amsterdam: North Holland Publishing Co.

Niu, M. C. and V. C. Twitty. (1953) The differentiation of gastrula ectoderm in medium conditioned by axial mesoderm. Proc. Natl. Acad. Sci. USA 39: 985-989.

Norton, T. T. (1974) Receptive-field properties of superior colliculus cells and development of visual behaviour in kittens. J. Neurophysiol. 37: 674-690.

O'Flaherty, J. J. (1971) The optic nerve of the Mallard duck: Fibre diameter frequency distribution and physiological properties. J. Comp. Neurol. 143: 17-24.

Öhman, P. (1977) Fine structure of the optic nerve of Lampetra fluviatilus (Cyclastomi). Vision Res. 17: 719-722.

Orkand, R. K., J. G. Nicholls and S. W. Kuffler. (1966) Effect of nerve impulses on the membrane potential of glial cells in the central nervous system of the amphibia. J. Neurophysiol. 29: 788-806.

Palay, S. L. and V. C. Chan-Palay. (19 4) The Cerebellar Cortex: Cytology and Organization. Berlin: Springer-Verlag.

Pappas, G. D. and D. P. Purpura. (1961) Fine structure of dendrites in the superficial neocortical neuropil. Exp. Neurol. 4: 507-530.

Peretz, B. (1969) Vertical distribution of optic nerve fibre terminations in the frog optic tectum. Am. J. Physiol. 217: 181-187.

Peters, A. (1960 a) The structure of myelin sheaths in the central nervous systems of Xenopus laevis (Daudin). J. Biophys. Biochem. Cytol. 7: 121-126.

Peters, A. (1960 b) The formation and structure of myelin sheaths in the central nervous system. J. Biophys. Cytol. 8: 431-446.

Peters, A. (1964) Further observations on the structure of myelin sheaths in the central nervous system. J. Cell Biol. 20: 281-296.

Peters, A. (1968) The Morphology of Axons of the Central Nervous System. In: The structure and function of Nervous Tissue. G. H. Bourne (Ed.). New York: Academic Press, Vol. 1. pp 141-186.

Peters, A., S. L. Palay and H. de F. Webster. (1970) The Fine Strucutre of the Nervous System. The cells and their processes. New York: Harper and Row.

Pettigrew, J. D. (1974) The effect of visual experience on the development of stimulus specificity by kitten cortical neurones. J. Physiol. (Lond.) 235: 49-74.

Picouet, M. J. and P. Clairambault. (1976) Une nouvelle voie visuelle chez un amphibien anoure, Discoglossus pictus. C. R. Acad. Sci. (Paris), 282: 2195-2198.

Pomeranz, B. (1972) Metamorphosis of frog vision: Changes in ganglion cell physiology and anatomy. Exp. Neurol. 34: 187-199.

Pomeranz, B. and S. H. Chung. (1970) Dendritic tree anatomy codes form-vision physiology in tadpole retina. Science 170: 983-985.

Potter, D. D., E. J. Furshpan and E. S. Lennox. (1966) Connections between cells of the developing squid as revealed by electrophysiological methods. Proc. Nat. Acad. Sci. U.S.A. 55: 328-326.

Potter, H. D. (1965) Mesencephalic auditory region of the bullfrog. J. Neurophysiol. 28: 1132-1154.

Potter, H. D. (1969) Structural characteristics of cell and fiber populations in the optic tectum of the frog (Rana catesbeiana). J. Comp. Neurol. 136: 203-232.

Potter, H. D. (1972) Terminal arborizations of retinotectal axons in the bullfrog. J. Comp. Neurol. 144: 269-284.

Prestige, M. C. (1965) Cell turnover in the spinal ganglia of Xenopus laevis tadpoles. J. Embryol. Exp. Morphol. 13: 63-72.

Prestige, M. C. (1967 a) The control of cell number in the lumbar spinal ganglia during the development of Xenopus laevis tadpoles. J. Embryol. Exp. Morphol. 17: 453-471.

Prestige, M. C. (1967 b) The control of cell number in the lumbar ventral horns during the development of Xenopus laevis tadpoles. J. Embryol. Exp. Morphol. 18: 359-387.

Prineas, J., C. S. Raine and H. Wisniewski. (1969) An ultrastructural study of experimental demyelination and remyelination: III. Chronic experimental allergic encephalomyelitis in the central nervous system. Lab. Invest. 21: 472-483.

Rager, G. (1976 a) Morphogenesis and physiogenesis of the retino-tectal connection in the chicken. I. The retinal ganglion cells and their axons. Proc. R. Soc. (Lond.) B. 192: 331-352.

Rager, G. (1976 b) Morphogenesis and physiogenesis of the retinotectal connection in the chicken. II. The retiontectal synapses. Proc. R. Soc. (Lond.) B. 192: 353-370.

Rager, G. and U. Rager. (1976) Generation and degeneration of retinal ganglion cells in the chicken. Exp. Brain Res. 25: 551-553.

Rakic, P. (1971) Neuron-glia relationship during granule cell migration in developing cerebellar cortex: A Golgi and electronmicroscopic study in Macacus rhesus. J. Comp. Neurol. 141: 283-312.

Rakic, P. (1976) Prenatal genesis of connections subserving ocular dominance in the rhesus monkey. Nature (Lond.) 261: 467-471.

Rakic, P. (1977) Prenatal development of the visual system in rhesus monkey. Phil. Trans. R. Soc. Lond. B. 278: 245-260.

Rakic, P. and R. L. Sidman. (1970) Histogenesis of cortical layers in human cerebellum, particularly the lamina dissecans. J. Comp. Neurol. 139: 473-500.

Rakic, P. and R. L. Sidman. (1973) Weaver mutant mouse cerebellum: Defective neuronal migration secondary to abnormality of Bergmann glia. Proc. Natl. Acad. Sci. U.S.A. 70: 240-244.

Rall, W. and G. M. Shepherd. (1968) Theoretical reconstruction of field potentials and dendrodendritic synaptic interactions in olfactory bulb. J. Neurophysiol. 31: 884-915.

Ramon, P. (1890) Investigations de histologia comparanda en los centros opticas de distintos vertebrados. Thesis, cited in Ramon Y Cajal, S. (1911).

Ramon Y Cajal, S. (1911) Histologie du systeme nerveux de ('Lomme et des vertebres). Madrid: Instituto Ramon Y Cajal.

Reier, P. J. and A. Hughes. (1972) Evidence for spontaneous axon degeneration during peripheral nerve maturation. Am. J. Anat. 135: 147-152.

Reier, P. J. and H. de F. Webster. (1974) Regeneration and remyelination of Xenopus tadpole optic nerve fibres following transection or crush. J. Neurocytol. 3: 591-618.

Reuter, T. (1969) Visual pigments and ganglion cell activity in the retina of tadpoles and adult frogs (Rana temporaria). Acta. Zool. Fenn. 122: 1-64.

Robertson, J. D. (1960) The molecular structure and contact relationships of cell membranes. Progr. Biophys. Biophys. Chem. 10: 343-418.

Rogers, L. A. and W. M. Cowan. (1973) The development of the mesencephalic nucleus of the trigeminal nerve in the chick. J. Comp. Neurol. 147: 291-320.

Rosenbluth, J. (1965) Irregularities in myelin sheaths of toad brain. Anat. Rec. 151: 407.

Rosenbluth, J. (1966) Redundant myelin sheaths and other ultrastructural features of the toad cerebellum. J. Cell Biol. 28: 73-93.

Rosenbluth, J. and S. L. Palay. (1961) The fine structure of nerve cell bodies and their myelin sheaths in the eighth nerve ganglion of the goldfish. J. Biophys. Biochem. Cytol. 9: 853-877.

Ross, L. L., M. B. Bornstein and G. M. Lehrer. (1962) Electron microscopic observations of rat and mouse cerebellum in tissue culture. J. Cell Biol. 14: 19-30.

Rushton, W. A. H. (1951) A theory of the effects of fiber size in medullated nerve. J. Physiol. (Lond.) 115: 101-122.

Saunders, J. (1966) Death in embryonic systems. Science 154: 604-612.

Saunders, J. and J. F. Fallon. (1966) Cell death in morphogenesis. In: Major Problems in Developmental Biology. M. Locke (Ed.). New York: Academic Press. pp 289-314.

Scalia, F. (1973) Autoradiographic demonstration of optic nerve fibers in the stratum zonale of the frog's tectum. Brain Res. 58: 484-488.

Scalia, F. (1976) The optic pathway of the frog: Nuclear organization and connections. In: Frog Neurobiology - A Handbook. R. Llinás and W. Precht (Eds.). Heidelberg. Springer-Verlag. pp. 386-406.

Scalia, F. and D. R. Colman. (1974) Aspects of the central projection of the optic nerve in the frog as revealed by anterograde migration of horseradish peroxidase. Brain Res. 79: 496-504.

Scalia, F. and K. V. Fite. (1974) A retinotopic analysis of the central connections of the optic nerve in the frog. J. Comp. Neurol. 158: 455-478.

Scalia, F. and K. Gregory. (1970) Retinofugal projections in the frog: location of the postsynaptic neurons. Brain Behav. Evol. 1: 324-353.

Scalia, F., H. Knapp, M. Halpern and W. Riss. (1968) New observations on the retinal projection in the frog. Brain Behav. Evol. 1: 324:353.

Schmatolla, E. (1972) Dependence of tectal neuron differentiation on optic innervation in teleost fish. J. Embryol. Exp. Morphol. 27: 555-576.

Schmatolla, E. and H. A. Fischer. (1972) Axonal transport in embryonic visual system in zebrafish. Expl. Brain Res. 15: 168-176.

Schmatolla, E. and G. Erdman. (1973) Influence of retinotectal innervation on cell proliferation and cell migration in the embryonic teleost tectum. J. Embryol. Exp. Morphol. 29: 697-712.

Schmidt, J. T. (1976) Expansion of the half-retinal projection in goldfish. Ph.D. Thesis, University of Michigan.

Schönbach, C. (1969) The neuroglia in the spinal cord of the newt Triturus viridescens. J. Comp. Neurol. 135: 93-119.

Scott, T. M. (1974) The development of the retino-tectal projection in Xenopus laevis: an autoradiographic and degenerative study. J. Embryol. Exp. Morphol. 31: 409-414.

Scott, T. M. and G. Lázár. (1976) An investigation into the hypothesis of shifting neuronal relationships during development. J. Anat. 121: 485-496.

Shepherd, G. M. (1962) Transmission in the olfactory pathway. Ph.D. Thesis, Oxford University.

Shepherd, G. M. (1963) Neuronal systems controlling mitral cell excitability. J. Physiol. (Lond.) 168: 101-117.

Shepherd, G. M. (1974) The synaptic organization of the brain: an introduction. New York: Oxford University Press.

Shepherd, G. M. and L. B. Haberly. (1970) Partial activation of olfactory bulb: Analysis of field potentials and topographical relation between bulb and lateral olfactory tract. J. Neurophysiol. 33: 643-653.

Sidman, R. L. (1961) Histogenesis of mouse retina studies with thymidine-H^3. In: The structure of the eye. Smelser, G. K. (Ed.) New York: Academic Press.

Silver, J. (1972) The role of cell degeneration in the developing rat eye. Anat. Rec. 172: 406.

Silver, J. and A. F. W. Hughes. (1973) The role of cell death during morphogenesis of the mammalian eye. J. Morphol. 140: 159-170.

Singer, M. and M. C. Steinberg. (1972) Wallerian degeneration: A reevaluation based on transected and colchicine-poisoned nerves in the amphibian Triturus. Am. J. Anat. 133: 51-83.

Skarf, B. (1973) Development of binocular single units in the optic tectum of frog raised with disparate stimulation to the eyes. Brain Res. 51: 352-357.

Skarf, B. and M. Jacobson. (1974) Development of binocularity driven single units on frogs raised with assymmetrical visual stimulation. Exp. Neurol. 42: 669-686.

Skoff, R. P., D. L. Price and A. Stocks. (1976 a) Electron microscopic autoradiographic studies of gliogenesis in rat optic nerve: I. Cell proliferation. J. Comp. Neurol. 169: 291-312.

Skoff, R. P., D. L. Price and A. Stocks. (1976 b) Electron microscopic autoradiographic studies of gliogenesis in rat optic nerve. II. Time of origin. J. Comp. Neurol. 169: 313-334.

Smith, R. S. and Z. J. Koles. (1970) Myelinated nerve fibres: computed effect of myelin thickness on conduction velocity. Am. J. Physiol. 219: 1256-1258.

Sohal, G. S. (1976) Effects of deafferentiation on the development of the isthmo-optic nucleus in the duck (Anas platyrhynchos). Exp. Neurol. 50: 161-173.

Speidel, C. C. (1932) Studies of living nerves. I. The movements of individual sheath cells and nerve sprouts correlated with the process of myelin-sheath formation in amphibian larvae. J. Exp. Zool. 61: 279-314.

Speidel, C. C. (1933) Studies on living nerves. II. Activities of ameboid growth cones, sheath cells and myelin segments, as revealed by prolonged observation of individual nerve fibres in frog tadpoles. Am. J. Anat. 52: 1-79.

Sperry, R. W. (1943) Visuomotor co-ordination in the newt (Triturus viridescens) after regeneration of the optic nerve. J. Comp. Neurol. 79: 33-55.

Sperry, R. W. (1944) Optic nerve regeneration with return of vision on anurans. J. Neurophysiol. 7: 57-69.

Stein, B. E., E. Labos and L. Kruger. (1973) Sequence of changes in properties of neurons of superior colliculus of the kitten during maturation. J. Neurophysiol. 36: 667-679.

Stone, J. and J. A. Freeman. (1971) Synaptic organization of the pigeon's optic tectum: A Golgi and current source-density analysis. Brain Res. 27: 203-221.

Straznicky, K. (1973) The formation of the optic fibre projection after partial tectal removal in Xenopus. J. Embryol. Exp. Morphol. 29: 397-409.

Straznicky, K. (1976) Reorganization of retino-tectal projection of compound eyes after various tectal lesions in Xenopus. J. Embryol. Exp. Morphol. 35: 41-57.

Straznicky, K. and R. M. Gaze. (1971) The growth of the retina in Xenopus laevis: an autoradiographic study. J. Embryol. Exp. Morphol. 26: 469-474.

Straznicky, K. and R. M. Gaze. (1972) The development of the tectum in Xenopus laevis: an autoradiographic study. J. Embryol. Exp. Morphol. 28: 87-115.

Straznicky, K., R. M. Gaze and M. J. Keating. (1971) The retinotectal projections after uncrossing the optic chiasma in Xenopus with one compound eye. J. Embryol. Exp. Morphol. 26: 523-542.

Straznicky, K., R. M. Gaze and M. J. Keating. (1974) The retinotectal projection from a double-ventral compound eye in Xenopus laevis. J. Embryol. Exp. Morphol. 31: 123-137.

Straznicky, K. and D. Tay. (1977) Retinal growth in double dorsal and double ventral eyes in Xenopus. J. Embryol. Exp. Morphol. 40: 175-185.

Sturrock, R. R. (1975) A light and electron microscope study of proliferation and maturation of fibrous astrocytes in the optic nerve of the human embryo. J. Anat. 119: 223-234.

Sutterlin, A. M. and C. L. Prosser. (1970) Electrical properties of goldfish optic tectum. J. Neurophysiol. 33: 36-45.

Székely, G. (1973) Anatomy and synaptology of the optic tectum. In: Handbook of Sensory Physiology V11/3 Central Visual Information B. (Ed.) Jung, R. Berlin: Springer-Verlag.

Székely, G. and G. Lázár. (1976) Cellular and synaptic architecture of the optic tectum. In: Frog Neurobiology: A Handbook. (Eds.) Llinás, R. and Precht, W. Heidelberg: Springer-Verlag.

Székely, G., Sétáló, G. and Lázár, G. (1973) Fine structure of the frog's optic tectum: optic fibre termination layers. J. Hirnforsch. 14: 189-225.

Tapp, R. L. (1973) The structure of the optic nerve of the teleost: Eugerres plumieri. J. Comp. Neurol. 150: 239-251.

Tapp, R. L. (1974) Axon numbers and distribution myelin thickness, and reconstruction of compound action potential in the optic nerve of the teleost: Eugerres plumieri. J. Comp. Neurol. 153: 267-274.

Tasaki, K. (1970) Three fiber groups in the frog optic nerve. J. Physiol. Soc. Jap. 32: 1-2.

Taylor, A. C. and J. J. Kollros. (1946) Stages in the normal development of Rana pipiens larvae. Anat. Rec. 94: 7-23.

Thomas, R. C. and V. J. Wilson. (1965) Precise localization of renshaw cells with a new marking technique. Nature (Lond.) 206: 211-213.

Trachtenberg, M. C. and D. Ingle. (1974) Thalamo-tectal projections in the frog. Brain Res. 79: 419-430.

Treff, W. M., E. Meyer-Koenig and W. Schlote. (1972) Morphometric analysis of a fibre system in the central nervous system. J. Microsc. (Oxf.) 95: 337-342.

Tucker, G. S. and J. G. Hollyfield. (1977) Modifications by light and synaptic density in the inner plexiform layer of the toad, Xenopus laevis. Exp. Neurol. 55: 133-151.

Turner, J. E. and K. A. Glaze. (1977) The early stages of Wallerian degeneration in the severed optic nerve of the newt (Triturus viridescens). Anat. Rec. 187: 291-311.

Turner, J. E. and M. Singer. (1974) An electron microscopic study of the newt (Triturus viridescens) optic nerve. J. Comp. Neurol. 156: 1-17.

Turner, J. E. and M. Singer. (1975) The ultrastructure of Wallerian degeneration in the severed optic nerve of the newt (Triturus viridescens). Anat. Rec. 267-285.

Udin, S. B. (1977) Rearrangements of the retinotectal projection in Rana pipiens after unilateral caudal half-tectum ablation. J. Comp. Neurol. 173: 561-582.

Valverde, F. (1965) 'Studies on the piriform lobe.' Harvard University Press.

Valverde, F. (1970) The Golgi Method. A tool for comparative structural analyses. In: Contemporary Research Methods in Neuroanatomy. W. J. H. Nauta and S. O. E. Ebesson (Eds.) New York: Springer-Verlag. pp 12-31.

Vanegas, H., J. Amat and E. Essáyag-Millán. (1974) Postsynaptic phenomena in optic tectum neurones following optic nerve stimulation in fish. Brain Res. 77: 25-38.

Vanegas, H., E. Essáyag-Millán and M. Laufer. (1971) Response of the optic tectum to stimulation of the optic nerve in the teleost Eugerres plumiere. Brain Res. 31: 107-118.

Vanegas, H. and B. Williams. (1977) Cerebelloid circuit in the teleost in optic tectum? Parallel course, action potential and on-beam postsynaptic effects of marginal fibres. Proc. Int. Inst. Physiol. 27: Abs. 2311.

Vaney, D. I. and A. Hughes. (1976) The rabbit optic nerve: Fibre diameter spectrum, fibre count, and comparison with a retinal ganglion cell count. J. Comp. Neurol. 170: 241-251.

Vaughn, J. E. (1969) An electron microscopic analysis of gliogenesis in rat optic nerves. Z. Zellforsch. Mikrosk. Anat. 140: 145-167.

Vaughn, J. E. and A. Peters. (1967) Electron microscopy of the early postnatal development of fibrous astrocytes. Amer. J. Anat. 121: 131-151.

Vignal, W. (1883 a) Aeroissement en longeur des tubes nerveux par la formation des segments intercalaires. Arch. Physiol. 15: 336-348.

Vignal, W. (1883 b) Memoire sur le development des tubes nerveux chez les embryous de mammifres. Arch. Physiol. 15: 513-534.

Voeller, K., G. O. Pappas and D. P. Pupura. (1963) Electron microscope study of development of cat superficial neocortex. Exp. Neurol. 7: 107-130.

Webster, H. de F. and D. Spiro. (1960) Phase and electronmicroscopic studies of experimental demyelination. I. Variations in myelin sheath contour in normal guinea pig sciatic nerve. J. Neuropath. Exp. Neurol. 19: 42-69.

Weidman, T. A. and T. Kuwabara. (1968) Postnatal development of the rat retina. An electron microscopic study. Arch. Ophthalmol. 79: 470-484.

Wendell-Smith, C. P., M. J. Blunt and F. Baldwin. (1966) The ultrastructural characterization of macroglial cell types. J. Comp. Neurol. 127: 219-240.

Werblin, F. S. and J. E. Dowling. (1969) Organization of the retina of the mudpuppy, Necturus maculosus. II. Intracellular recording. J. Neurophysiol. 32: 339-355.

Wiesel, T. N. and D. H. Hubel. (1963 a) Effects of visual deprivation on morphology and physiology of cells in the cat's lateral geniculate body. J. Neurophysiol. 26: 978-993.

Wiesel, T. N. and D. H. Hubel. (1963 b) Single-cell responses in striate cortex of kittens deprived of vision in one eye. J. Neurophysiol. 26: 1003-1017.

Wiesel, T. N. and D. H. Hubel. (1974) Ordered arrangement of orientation columns in monkeys lacking visual experience. J. Comp. Neurol. 158: 307-318.

Wilczynski, W. and R. G. Northcutt. (1977) Afferents to the optic tectum of the leopard frog: an HRP study. J. Comp. Neurol. 173: 219-230.

Wilson, M. (1971) Optic nerve fibre counts and retinal ganglion cell counts during development of Xenopus laevis (Daudin). Q. J. Exp. Physiol. 56: 83-91.

Wilt, F. H. and N. K. Wessells. (Eds.) (1967) Methods in Developmental Biology. New York: Thomas Y. Cromwell Co.

Wise, S. P. and E. G. Jones. (1976) The organization and postnatal development of the commissural projection of the rat somatic sensory cortex. J. Comp. Neurol. 168: 313-344.

Wisniewski, H. and C. S. Raine. (1971) An ultrastructural study of experimental demyelination and remyelination: V. Central and peripheral nervous system lesions caused by diphtheria toxin. Lab. Invest. 25: 73-80.

Witkovsky, P., E. Gallin, J. G. Hollyfield, H. Ripps and C. D. B. Bridges. (1976) Photoreceptor thresholds and visual pigment levels in normal and vitamin A-deprived Xenopus tadpoles. J. Neurophysiol. 39: 1272-1287.

Witpaard, J. and H. E. D. J. ter Keurs. (1975) A reclassification of retinal ganglion cells in the frog, based upon tectal endings and response properties. Vision Res. 15: 1333-1338.

Wlassak, R. (1893) Die optischen Leitungsbahnen des Frosches. Arch. Anat. Physiol., Physiol. Abth., Suppl. 1-28.

Yamamoto, T. (1966) Electron microscopic observation on human optic nerves. Jpn. J. Ophthal 10: 40-53.

Yoon, M. (1971) Reorganization of retinotectal projection following surgical operations on the optic tectum in goldfish. Exp. Neurol. 33: 395-411.

Zečević, N. and P. Rakic. (1976) Differentiation of Purkinje cells and their relationship to other components of developing cerebellar cortex in man. J. Comp. Neurol. 167: 27-48.